Stony Brook University

Synthesis of 2,6-Pyridine-Based Diacetylene Macrocycle and its Possible Formation to a Covalently Bonded Tubular Structure via Topochemical Polymerization

By

Steven Kit Chow

To

The Graduate School

In Partial Fulfillment of the

Requirements

For the Degree of

Master of Science

In

Chemistry

Stony Brook University

August 2008

Stony Brook University

The Graduate School

Steven Kit Chow

We, the thesis committee for the above candidate for the Master of Science degree, hereby recommend acceptance of this thesis.

Dr. Frank W. Fowler, Advisor, Department of Chemistry

Dr. Joseph W. Lauher, Advisor, Department of Chemistry

Dr. Nancy S. Goroff, Chair Committee, Department of Chemistry

Dr. Andreas Mayr, Third Member, Department of Chemistry

This thesis is accepted by the Graduate School

Lawrence Martin
Dean of the Graduate School

Abstract of the Thesis

Synthesis of 2,6-Pyridine-Based Diacetylene Macrocycle and its Possible Formation to a Covalently Bonded Tubular Structure via Topochemical Polymerization

By

Steven Kit Chow

Master of Science

In

Chemistry

Stony Brook University

2008

Molecular macrocycles have been widely studied because of their open structures, their binding ability, and their interesting supramolecular structures. There have been many studies that show the construction of tubular structures via intermolecular interactions, but the construction of a covalent bonded tubular structure based on molecular macrocycles has not yet been achieved. The research goal of this project is to apply supramolecular chemistry to prepare a covalently bonded tubular structure from a pyridine-based diacetylene macrocycle in the solid state. Using the "Host-Guest" strategy, each diacetylene macrocycle unit may be directed into a correct spacing distance (5.0 Å) for a proper diacetylenic 1,4-polymerization. Diacetylene macrocycles are prepared via a planned synthesis. In this thesis, the main focus will be the synthesis of a 2,6-pyridine-based diacetylene macrocycle.

The synthesis of the 2,6-pyridine-based macrocycle has proven to be difficult. Even though the planned synthetic steps were short, there were many complications. Therefore, an alternative synthetic route has been developed. The final crude product is insoluble in common organic solvents, and thus the desired macrocycle was not isolated. The monocyclic by-product obtained from the original synthetic route was subjected to X-Ray crystallography for structural analysis, and the structure was compared with previously made 3,5-pyridine-based monocyclic by-product. It is suggested that the introduction of electron withdrawing groups into the pyridine ring position of the macrocycle may assist the macrocyclic formation and its stacking patterns in solid state.

Table of Contents

Page

List of Figures vii
List of Schemes viii
List of Tables ix

Chapter 1. Introduction 1
1.1 From Nanotube to Macrocyclic Supramolecular Structure 1
1.2 Ancestor of Macrocycle: The Crown Ether, and General Design of Macrocycles 2
1.3 Macrocycle Synthesis Technique 4
1.4 Intermolecular Interactions and Crystal Engineering 8
1.5 Formations of Tubular Structure from Macrocycles 12
1.6 Formations of Tubular Structure from Cyclic Peptides 17
1.7 Summary 18
Endnotes 19

Chapter 2. Synthesis of Diacetylene and its Polymerization 21
2.1 Acetylene and Conductive Polymers 21
2.2 Applying Metal Catalyzed Coupling Reactions to Construct Diacetylene Linkage and π-Bond Conjugated Polymers 23
2.3 The 1,4-Polymerization of Diacetylene – Topochemical Polymerization 28
2.4 The Host-Guest Strategy, An Approach for a Proper Diacetylene Organization 29
2.5 The "Turn-Stile" and "Swinging-Gate" Mechanism 32
2.6 Summary 35
Endnotes 36

Chapter 3. Synthesis of Pyridine-Based Diacetylene Macrocycle and Covalently-Bonded Tubular Structure (Part I) – Experimental Plan 38
3.1 Research Goal and Hypothesis 38
3.2 The Planned Synthetic Route to Pyridine-Based Diacetylene Macrocycles 43
Endnotes 46

Chapter 4. Synthesis of Pyridine-Based Diacetylene Macrocycle and Covalently-Bonded Tubular Structure (Part II) – Result and Discussion 47
4.1 Molecular Synthesis 47

Page
4.2 Alternate Synthetic Steps 51
4.3 Crystal Structure Analysis and Comparison 54
4.4 Future Plan 58
4.5 Conclusion 60
Endnotes 61

Chapter 5. Experimental Section 62
5.1 Synthesis of Macrocycle **4** and **4(m)** 63
5.2 Synthesis of Macrocycle **4a** and **4a(m)** 69
Endnotes 70

Bibliography 71

Appendix 1 80
A. Crystallographic Data for Compound **2** 80
B. Crystallographic Data for Compound **5(d)** 85
C. Crystallographic Data for Compound **4(m)** 93
D. ^{1}H-NMR and ^{13}C-NMR Spectra 98

List of Figures

Figure		Page
1.1	Ortho-, meta-, and para- isomers of [8,8]cyclophane	3
1.2	Macrocycles synthesized by Tobe and co-workers	13
1.3	Macrocycle concepts by Gleiter and co-workers	14
1.4	X-ray crystal structure of one of the macrocycles synthesized by Gleiter and co-workers	14
1.5	Macrocycle synthesized by Tykwinski et. al.	16
1.6	Crystal structure of Tykwinski's macrocycle (Red) while excess amount of porphyrin (Green) remains in the crystal structure	16
1.7	Shimizu and co-workers' macrocycle	17
1.8	Concepts and design of Ghadiri and co-workers' macrocycle	18
2.1	Examples of conductive polymers	22
2.2	Case (a) – Hydrogen bonding network of amide substituted diacetylene, synthesized by Amano and co workers	30
2.3	Case (b) – A co-crystal proposed by co-worker Ti Wang	30
2.4	A library of host functional groups that obtain a variety of spacing distance	31
2.5	Case 1 – Two co-crystals that apply (a): the urea of glycine host, and (b): the oxalamide of glycine host	33
2.6	Case 2 – Co-crystal of 4-butadiynylbenzyl ammonium salt with oxalamide of glycine, done by co-worker Zhong Li	34
2.7	(a) The "Turn-Stile" and (b) "Swinging-Gate" mechanism for diacetylene	35
3.1	The designed macrocycles in this project	39
3.2	Curtis' proposed macrocycle **4a'** in comparison to Tykwinski's macrocycle structure **3.1**.	40
3.3	The single crystal structure of macrocycle **4a**	43
4.1a	Crystal structure of 2,6-pyridine-based macrocycle monomer **4(m)**	56
4.1b	Crystal structure of 3,5-pyridine-based macrocycle monomer **4a(m)**	57
4.2	The side view of (a) the 2,6-pyridine-based macrocycle monomer **4(m)**, and (b) the 3,5-pyridine-based macrocycle monomer **4a(m)**	58
4.3	(a) The proposed refinement of macrocycle **4** by introducing electron withdrawing group. (b) The proposed new macrocycle structure form by homocoupling of **3** and **3a**	59
4.4	A plausible copper-diether **3** coordination complex that may alter the favorability during the Hay coupling condition on the original synthetic route	60

List of Schemes

Scheme		Page
1.1	Williamson ether synthesis of a crown ether	4
1.2	A possible side-reaction that might lead to polymerization of 2 reactants	5
1.3	Potassium cation serves as a templates and the reactants are topologically fixed for a desired cyclization product **1.12**	6
1.4	Höger and co-workers used a covalently bonded template to assist the formation of diacetylene linkage via homocoupling reaction	7
2.1	General reaction schemes for homocoupling and heterocoupling reactions of acetylene	23
2.2	Polymerization steps for Le Moigue's polymers	24
2.3	TBDMS-substituted polytriacetylene oligomer synthesized by Diederich and co-workers	25
2.4	The supramolecular polymer constructed by Wilson and Anderson that uses a porphyrin-based diacetylene as building blocks	26
2.5	Metal-coordinated diacetylenic polymer synthesized by Bunz and co-workers	27
2.6	Dimerization of the pyridine-based dialkyne into a rigid macrocycle	27
2.7	The 1,4-topochemical polymerization of diacetylene	29
3.1	General scheme for the synthesis of macrocycle **4a'**	40
3.2	Modified steps for the synthesis of **3a'(p)**	41
3.3	The expected 1,4-polymerization of diacetylene macrocycle **4a** under co-crystal with oxalamide of glycine	42
3.4	General scheme for the synthesis of pyridine based diacetylene macrocycle **4**, **4a**, and **4b**	44
3.5	general scheme for the synthesis of macrocycle **4c**	45
4.1	The synthesis steps of 3,5-pyridine-based macrocycle **4a**	47
4.2	The first synthetic steps of 2,6-pyridine-based macrocycle **4**	48
4.3	The copper-free Sonogashira coupling reaction system applies in the coupling of 2,6-dibromopyridine **1** and 3,5-dibromopyridine **1a** with propargyl alcohol	49
4.4	Sonogashira coupling of 2,6-dibromopyridine with propargyl ether using standard reaction system	50
4.5	Homocoupling of **3** via Hay coupling condition. The major product in this reaction was **4(m)**	50
4.6	The alternative synthetic route for the synthesis of 2,6-pyridine-based macrocycle **4**	52
4.7	Reaction scheme for the terminal alkyne protection	53

List of Tables

Table		Page
1.1	[8,8]cyclophane connectivity as it relates to cavity dimension	3
1.2	Selected properties and examples of hydrogen bonds	11
4.1	Unit cell parameters for [1 + 1] side products **4(m)** and **4a(m)**	55

Chapter 1. Introduction to Macrocycle and Tubular Structure

1.1 Macrocyclic Supramolecular Structure

Chemists and material scientists have been interested in tubular structures since the debut of carbon nanotubes. This type of tubular structure has lead to extensive research, and numerous applications in human technology that we are currently using today. Even though nanotubes have useful properties that can be applicable in material,[1] electrical,[2] and medical developments,[3] similar tubular structure can also be prepared via supramolecular chemistry or self-aggregation by using macrocycles as building blocks.[4] These type of tubular supramolecular structures may have an unique architecture and exhibit interesting binding properties.[4,5,6] They may also have interesting properties that can be applicable in material, electrical, and medical developments just like nanotubes.[4,5,7]

While nanotubes are mostly covalently bonded sp^2 hybridized carbon atoms, tubular structures that form from macrocycle building blocks are held together by intermolecular interactions.[4, 8] Networked intermolecular tubular structures existed in biological systems before carbon nanotubes were discovered. They can be found, for example, in a cell's membrane channels, which are essential for ion exchange and molecular signaling of a cell.[4b, 9] Protein folding into tubular structures is also well studied by biochemists.[4b,9] Applying intermolecular interactions, chemists and material scientists can induce macrocycles to form tubular structures. By establishing a design of a single macrocycle building block, chemists and material chemists are able to engineer the architecture of these tubular structures and enable these structures to exhibit their unique

stacking patterns and/or properties. While macrocycles and their supramolecular structures are widely studied, attempts to synthesize macrocycles are still challenging to chemists and material scientists.

1.2 Ancestor of Macrocycle: The Crown Ether, and General Design of Macrocycles

One of the functions of a macrocycle is to bind atoms or molecules.[10] One of the simplest examples of macrocycles, the crown ethers, have the ability to bind different cations based on their ring size.[5] Metal cations can be trapped by coordination with oxygen atoms in crown ethers. Even though the discovery of crown ethers by Pedersen in 1967 was accidental,[5,10] the crown ethers made scientists to become interested in their coordination properties. Then, the applications of macrocycles were further expended. Chemists and other scientists have used macrocycles to study their molecular recognition,[4,5,6] their coordination chemistry,[5] and their supramolecular chemistry.[4,5,8] They have also designed different macrocycles with unique size, shape, and binding properties using various synthetic techniques.[11,12]

In order to study macrocycles' supramolecular structure, the structural designs of macrocycles have become more rigid recently. Carbon-carbon triple bond linkages (*sp* hybridized carbon framework) have been used frequently.[4,7,11,12] The advantage of using acetylene as a linkage is that there is no cis-trans isomerization compared to a double bond framework.[13,14] There is less steric hindrance either because no branch is present in the acetylene linkage.[13,14] The size of a macrocycle depends on the length of the triple bond linkages and the linkages' position in a aromatic ring. Using the ortho-, metha-, and

para- isomers of [8,8]cyclophane **1.1**, **1.2** and **1.3** as examples, the cavity area of these macrocycles are different in each of these isomers. In comparisons, the para- isomer obtains the largest area (Figure 1.1, Table 1.1).[15]

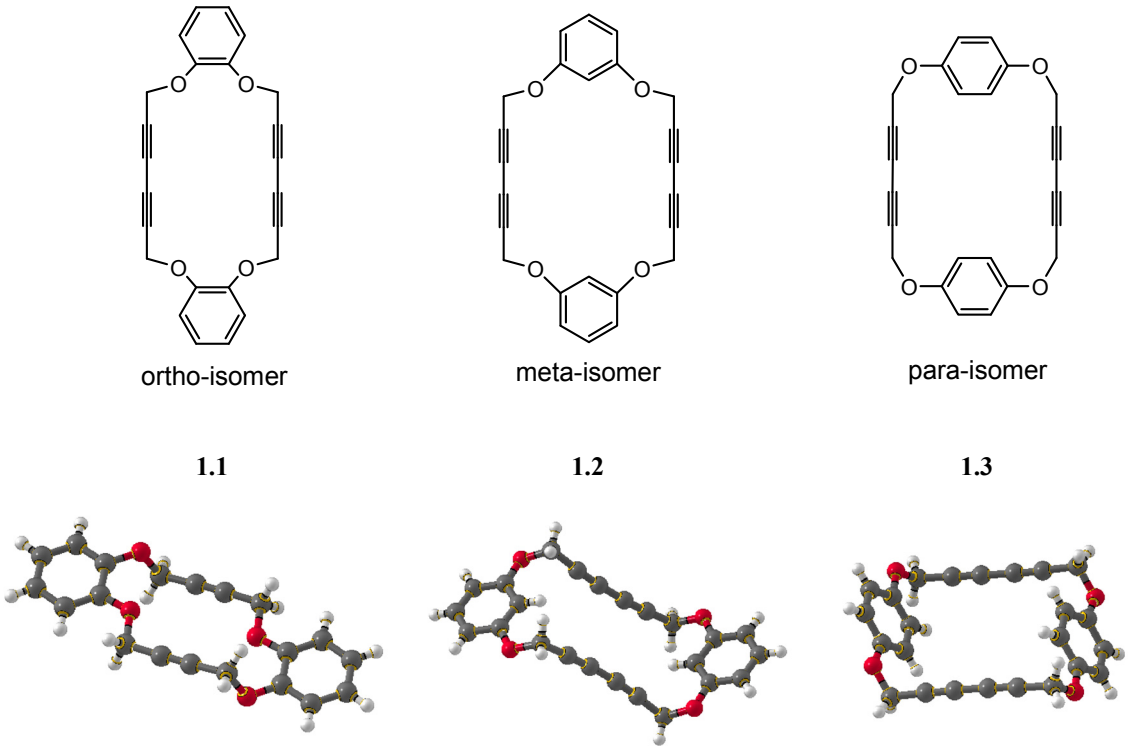

Figure 1.1: Ortho-, meta-, and para- isomers of [8,8]cyclophane.[15,16]

	Ortho isomer **1.1**	Meta isomer **1.2**	Para isomer **1.3**
Dimension Area	4.1 Å × 10.2 Å (41.8 Å^2)	4.4 Å × 10.4 Å (45.8 Å^2)	7.0 Å × 7.9 Å (55.3 Å^2)

Table 1.1: [8,8]cyclophane connectivity as it relates to cavity dimension.[15,16]

In Sections 1.5 to 1.7, we can see how macrocycles induce tubular supramolecular structures by looking at various literature examples. We will also see more examples in the formation of tubular structures using cyclic peptides.

1.3 Macrocycle Synthesis Techniques

Before going on to literature examples, we shall turn our attention to the synthesis techniques for the preparation of macrocycle. We shall take the synthesis of a crown ether for example. Via Williamson ether synthesis, a crown ether can be formed as a [2 + 2] cycloaddition product **1.6** by promoting a 2-component ring closure (Scheme 1.1).[5,10] The problem is, however, the formation of a [1 + 1] cycloaddition product **1.7**, or polymerization that leads to the formation of polymer **1.8** may also occur (Scheme 1.1-1.2). This may lead to undesired side products and/or polymer.[5]

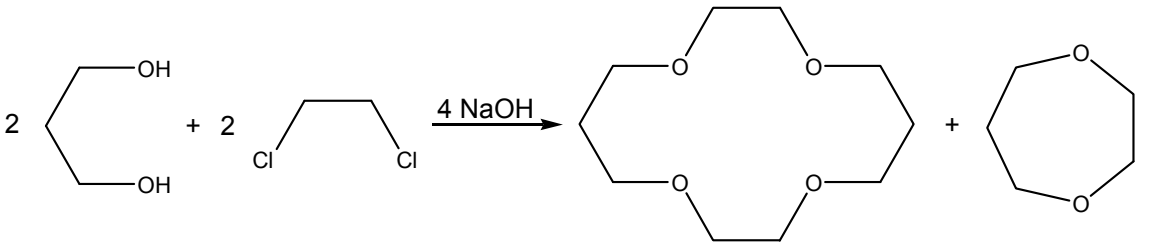

1.4 **1.5** **1.6** **1.7**

[2 + 2] Product [1 + 1] Product

Scheme 1.1: Williamson ether synthesis of a crown ether. The [2 + 2] cycloaddition product is made by the combination of 2 eq. of each reactant. On the other hand, the [1 + 1] cycloaddition product is the combination of 1 eq. of each component.[5]

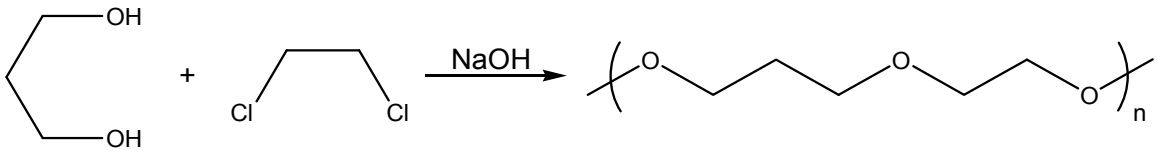

1.4 **1.5** **1.8**

Scheme 1.2: A possible side-reaction that may lead to polymerization of 2 reactants.

To avoid such complications, macrocycle synthesis can be efficiently accomplished by either: (a) applying a template,[5,11,17] or (b) high dilution.[5,11,18]

(a) – The Template effect: A molecule act as a template is used to hold reactants in place. When the reactants are in a fixed position, the reaction favors cyclization and forms a cyclization product.[17] Therefore, a template must be able to bind with reactants either by chemical bonding[19] or by intermolecular attraction.[5] Templated cyclization reactions give chemists more geometric or topological control and thus polymerization can be avoided. For example, potassium cation coordinates with reactants in a crown ether synthesis (Scheme 1.3).[5]

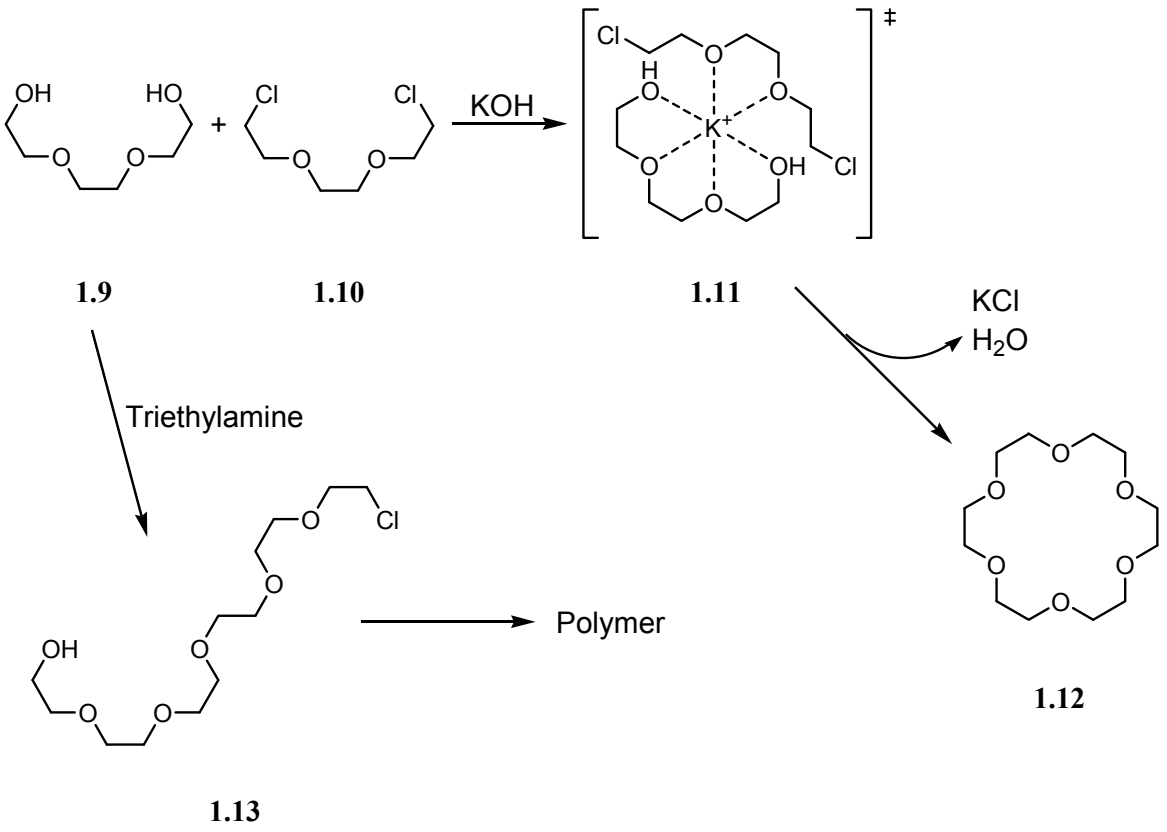

Scheme 1.3: Potassium cation serves as a template and the reactants are topologically fixed for a desired cyclization product **1.12**.[5]

In the above crown ether synthesis, potassium cation coordinates with reactants and forms coordination complex **1.11** when using KOH as the base. On the other hand, without the presence of potassium cation, **1.9** and **1.10** tend to polymerize. Therefore, potassium cation promotes cyclization for the desired crown ether **1.12** by pre-organizing the position of reactants with the formation of a ligand-metal complex (intermediate **1.11**) and enhancing the rate of cyclization. Thus, the above crown ether synthesis using KOH is under kinetic template effect.[5]

Even though there are many successful cases of macrocycle synthesis using templated cations[5,11] and metals[11] for coordination with reactants, there are also cases in

which the template is covalently bonded to the starting materials. After cyclization reactions, the covalently bonded templates should be able to cleave easily without complication. Höger et. al. applied such template to synthesized their acetylene based macrocycle **1.16** (Scheme 1.4).[19]

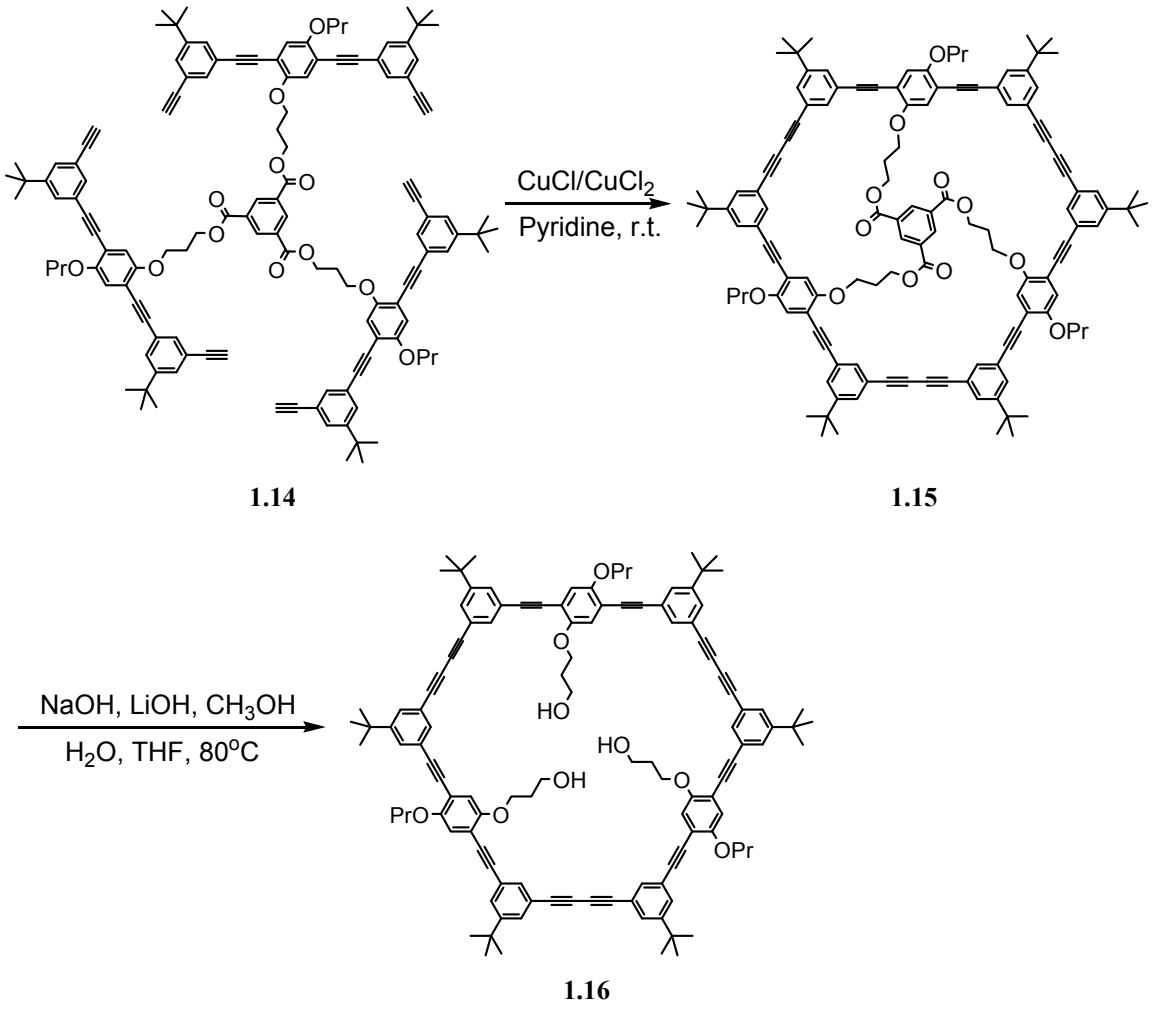

Scheme 1.4: Höger and co-workers used a covalently bonded template to assist the formation of diacetylene linkage via homocoupling reaction. The template was then cleaved under basic conditions after the formation of the templated-macrocycle.[19]

(b) – High Dilution: A huge amount of solvent is used to dissolve reactants in a reaction system. The main objective of high dilution is to prevent polymerization of

starting materials, so that reactants can be able to proceed with ring closure and form a [1 + 1] cyclization product.[18] Thus, the probability of polymerization can be further reduced. Let r_c be the rate of cyclization and r_p be the rate of polymerization. The rate expression can be represented as $r_c = k_c$ [Reactant], and $r_p = k_p$ [Reactant]^2, and then the following expression can be derived when we compare the ratio between the rate of cyclization and the rate of polymerization:[5]

$$\frac{r_c}{r_p} = \frac{k_c[\text{Reactant}]}{k_p[\text{Reactant}]^2} = \frac{k_c}{k_p[\text{Reactant}]} \qquad \text{(Eq. 1.1)}^5$$

Based on Eq. 1.1, it is reasonable that if the concentration of reactant decreases, the ratio of cyclization product compare to polymer product increases. In order to enhance the yield of the cyclized product, high dilution has been applied frequently in macrocycle synthesis.[5,11,18]

1.4 Intermolecular Interactions and Crystal Engineering

The term "crystal engineering" was introduced by G. M. J. Schmidt in 1971. He applied different packing patterns of cinnamic acids to demonstrate the differences in their photodimerization behavior in the solid state.[20] A more well-defined concept of crystal engineering was suggested by G. R. Desiraju 18 years after.[21] The analogy of crystal engineering is the formation of an organized crystal by intermolecular bonding of molecules, just as how atoms bond together to form a molecule.[5] Supramolecular chemistry is therefore an important concept for crystal engineering, or the formation of crystal structures.[22] Herein, we shall list different kinds of intermolecular interactions that are applicable in supramolecular chemistry:[5,16,23]

Ion-ion interactions – Anions and cations attracted to each other via charge-charge attractions.

Ion-dipole interactions – Anions or cations attracted to a polar molecule. Anion will be attracted to the positive end of the dipole of a molecule, while cation will be attracted to the negative end of the dipole of a molecule.

Dipole-dipole interactions – Two dipoles interact in a fashion such that the negative end of one dipole is attracted to the positive end of the other dipole.

Hydrogen bonding – Hydrogen atom to an electronegative atom or an electron withdrawing group (H-Bond donor) attracted to a functional group or a dipole of an adjacent molecule (H-Bond acceptor).[24]

Cation-π interactions – A Cation (usually transition metal) attracted to the π-orbital of an aromatic ring.

π-π stacking – Electrostatic interaction between two aromatic rings. There are two types of π-π stacking: (a) Face-to-face π-π stacking. The partially positive charged aromatic ring center in an aromatic ring attracts the partially negative charged delocalized π system of another aromatic ring. Thus the aromatic rings are on top of each other.[25] (b) Edge-to-face π-π stacking. Electron poor hydrogen atoms from an aromatic ring attract the electron rich π system of another aromatic ring.

van der Waals forces – Polarized electron cloud of an molecule attracts an adjacent molecule while they polarize each other. The resulted intermolecular attraction is relatively weak, however.

In crystal engineering, hydrogen bonding has been applied more frequently then other intermolecular interactions, because this type of intermolecular interaction is strong enough (approximately 120kJ/mol is the strongest case), has predictable bond angles, and manageable by just manipulating the function groups of a molecule. To demonstrate the strength of hydrogen bonding, a list of hydrogen bond properties are listed on Table 1.2.[16,23] The strength of hydrogen bonding, as shown in Table 1.2, depends on the polarity and electronegativity of the functional group.

	Strong	Moderate	Weak
D-H•••A interaction	mostly covalent	mostly electrostatic	Electrostatic
Bond lengths	D-H ≈ H•••A	D-H < H•••A	D-H <<H•••A
H•••A (Å)	~1.2-1.5	~1.5-2.2	2.2-3.2
D•••A (Å)	2.2-2.5	2.5-3.2	3.2-4.0
Bond angles (°)	175-180	130-180	90-150

Examples		Donors:	Donors:
	$[F\bullet\bullet\bullet H\bullet\bullet\bullet F]^-$	S-H, C-N(H)H, O-H	C-H, Si-H (?)
	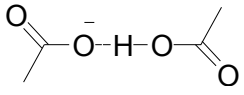	Acceptors: 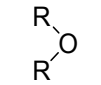  	Acceptors:  

Table 1.2: Selected properties and examples of hydrogen bonds.[24]

To further understand the pattern of hydrogen bonding, a proposal from Etter et. al. has suggested the following hydrogen bonding rules,[26] which are useful for predicting hydrogen bonding pattern, and designing hydrogen bonding network for crystal engineering.

(1) All good proton donors and acceptors are used in hydrogen bonding.

(2) Six-membered ring intramolecular hydrogen bonds form in preference to intermolecular hydrogen bonds.

(3) The best proton donors and acceptors remaining after intramolecular hydrogen-bond formation form intermolecular hydrogen bonds to one another.

To demonstrate the applications of intermolecular interactions, we shall take a look at some literature examples presented in Section 1.5-1.7.

1.5 Formations of Tubular Structure from Macrocycles

To demonstrate how the polarity of solvents affect the stacking pattern of macrocycles, Tobe et. al. studied macrocycles' self-aggregation properties in a theoretical approach by making rigid macrocycles **1.17**, **1.18**, and **1.19**, that used diacetylene linkages and aromatic rings (Figure 1.2).[14] The diacetylene linkages in their macrocycles may have a potential to polymerize and form covalent bonded tubular structures with interesting electrical and optical properties.[14] They observed their macrocycles' self-aggregation behavior by ^{1}H-NMR spectrometry. The chemical shifts of phenyl hydrogens in these macrocycles change while π-π stacking interactions occurr.[14,27] Using the data they obtained by observing the change of chemical shifts, they applied Eq. 1.1 to determine the self-aggregation constant K_E. Under different solvent systems, the tendency of self-aggregation, or π-π stacking interaction, can be observed by comparing K_E in different macrocycle cases.[14]

$$\delta = \delta_m + (\delta_a - \delta_m)\left(1 + \frac{1-\sqrt{4K_E C_t + 1}}{2K_E C_t}\right) \qquad \text{(Eq. 1.2)}^{14}$$

An assumption was made, that macrocycles undergo isodesmic (infinite) association, and $K_2 = K_3 = K_4 = \ldots = K_n = K_E$. δ_a is the average chemical shift of the aggregated macrocycles and δ_m is the chemical shift of a single unit of the macrocycles. Under a more polar or aromatic solvent, the association constant K_E increases compared to the

standard solvent $CDCl_3$. Therefore, this result indicates that π-π stacking interactions of the macrocycles are favorable due to solvophobic interactions.[14]

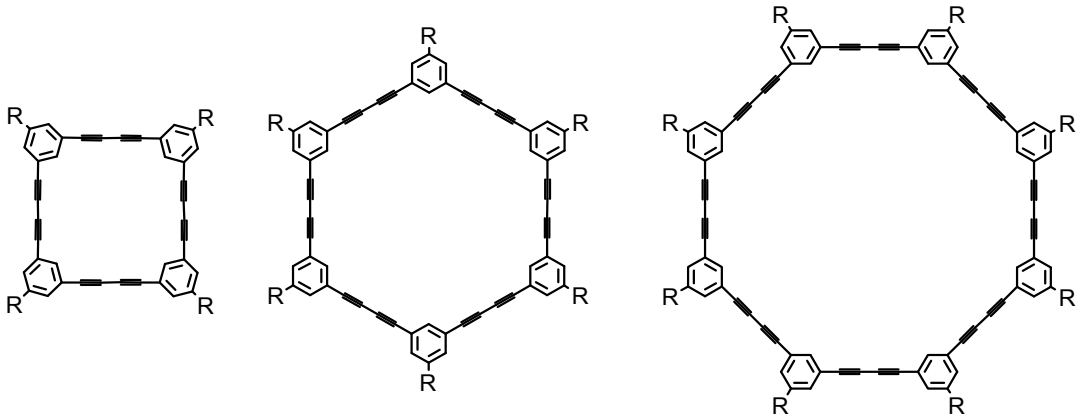

1.17 **1.18** **1.19**

R = $COOC_8H_{17}$, $COOC_{16}H_{33}$, $COO(CH_2CH_2O)_3CH_3$, H

Figure 1.2: Macrocycles synthesized by Tobe and co-workers. Their self-aggregation behavior was observed via ^{1}H-NMR.[14]

In a more crystallographic approach, Gleiter et. al. synthesized their macrocycles and obtained their tubular supramolecular structures. Their designs enable these macrocycles to be more flexible while they applied an alkyl chain to attach the rigid diacetylene linkages. The soft heteroatoms in their macrocycles also enabled the tubular structures to obtain chalcogen-chalcogen interaction with the adjacent tubular network. The macrocycles obtain a chair conformation while they self-assembled and formed a tubular network (Figure 1.3-1.4).[28]

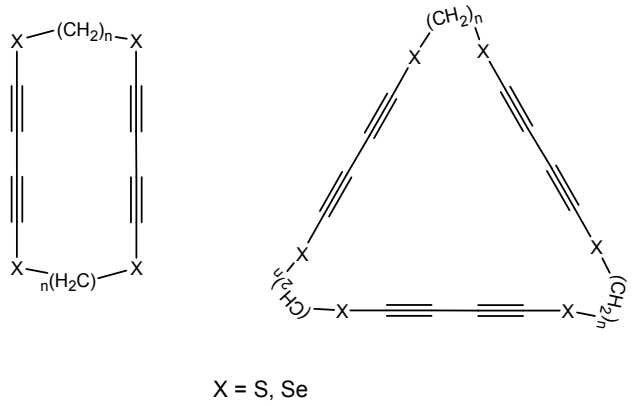

Figure 1.3: Macrocycle design concepts by Gleiter and co-workers. The flexible alkyl chains allow these type of macrocycles to be more flexible and exhibit a chair conformation.[28]

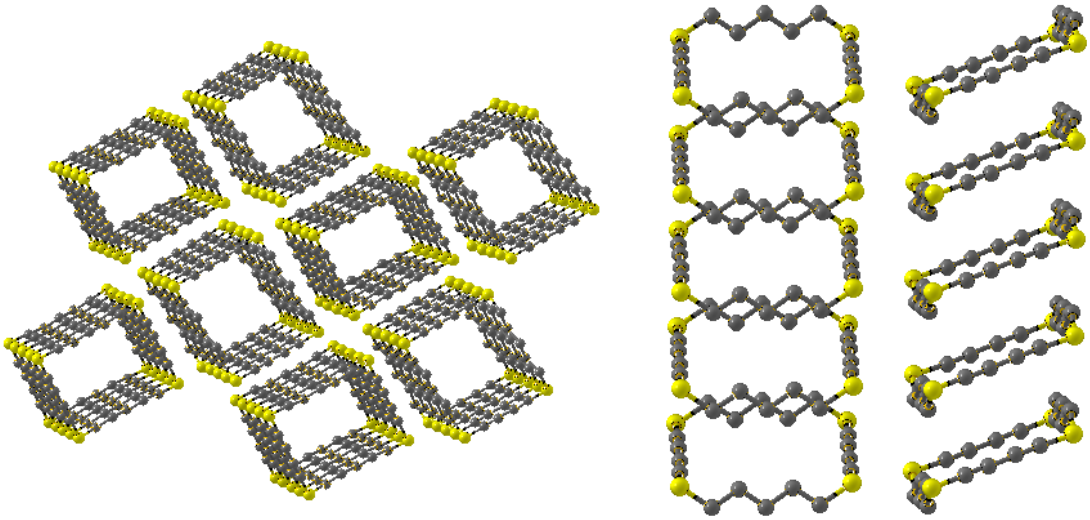

Figure 1.4: X-ray crystal structure of one of the macrocycles synthesized by Gleiter and co-workers. Yellow atom is sulfur (See also Figure 1.3). This macrocycle formed a tubular supramolecular structure via van der Waals interactions, and each macrocycle building block is in a chair conformation.[28]

They had observed the relationship between the solvent-accessible volume (inside the tubular structure) and the torsional angle φ of the diacetylene arms in these macrocycles

caused by high flexibility. This observation led to the conclusion that the smaller the torsional angle φ, the larger the solvent-accessible volume.[28]

Tykwinski et. al. also attempted to synthesize macrocycles in order to study their supramolecular structures. They introduced their rigid macrocycles' design, such as macrocycle **1.20**. While they made most of their efforts in forming single crystals of their designed macrocycles, they used ruthenium-coordinated porphyrin to coordinate their macrocycle, in order to resolve the purification and solubility problems (Figure 1.5).[29] Even though some of their macrocycle derivatives failed to crystallize, they still obtained some macrocycles' single crystal and confirmed their structure based on X-ray crystallographic analysis (Figure 1.6).[29]

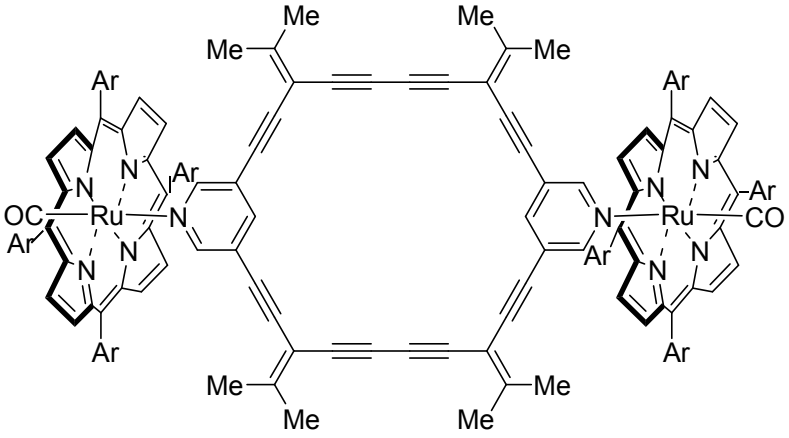

1.20

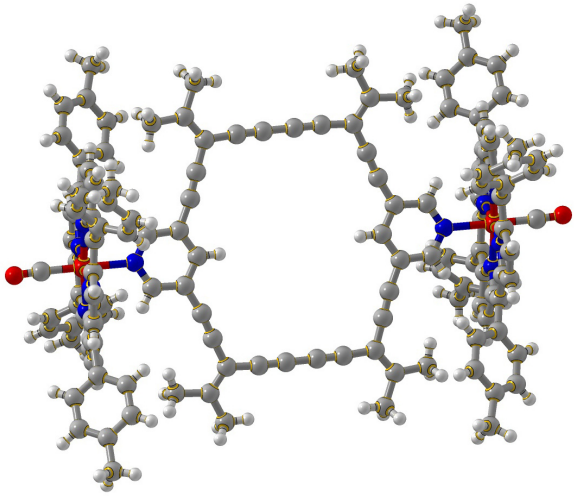

Figure 1.5: Macrocycle synthesized by Tykwinski et. al. Pyridines in the macrocycle were coordinated with the ruthenium metal in the porphyrin.[29]

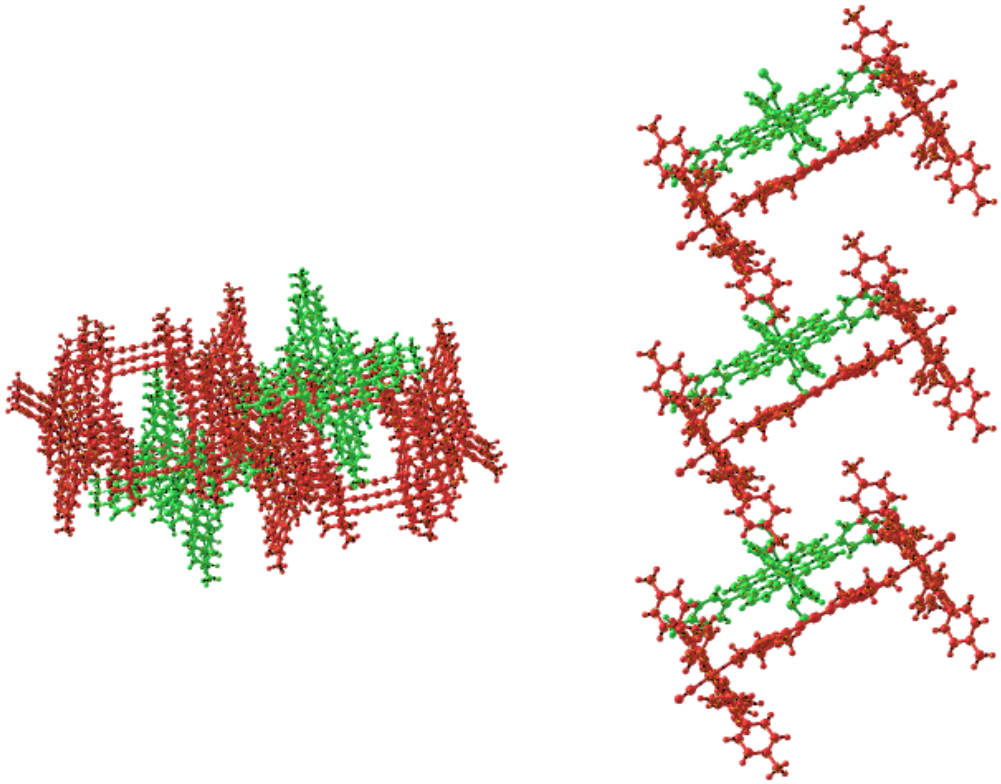

Figure 1.6: Crystal structure of Tykwinski's macrocycle (Red) with excess amount of porphyrin (Green) remains in the crystal structure.[29]

The crystal structure of Tykwinski's macrocycle (Figure 1.6) has shown that the spacing distance between each single macrocycle unit is huge and the excess amount of porphyrin is stacked in between each macrocycle via π-π stacking interactions.

Shimizu et. al. applied urea as the functional group for hydrogen bonding in their macrocycles and formed a hydrogen-bonding-networked tubular structure. The recognition for hydrogen bonding by the urea functional groups in the macrocycles has leaded to a tubular structure formation. Rigid aromatic rings is also presented in their macrocycles, thus they also observed an edge-to-face π-π stacking interaction (Figure 1.7).[30]

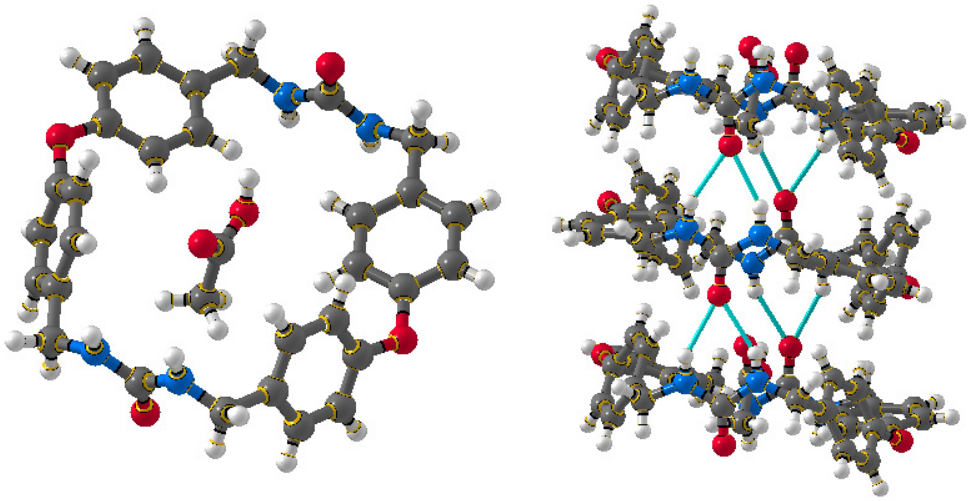

Figure 1.7: Shimizu and co-workers' macrocycle. By applying the urea functional group, the macrocycle can be able to form a hydrogen bonding network to the next macrocycle. Thus a tubular structure has formed.[30]

1.6 Formations of Tubular Structure from Macrocyclic Peptides

Due to a board application of tubular structures in biological systems,[4b,9] Ghadiri et. al. introduced a cyclic peptide concept based on the finding by DeSantis et. al., that

cyclic peptides can be formed by alternating an even number amount of D- and L- amino acids.[23,31] Ghadiri and co-workers synthesized a peptide ring using L-glutamine and D-alanine in an alternating manner. The synthesized peptide-based macrocycle formed a tubular structure based on the hydrogen bonding network from the amino linkage (Figure 1.8).[32] In this case, hydrogen bonding has taken an essential role on the construction of this peptide-based tubular structure. Even though this tubular structure is constructed by intermolecular interactions, it has a similar architecture as a transmembrane ion channel and can also be considered as an organic nanotube.

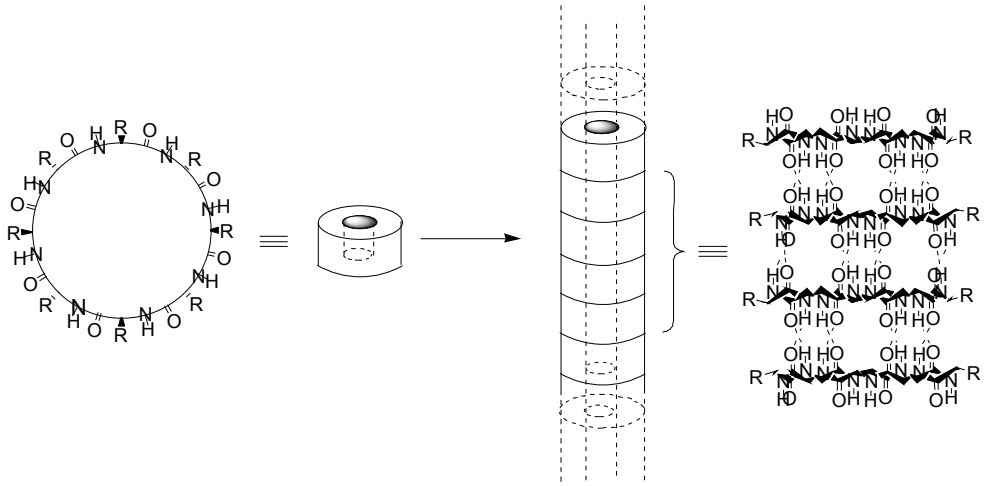

Figure 1.8: Concepts and design of Ghadiri and co-workers' macrocycle. This peptide macrocycle forms a tubular supramolecular structure by hydrogen bonding at the amine- and carboxyl- linkage of the amino acids in the macrocycle.[32]

1.7 Summary

Due to tubular structure's pre-existence in biological systems and its potential applications, chemists and material scientists have a great interest in this type of hollow structure. Tubular structures can be formed covalently such as the nanotube, or by crystal engineering via supramolecular interactions of macrocycle building blocks.

Intermolecular interactions such as ion-ion interactions, ion-dipole interactions, dipole-dipole interactions, hydrogen bonding, cation- π interactions, π-π stacking interactions, and van der Waals forces had become an important aspect of supramolecular chemistry and coordination chemistry. These supramolecular interactions dictate the macrocycles' packing pattern when they form supramolecular structures. In the next chapter, we will see how the concept of supramolecular chemistry assists the polymerization of diacetylene. We will also see how supramolecular chemistry is the basis of our research goals.

Endnotes:

[1] (a) Simmons, T. J.; Hashim, D.; Vajtai, R.; Ajayan, P. M. *J. Am. Chem. Soc.* **2007**, *129*, 10088-10089.; (b) Zhang, M.; Fang, S.; Zakhidou, A. A.; Lee, S. B.; Aliev, A. E.; Williams, C. D.; Atkinson, K. R.; Baughman, R. H. *Science*, **2005**, *309*, 1215-1219.; (c) Dalton, A. B.; Collins, S.; Muñoz, E.; Razal, J. M.; Ebron, V. E.; Ferraris, J. P.; Coleman, J. N.; Kim, B. G.; Baughman, R. H. *Nature*, **2003**, *423*, **6941**, 703.

[2] (a) Bradley, K.; Gabriel, J.-C. P.; Grünert, G. *Nano Lett.* **2003**, *3*, 1353-1355.; (b) Gabriel, J. C.-P. *Mat. Res. Soc. Symp. Proc.* **2003**, *776*, 271-277.; (c) Collins, P. G.; Arnold, M. S.; Avouris, P. *Science*, **2001**, *292*, 706-709.; (d) Postma, H. W. C.; Teepen, T.; Yao, Z.; Grifoni, M.; Dekker, C. *Science*, **2001**, *293*, 76-79.; (e) Tseng, Y.-C.; Xuan, P.; Javey, A.; Malloy, R.; Wang, Q.; Bokor, J.; Dai, H. *Nano Lett.* **2004**, *4*, 123-127.

[3] (a) Singh, R.; Pantarotto, D.; McCarthy, D.; Chaloin, O.; Hoebeke, J.; Partidos, C. D.; Briand, J.-P.; Prato, M.; Bianco, A.; Kostarelos, K. *J. Am. Chem. Soc.* **2005**, *127*, 4388-4396.; (b) Gannon, C. J.; Cherukuri, P.; Yakobson, B. I.; Cognet, L.; Kanzius, J. S.; Kittrell, C.; Weisman, R. B.; Pasquali, M.; Schmidt, H. K.; Smalley, R. E.; Curley, S. A. *Cancer*, **2007**, *110*, 2654-2665.

[4] (a) Moore, J. S. *Acc. Chem. Res.* **1997**, *30*, 402-413. (b) Bong, D. T.; Clark, T. D.; Granja, J. R.; Ghadiri, M. R. *Angew. Chem. Int. Ed.* **2001**, *40*, 988-1011.; (c) Shu, L.; Mayor, M. *Chem. Comm.* **2006**, 4134-4136.

[5] Steed, J. W.; Atwood, J. L. Supramolecular Chemistry, John Wiley & Sons, Chichester, 2000.

[6] Katayev, E. A.; Sessler, J. L.; Khrustalev, V. N.; Ustynyuk, Y. A. *J. Org. Chem.* **2007**, *72*, 7244-7252.

[7] (a) Zhao, D.; Moore, J. S. *Chem. Comm.* **2003**, 807-818.; (b) Höger, S. *J. Polym. Sci. Part A: Polym. Chem.* **1999**, *37*, 2685-2698.

[8] Burnsveld, L.; Folmer, B. J. B.; Meijer, E. W.; Sijbesma, R. P. *Chem. Rev.* **2001**, *101*, 4071-4097.

[9] (a) Eisenberg, B. *Acc. Chem. Res.* **1998**, *31*, 117-123.; (b) Sigler, P. B.; Xu, Z.; Rye, H. S.; Burston, S. G.; Fenton, W. A.; Horwich, A. L. *Annu. Rev. Biochem.* **1998**, *67*, 581-608.; (c) Horwich, A. L.; Weber-Ben, E. U.; Finley, D. *Proc. Natl. Acad. Sci. USA* **1999**, *96*, 11033-11040.; (d) Voges, D.; Zwickl, P.; Baumeister, W. *Annu. Rev. Biochem.* **1999**, *68*, 1015-1068.

[10] Pedersen, C. J. *J. Am. Chem. Soc.* **1967**, *89*, 7017.

[11] Zhang, W.; Moore, J. S. *Angew. Chem. Int. Ed.* **2006**, *45*, 4416-4439.

[12] Siemsen, P.; Livingston, R. C.; Diederich, F. *Angew. Chem. Int. Ed.* **2000**, *39*, 2632-2657.

[13] Viehe, H. G. Chemistry of Acetylene, Marcel Dekker, New York, 1969.

[14] Tobe, Y.; Utsumi, N.; Kawabata, K.; Nagano, A.; Adachi, K.; Araki, S.; Sonoda, M.; Hirose, K.; Naemura, K. *J. Am. Chem. Soc.* **2002**, *124*, 5350-5364.
[15] Srinivasan, M.; Sankararaman, S.; Hopf, H.; Dix, I.; Jones, P. G. *J. Org. Chem.* **2001**, *66*, 4299-4303.
[16] Curtis, S. M. Ph.D. Thesis (Chemistry), SUNY at Stony Brook, 2003.
[17] Busch, D. H.; Stephenson, N. A. *Coord. Chem. Rev.* **1990**, *110*, 119-154.
[18] Illuminati, G.; Mandolini, L. *Acc. Chem. Res.* **1981**, *14*, 95-102.
[19] Höger, S.; Meckenstock, A.-D.; Pellen, H. *J. Org. Chem.* **1997**, *62*, 4556-4557.
[20] Schmidt, G. M. J. *Pure Appl. Chem.* **1971**, *27*, 647-648.
[21] Desiraju, G. R. Crystal Engineering: The Design of Organic Solids, Elsevier, Amsterdam, 1989.
[22] Desiraju, G. R. *Angew. Chem. Int. Ed. Engl.* **1995**, *34*, 2311-2327.
[23] Wang, T. M.S. Thesis (Chemistry), SUNY at Stony Brook, 2005.
[24] (a) Pimental, G. C.; McClellan, A. L. The Hydrogen Bond, Freeman, San Francisco, 1960.; (b) Jeffrey, G. A. An Introduction to Hydrogen Bonding, Oxford University Press, Oxford, 1997.
[25] Hunter, C. A.; Sanders, J. K. M. *J. Am. Chem. Soc.* **1990**, *112*, 5525-5534.
[26] Etter, M. C. *Acc. Chem. Res.* **1990**, *23*, 120-126.
[27] (a) Höger, S.; Bonrad, K.; Mourran, A.; Beginn, U.; Möller, M. *J. Am. Chem. Soc.* **2001**, *123*, 5651-5659.; (b) Kakamura, K.; Okubo, M.; Yamaguchi, M. *Org. Lett.* **2001**, *3*, 1097-1099.; (c) Martin, R. B. *Chem. Rev.* **1996**, *96*, 3043-3064.
[28] Werz, D. B.; Gleiter, R.; Rominger, F. *J. Org. Chem.* **2004**, *69*, 2945-2952.
[29] (a) Campell, K.; McDonald, R.; Branda, N. R.; Tykwinski, R. R. *Org. Lett.* **2001**, *3*, 1045-1048.; (b) Campell, K.; McDonald, R.; Tykwinski, R. R. *J. Org. Chem.* **2002**, *67*, 1133-1140.
[30] Shimizu, L. S.; Hughes, A. D.; Smith, M. D.; Davis, M. J.; Zhang, B. P.; Loye, H.-C.; Shimizu, K. D. *J. Am. Chem. Soc.* **2003**, *125*, 14972-14973.
[31] DeSantis, P.; Morosetti, S.; Rizzo, R. *Macromolecules* **1974**, *7*, 52-58.
[32] (a) Ghadiri, M. R.; Granja, J. R.; Milligan, R. A.; McRee, D. E.; Khazanovich, N. *Nature*, **1993**, *366*, 324-327.; (b) Hartgerink, J. D.; Granja, J. R.; Milligan, R. A.; Ghadiri, M. R. *J. Am. Chem. Soc.* **1996**, *118*, 43-50.

Chapter 2. Synthesis of Diacetylene Linkages and Acetylenic Polymers

2.1 Acetylene and Conductive Polymers

Having sp hybridized bonding orbitals, carbon-carbon triple bond has a rich electron density and forms a strong bond. The bond dissociation energy of a carbon-carbon triple bond is approximately 837 kJ/mol, which is much stronger then a saturated carbon-carbon single bond or a sp^2 hybridized carbon-carbon double bond.[1] The sp hybridized orbital in triple bond also enable the geometry of this carbon-carbon linkage to be linear. Even though carbon-carbon triple bonds usually serve as a linear linkage in a molecule, it may also promote a pericyclic or an intramolecular cyclization reaction[2,3] into a multi-ring structure if there is another adjacent acetylene linkage within an appropriate distance, and also with suitable reagents and/or reaction environment. Therefore, compound with the acetylene linkage is considered as a reactive species.

If acetylenic compounds have such reactivity, we can also envision their polymerization. Polyacetylene, a type of π-bond conjugated polymer, was found to exhibit conductivity by Shirakawa and co-workers. They subjected their synthesized polyacetylene film to oxidative doping and observed this polymer has electronic conductivity.[4] These conductive polymers have been further modified and applied by many chemists and material scientists. Potential applications of conductive polymers in the development of electronics,[5] molecular devices/sensors,[6] nonlinear optical devices,[7] etc. attracted scientists to study their conductivity and other properties. They also attracted synthetic chemists to synthesize and modify these type of polymers.

The main feature of conductive polymers is their overlapping π-orbital. It is essential for these polymers to obtain a π-bond conjugation, so that the π-orbital in the polymer chains can be delocalized and ensure electron flow within the polymers. Therefore, double bond or triple bond linkages are often applied in conducting polymers. Examples of π-bond conjugated polymers (such as acetylenic polymers) are shown in Figure 2.1.

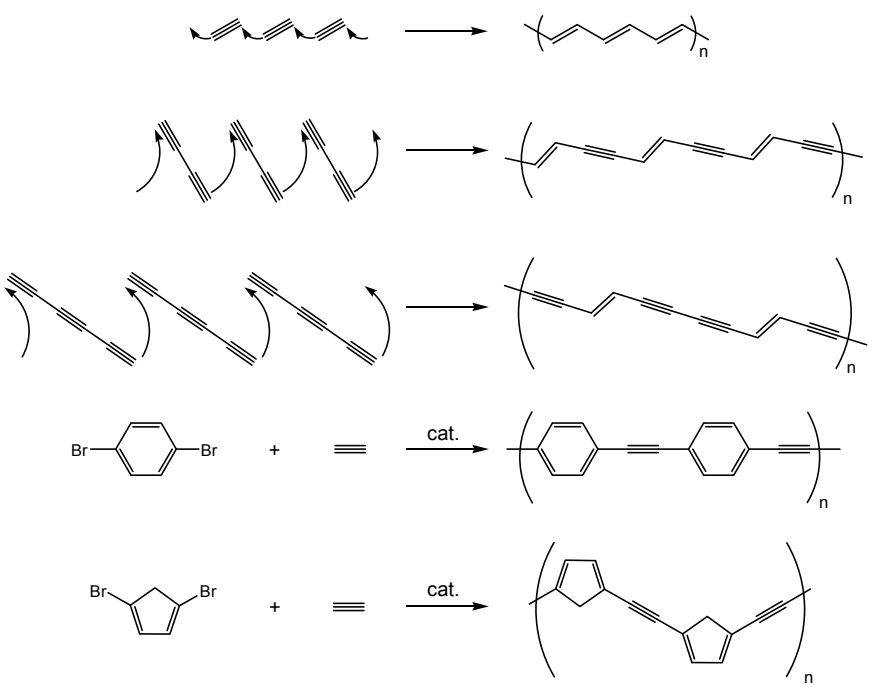

Figure 2.1: Examples of conductive polymers. They all obtain π-bond conjugation. Acetylene linkages can be formed via polymerizations.

To construct a π-bond linkage, one may apply a metal catalyzed coupling reaction to do so.[8] Another method to construct the π-bond linkage is by topochemical polymerization in solid state.[9,10] In Section 2.2 and 2.3, we shall explore these two strategies for the synthesis of acetylenic polymers, a type of conductive polymer.

2.2 Applying Metal Catalyzed Coupling Reactions to Construct Diacetylene Linkage and π-Bond Conjugated Polymers

To synthesize 1-dimensional acetylenic polymers, one straightforward strategy is to apply an oxidative coupling reaction to acetylene. Polymerization can be done via homo coupling using the Hay coupling condition, [11] or in some other cases, heterocoupling of acetylenes using the Sonogashira[12] or Cadiot-Chodkiewicz coupling conditions (Scheme 2.1). [13] Even though it is possible to achieve polymerization by using these coupling reactions, they are much more useful in synthesizing acetylene, or diacetylene linkage in a molecule.[8]

(a) Sonogashira Coupling

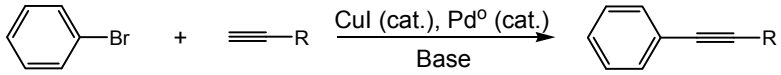

(b) Hay Coupling

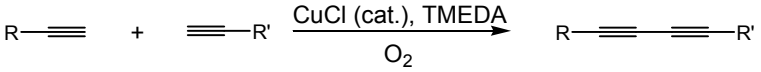

(c) Cadiot-Chodkiewicz Coupling

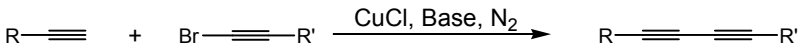

Scheme 2.1: General reaction schemes for homocoupling and heterocoupling reactions of acetylene. (a) The Sonogashira coupling condition; (b) The Hay coupling condition; (c) The Cadiot-Chodkiewicz coupling condition.

To further demonstrate the usefulness of these reaction systems, we shall explore literature examples for the application of these reactions into their synthesis of acetylenic polymers.

Taking Le Moigue and co-workers' polymer for example, they applied the Sonogashira coupling condition to synthesize their π-bond conjugated polymers **2.3** using aromatic halides and terminal alkynes as reactants (Scheme 2.2).[14] As mentioned before, however, Sonogashira coupling reaction applies more frequently in the construction of aryl alkynes, which are much more useful as building blocks for controllable polymerizations[8] or cyclization reactions.[2,3]

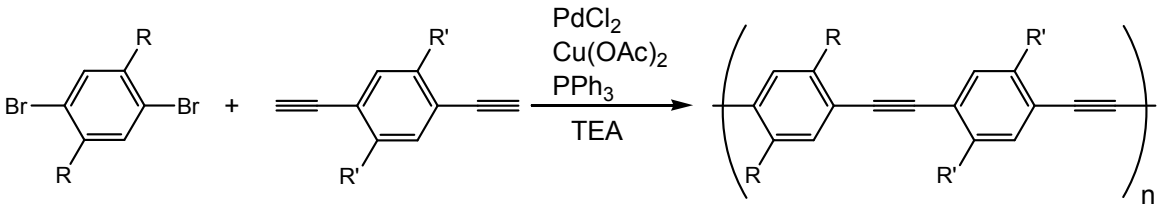

2.1 **2.2** **2.3**

R, R' = H, NO_2, alkyl ether, alkyl thioether, alkyl ester

Scheme 2.2: Polymerization step for Le Moigue's polymers. This key step is to connect the acetylene linkage by using Sonogashira coupling reaction.[14]

Diederich et. al. applied the Hay coupling condition for the synthesis of TBDMS-substituted polytriacetylene oligomers **2.6** (Scheme 2.3).[8,15,17] One of the complications, however, is that the chain growth may be uncontrollable during the reaction. The resulting crude product may be very insoluble and difficult to separate. To solve this problem, Diederich et. al. applied the protecting group strategy, originally applied by Walton et. al., in order to obtain a better control for the polymerization process.[8,16] They observed that the length of their oligomers were statistical based on the selective deprotection of the reactant before the actual homocoupling reaction, and were dependent on the ratio of the two starting materials.[8,15,17]

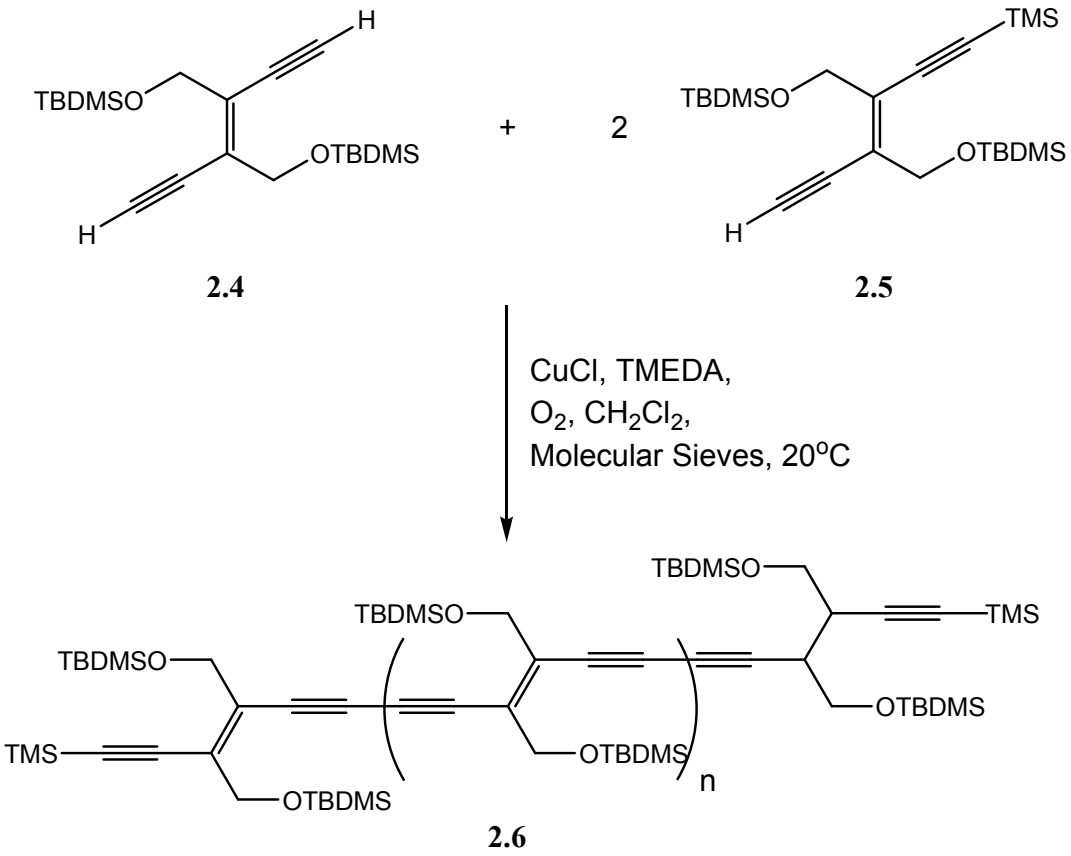

2.4 **2.5** **2.6**

Scheme 2.3: TBDMS-substituted polytriacetylene oligomer synthesized by Diederich and co-workers. TMS-protected terminal alkyne was applied for a better chain-growth control.[8,15,17]

Other research groups also obtained their desired polymers with acetylene linkages by using the Hay coupling condition. Wilson and Anderson applied this coupling condition to construct the porphyrin building blocks with diacetylene linkage (compound **2.8**) for their supramolecular polymer (Scheme 2.4).[18] Bunz et al. also employed the similar method to prepare their π-bond conjugated polymer **2.11** with interesting material properties (Scheme 2.5).[19]

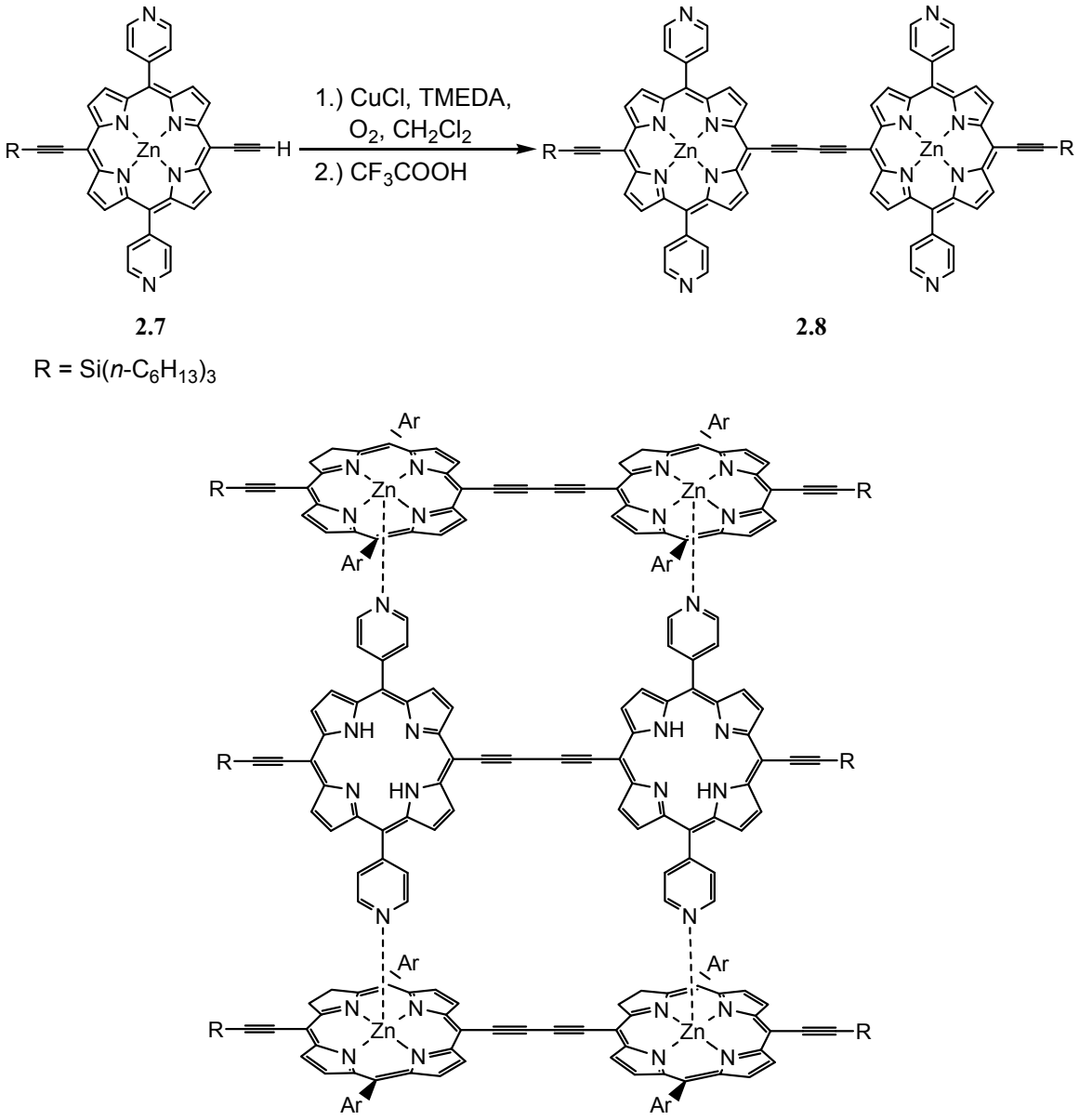

Scheme 2.4: The supramolecular polymer constructed by Wilson and Anderson that uses a porphyrin-based diacetylene as building blocks.[8,18]

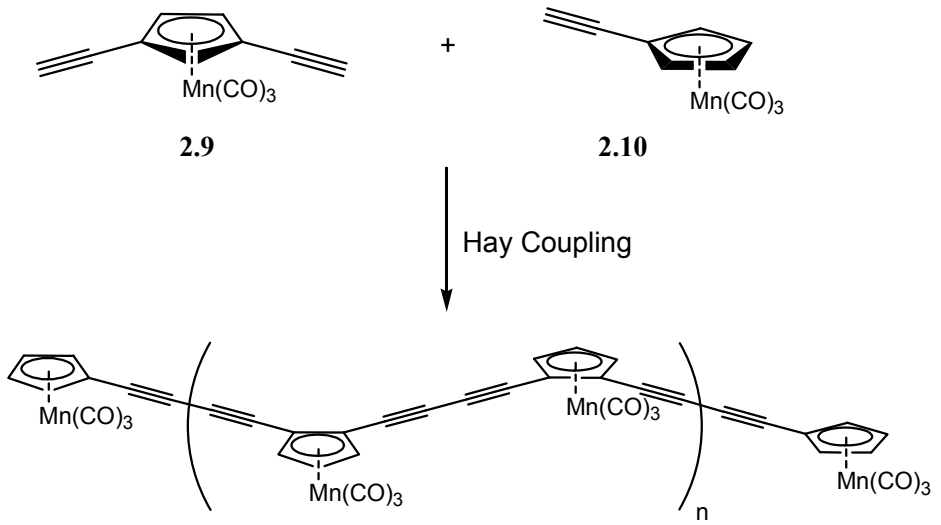

2.9 **2.10**

2.11

Scheme 2.5: Metal-coordinated diacetylenic polymer synthesized by Bunz and co-workers.[8,19]

Homocoupling reaction is also applicable for macrocycle ring closing. In many literature reports, scientists employed the Hay coupling condition for ring closing for their desired macrocycles.[8] We can also see that Tykwinski et. al. dimerized their 3,5-dialkynyl pyridine **2.12** into their desired macrocycle **2.13** as shown in Scheme 2.6.[20]

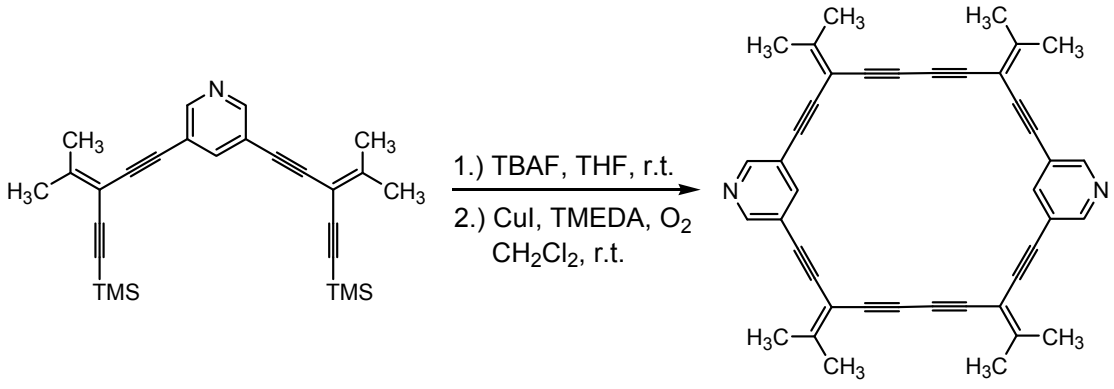

2.12 **2.13**

Scheme 2.6: Dimerization of the pyridine-based di-alkyne into a rigid macrocycle. Note that this reaction was done in high dilution. This reaction is performed by Tykwinski and co-workers.[20]

In later chapters, we will also see that the Hay coupling condition plays an important role for the ring closing reaction in the synthesis of our designed macrocycle as well in this project.

2.3 The 1,4-Polymerization of Diacetylene – Topochemical Polymerization

Another approach to synthesize acetylenic polymer is to apply topochemical polymerization in solid state. The idea of topochemistry was suggested by Kohlsvhutter[21] and the principle was established by G. M. J. Schmidt later on.[22] Schmidt developed this theory based on his observation of the dimerization of cinnamic acid derivatives in solid state. Because topochemical reaction occurs in a highly-ordered-state, the reaction has a high degree of regio- and stereo- selectivity.[21] However, one of the difficult problems for generating topochemical reaction is how to promote this type of reaction to occur in solid state, which it depends on the distance between each reactive unit.[10] Also, even though a crystal structure may change after a topochemical reaction, it should only allow a minimum amount of motion of each molecule in order to not destroying the crystal structure.[10] Therefore, to promote a topochemical reaction, the solid itself must be highly-ordered, so that reactants in the solid can line up properly. It requires a well designed intermolecular interaction network in application to supramolecular chemistry. In Section 2.4, we will introduce a technique for designing this type of supramolecular network.

To demonstrate how topochemical reaction depends on the spacing distance, we shall look at the case we will going to apply in this project: The topochemical 1,4-polymerization of diacetylene (Scheme 2.7). G. Wegner was the first scientist to polymerize diacetylene successfully by manipulating lattice structure in solid state.[9]

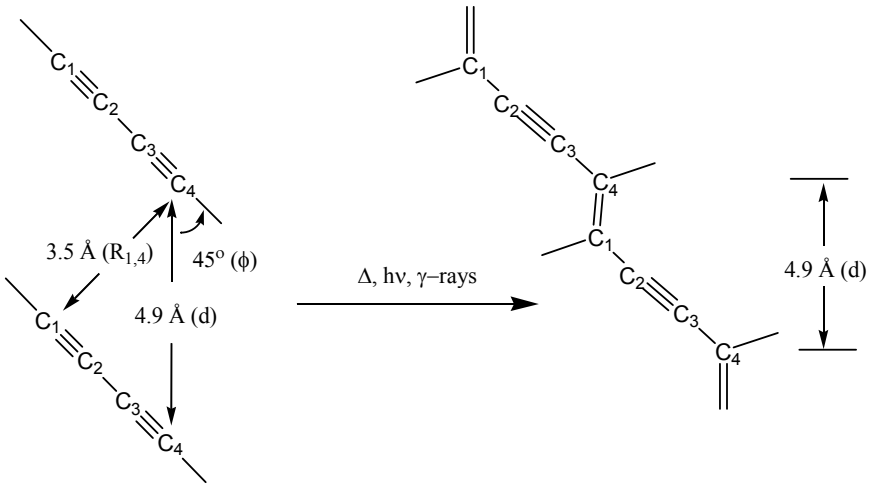

Scheme 2.7: The 1,4-topochemical polymerization of diacetylene. The C_1-C_4 distance ($R_{1,4}$) must be approximately 3.5 Å and the spacing distance (d) must be approximately 4.9 Å.

Intensive research on the 1,4-polymerization of diacetylene had lead to the understanding that the spacing distance between each diacetylene (d) is approximately 4.9 Å and the tilted angle (φ) should be approximately 45°.[10] Therefore, carbon 1 can be able to approach to carbon 4 for polymerization if they are approximately 3.5 Å apart from each other. The movement of the diacetylene unit can still be keep in minimal even though a slight change of the tilted angle (φ) will occur.

2.4 The Host-Guest Strategy, An Approach for a Proper Diacetylene Organization

How can we ensure the spacing of each diacetylene is correct? In order to obtain a correct spacing between each diacetylene unit, the diacetylene can (a): covalently bond with some functional groups that can lead to the correct spacing distance (Figure 2.2),[23] or (b): intermolecularly bind with molecules with such functional groups and form a supramolecular structure (Figure 2.3).[24]

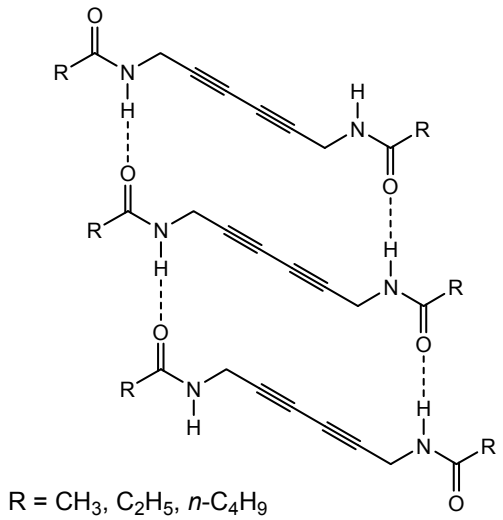

Figure 2.2: Case (a) – Hydrogen bonding network of amide substituted diacetylene, synthesized by Amano and co workers.[23]

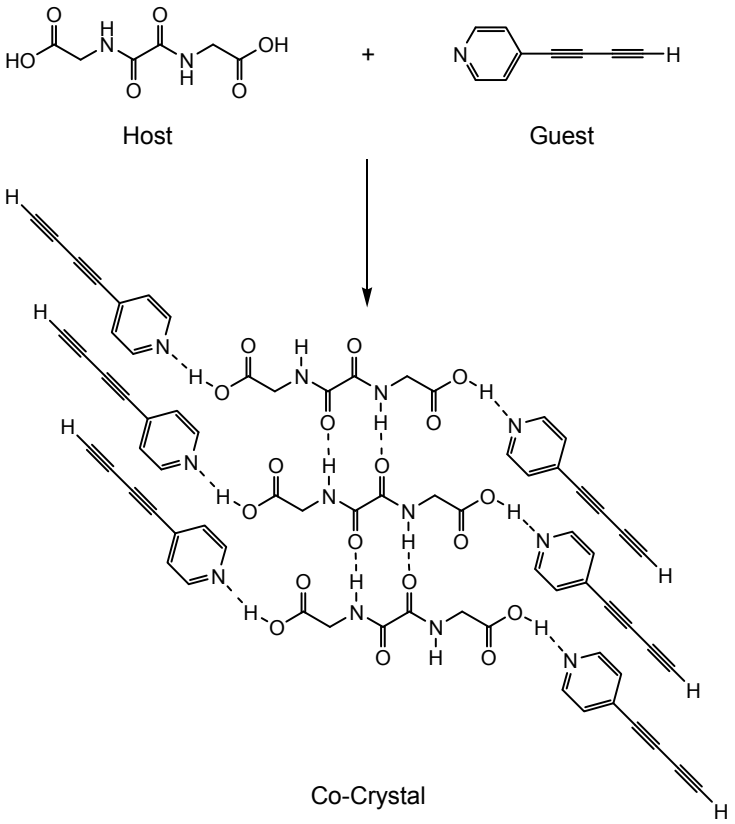

Figure 2.3: Case (b) – A co-crystal proposed by co-worker Ti Wang. The line-up of the terminal acetylenes is potentially favorable for topochemical polymerization.[25]

In case (a), a single crystal is formed and the molecule itself obtains the correct spacing for 1,4-polymerization. On the other hand, in case (b), a co-crystal is formed by involving two different molecules in a crystal structure. The spacing distance is "translated" from the functional group to the diacetylene. The functional group that leads the diacetylene to the correct distance can be named as "the host" molecule, and the diacetylene is then therefore "the guest" molecule. This strategy, introduced by our group, is called the Host-Guest Strategy.[24] The correct spacing for each diacetylene guest is obtained by binding with the host molecule via hydrogen bonding. Based on the investigations by our group, we had established a library of functional groups that provides a variety of spacing distances (Figure 2.4).[24,26]

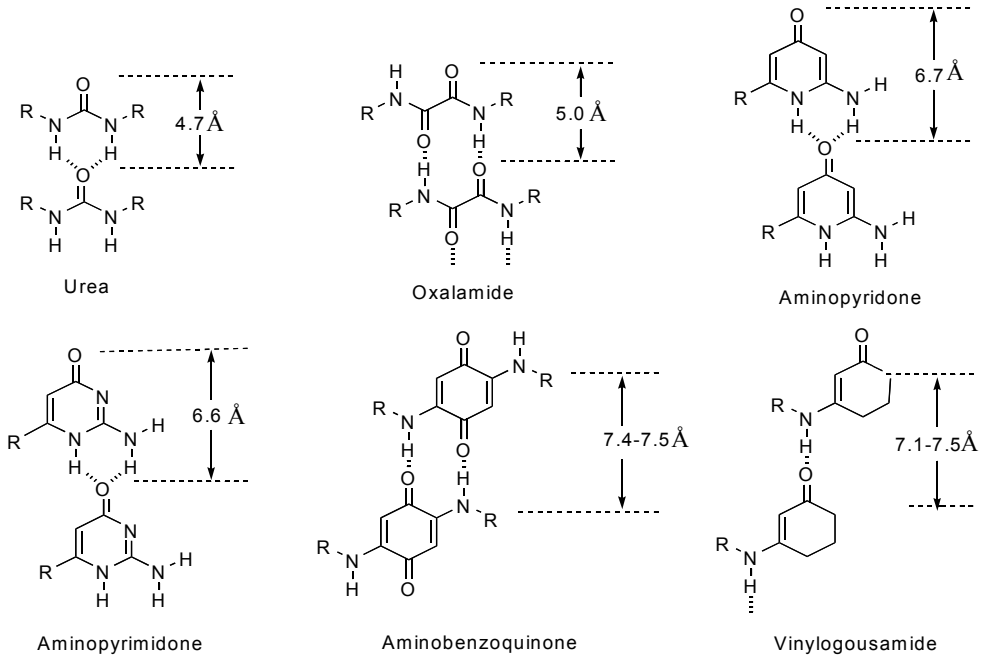

Figure 2.4: A library of host functional groups that obtain a variety of spacing distance.

The functional groups that will be useful for the 1,4-polymerization of diacetylene are urea (Spacing distance: 4.7 Å) and oxalamide (Spacing distance: 5.0 Å), because of the

spacing distance of these functional groups are close to the approximate spacing distance required for the polymerization.

2.5 The "Turn-Stile" and "Swinging-Gate" Mechanism

We have observed two types of 1,4-polymerization mechanisms in our projects: The "Turn-Stile" mechanism and the "Swinging-Gate" mechanism. Using our pervious experimental results as demonstrations, we can distinguish the difference between "Turn-Stile" and "Swinging-Gate" mechanism.

Case 1 – The "Turn-Stile" Mechanism: To prepare co-crystals with bispyridiyl-substituted diacetylene, we applied urea of glycine (Figure 2.5a) and oxalamide of glycine (Figure 2.5b) as hosts. The resulted spacing distance of the bispyridiyl-substituted diacetylene with urea of glycine host is 4.70 Å, which is a bit too short. The C_1-C_4 distance, on the other hand, is 4.12 Å, which is a bit too long. Even though this spacing distances lead to the destruction of crystal structure after the 1,4-polymerization, the application of the oxalamide of glycine host improves the result. The spacing distance and the C_1-C_4 distance in this case, is 4.97 Å and 3.38 Å, respectively.[24a]

(a)

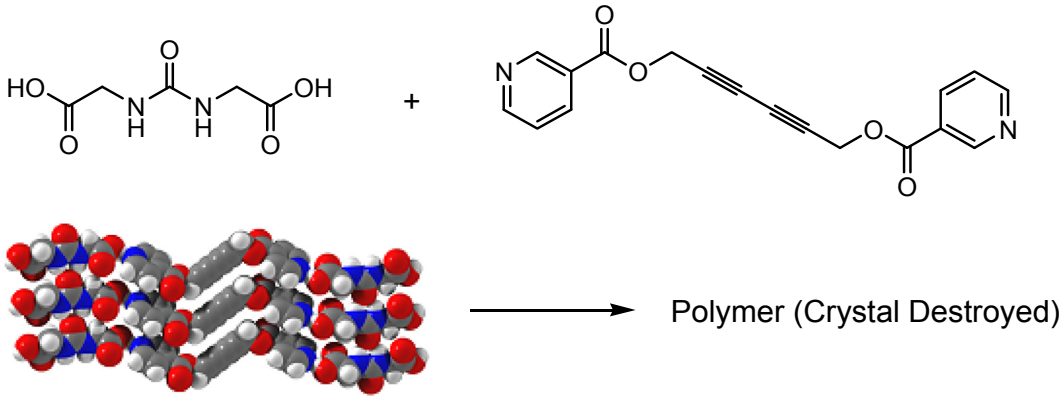

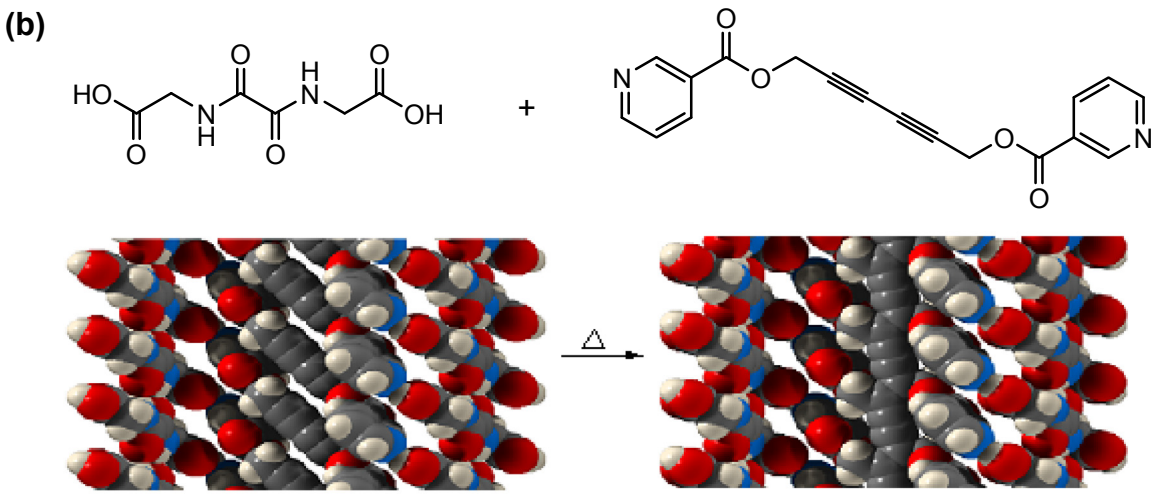

Figure 2.5: Case 1 – Two co-crystals that apply (a): the urea of glycine host, and (b): the oxalamide of glycine host. The co-crystal system (b) demonstrates the "Turn-Stile" mechanism for 1,4-polymerization.[24a]

Case 2 – The "Swinging-Gate" Mechanism: Co-crystal of 4-butadiynylbenzyl ammonium salt with oxalamide of glycine in 2:1 ratio was prepared and red crystals was observed after recrystallization. The observed repeat distance between each diacetylene is 4.94 Å. The tilted angle and the C_1-C_4 distance are 46.8˚ and 3.57 Å, respectively. With this approximately correct spacing distances and angle, the diacetylene undergoes 1,4-polymerization successfully and the movement of the aromatic ring in the guest molecules was also observed (Figure 2.6).[27]

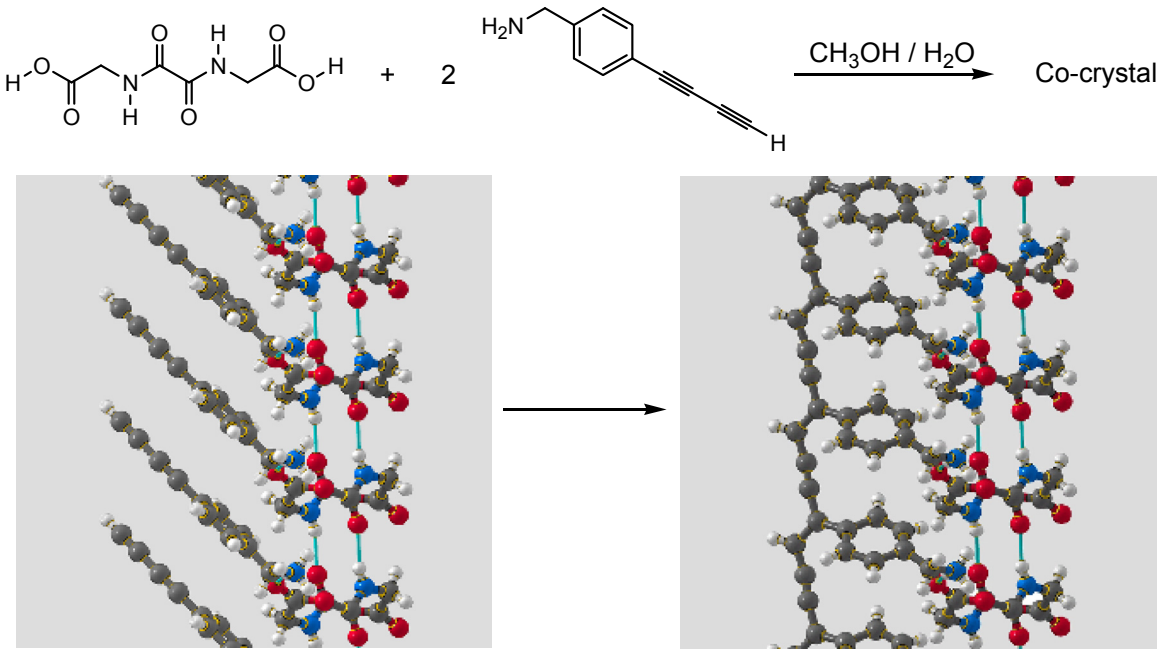

Figure 2.6: Case 2 – Co-crystal of 4-butadiynylbenzyl ammonium salt with oxalamide of glycine, done by co-worker Zhong Li. This co-crystal system promotes the "Swinging-Gate" mechanism during the 1,4-polymerization.[27]

In Case 1, we can observe the diacetylene guest molecules rotate after the 1,4-polymerization. The rotational axis is located between carbon 2 and carbon 3, which is in the middle of the diacetylene guest. This is a 1,4-polymerization that undergoes the "Turn-Stile" mechanism. This "Turn-Stile" mechanism had been observed frequently in non-terminal diacetylene guests (Figure 2.5). In Case 2, on the other hand, terminal diacetylene guest molecules undergo the "Swinging-Gate" mechanism, which the terminal acetylene guests "swing" downward in order to make the C_1-C_4 contact. The terminal carbon had moved for approximately 2.45 Å in this case (Figure 2.6). Figure 2.7 shows the general approach of how the diacetylene polymerizes under "Turn-Stile" and "Swinging-Gate" mechanism.

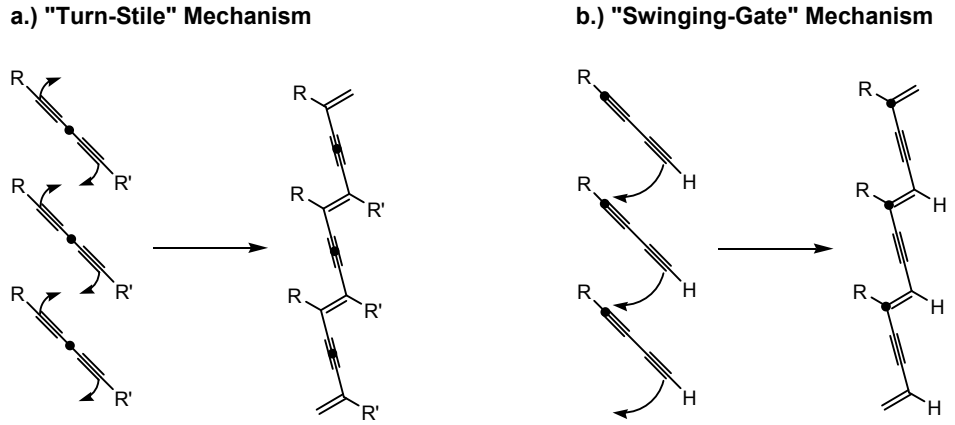

Figure 2.7: (a) The "Turn-Stile" and (b) "Swinging-Gate" mechanism for diacetylene.

2.6 Summary

Scientists have attempted to synthesize polydiacetylene because of its useful properties and its conductivity. In attempt to synthesize acetylenic polymers, metal catalyzed homocoupling or heterocoupling reactions such as Hay coupling, Sonogashira coupling, and Cadiot-Chodkiewicz coupling have been applied. These coupling reactions are also useful in synthesizing diacetylene linkages or acetylenic building blocks for crystal engineering. Other successful cases also applied topochemical polymerization to obtain polydiacetylene. Based on the aspect of solid-state polymerization, our group has developed the Host-Guest Strategy in order to obtain a correct spacing for each diacetylene guest. We have successfully polymerized the designed diacetylene guests in some of our co-crystal systems, thus have proven the concept of the Host-Guest Strategy. In the next chapter, we shall demonstrate the potential applications of the host-guest strategy into the 1,4-polymerization of our designed macrocycle building blocks. The experimental plan will therefore be introduced in the next chapter.

Endnotes:

[1] Zumdahl, S. S. Chemistry-4th Edition, Houghton Mifflin, Boston, 1997.
[2] (a) Cram, D. J.; Allinger, N. L.; Steinberg, H. *J. Am. Chem. Soc.* **1954**, *76*, 6132.; (b) Sondheimer, F.; Amiel, Y.; Wolovsky, R. *J. Am. Chem. Soc.* **1957**, *79*, 6263-6257.
[3] (a) Trost, B. M.; Rudd, M. T. *J. Am. Chem. Soc.* **2005**, *127*, 4763-4776.; (b) Dai, W.; Petersen, J. L.; Wang, K. K. *J. Org. Chem.* **2005**, *70*, 6647-6652.; (c) Basak, A.; Bag, S. S.; Majumder, P. A.; Das, A. K.; Bertolasi, V. *J. Org. Chem.* **2004**, *69*, 6927-6930.; (d) Zuercher, W. J.; Scholl, M.; Grubbs, R. H. *J. Org. Chem.* **1998**, *63*, 4291-4298.; (e) Nugent, W. A.; Thorn, D. L.; Harlow, R. L. *J. Am. Chem. Soc.* **1987**, *109*, 2788-2796.; (f) Zhou, Q.; Carroll, P. J.; Swager, T. M. *J. Org. Chem.* **1994**, *59*, 1294-1301.; (g) Son, S. U.; Yoon, Y. A.; Choi, D. S.; Park, J. K.; Kim, B. M.; Chung, Y. K. *Org. Lett.* **2001**, *3*, 1065-1067.
[4] (a) Itoh, T.; Shirakawa, H.; Ikeda, S. *J. Polym. Sci., Polym. Chem. Ed.* **1974**, *12*, 11-20.; (b) Shirakawa, H.; Louis, E. J.; MacDiarmid, A. G.; Chiang, C. K.; Heeger, A. J. *J. Chem. Soc., Chem. Comm.* **1977**, 578-580.; (c) Chiang, C. K.; Druy, M. A.; Gau, S. C.; Heeger, A. J.; Louis, E. J.; MacDiarmid, A. G.; Park, Y. W.; Shirakawa, H. *J. Am. Chem. Soc.* **1978**, *100*, 1013-1015.
[5] (a) Novak, P.; Muller, K.; Santhanam, K. S. V.; Haas, O. *Chem. Rev.* **1997**, *97*, 207-281.; (b) Pattil, A. O.; Heegar, A. J.; Wudl, F. *Chem. Rev.* **1998**, *88*, 183-200.; (c) Sailor, M. J.; Ginsburg, E. J.; Gorman, C. B.; Kumar, A.; Grubbs, R. H.; Lewis, N. S. *Science* **1990**, *249*, 1146-1149.; (d) Sailor, M. J.; Klavetter, F. L.; Grubbs, R. H.; Lewis, N. S. *Nature* **1990**, *346*, 155-157.; (e) Jozefiak, T. H.; Ginsburg, E. J.; Gorman, C. B.; Grubbs, R. H.; Lewis, N. S. *J. Am. Chem. Soc.* **1993**, *115*, 4705-4713.
[6] (a) Koopal, C. G. J.; Feiters, M. C.; Nolte, R. J. M.; de Ruiter, R. B. M. *Synth. Met.* **1992**, *51*, 397-405.; (b) McQuade, D. T.; Pullen, A. E.; Swager, T. M. *Chem. Rev.* **2000**, *100*, 2537-2574.
[7] (a) Sarkar, A.; Okada, S.; Nakanishi, H,; Matsuda, H. *Macromolecules* **1998**, *31*, 9174-9180.; (b) Sakwattanasinitt, M.; Lee, D.-C.; Kim. M.; Wang, X.; Li, L.; Kumar, J.; Tripathy, S. K.; Sandman, D. J. *Macromolecules* **1999**, *32*, 7361-7369.; (c) Sarkar, A.; Okada, S.; Matsuzawa, H.; Matsuda, H.; Nakanishi, H. *J. Mat. Chem.* **2000**, *10*, 819-828.; (d) Hide, F.; Diaz-Garcia, M. A.; Schwartz, B. J.; Andersson, M. R.; Pei, Q.; Heegar, A. J. *Science*, **1996**, *273*, 1833-1836.
[8] Siemsen, P.; Livingston, R. C.; Diederich, F. *Angew. Chem. Int. Ed.* **2000**, *39*, 2632-2657.
[9] Wegner, G. *Z. Naturforsch. (b)* **1969**, *24*, 824.
[10] (a) Enkelmann, V. Advances in Polymer Science 63 – Polydiacetylenes, Springer-Verlag, Berlin, 1984, pp91-136.; (b) Enkelmann, V. *Chem. Mater.* **1994**, *6*, 1337-1340.
[11] (a) Hay, A. S. *J. Org. Chem.* **1960**, *25*, 1275-1276.; (b) Hay, A. S. *J. Org. Chem.* **1962**, *27*, 3320-3321.
[12] (a) Sonogashira, K.; Tohda, Y.; Hagihara, N. *Tetrahedron Lett.* **1975**, 4467-4470.; (b) Takahashi, S.; Koroyama, Y.; Sonogashira, K.; Hagihara, N. *Synthesis* **1980**, *12*, 627-631.
[13] (a) Chodkiewicz, W.; Cadiot, P. *Compt. Rend.* **1955**, *241*, 1055-1057.; (b) Chodkiewicz, W. *Ann. Chim. (Paris) [13]* **1957**, *2*, 819-869.; (c) Chodkiewicz, W.; Alhuwalia, J. S.; Cadiot, P.; Willemart, A. *Compt. Rend.* **1957**, *245*, 322-324.
[14] Moroni, M.; Le Moigne, J.; Luzzati, S. *Macromolecules* **1994**, *27*, 562-571.
[15] (a) Martin, R. E.; Gubler, U.; Boudon, C.; Gramlich, V.; Bosshard, C.; Gisselbrecht, J.-P.; Günter, P.; Gross, M.; Diederich, F. *Chem. Eur. J.* **1997**, *3*, 1505-1512.; (b) Siemsen, P.; Gubler, U.; Bosshard, C.; Günter, P.; Diederich, F. *Chem. Eur. J.* **2001**, *7*, 1333-1341.
[16] (a) Eastmond, R.; Johnson, T. R.; Walton, D. R. M. *Tetrahedron* **1972**, *28*, 4601-4616.; (b) Eastmond, R.; Walton, D. R. M. *Tetrahedron* **1972**, *28*, 4591-4599.
[17] (a) Martin, R. E.; Mäder, T.; Diederich, F. *Angew. Chem.* **1999**, *111*, 834-838.; (b) Martin, R. E.; Mäder, T.; Diederich, F. Angew. *Chem. Int. Ed.* **1999**, *38*, 817-821.
[18] Wilson, G. S.; Anderson, H. L. *Chem. Commun.* **1999**, 1539-1540.
[19] (a) Bunz, U. H. F. *Synlett.* **1997**, 1117-1127.; (b) Bunz, U. H. F. *Pure Appl. Chem.* **1996**, *68*, 309-312.; (c) Bunz, U. H. F. *Top. Curr. Chem.* **1999**, *201*, 132-161.
[20] (a) Campell, K.; McDonald, R.; Branda, N. R.; Tykwinski, R. R. *Org. Lett.* **2001**, *3*, 1045-1048.; (b) Campell, K.; McDonald, R.; Tykwinski, R. R. *J. Org. Chem.* **2002**, *67*, 1133-1140.
[21] Kohlshutter, H. W. Z. *Anorg. Allg. Chem.* **1918**, *105*, 121.
[22] Schmidt, G. M. J. *Pure. Appl. Chem.* **1971**, *27*, 647-648.
[23] Kato, J.; Nakamura, K.; Yamazaki, S.; Tokushige, K, Amano, T. *J. Polym. Sci., Part A: Polym. Chem.* **1989**, *27*, 1853-1862.

[24] (a) Fowler, F. W.; Lauher, J. W. *J. Phys. Org. Chem.* **2000**, *13*, 850-857.; (b) Kane, J. J.; Nguyen, T.; Xiao, J.; Fowler, F. W.; Lauher, J. W. *Mol. Cryst. Liquid Cryst.* **2001**, *356*, 449-458.; (c) Kane, J. J.; Liao, R.-F.; Lauher, J. W.; Fowler, F. W. *J. Am. Chem. Soc.* **1995**, *117*, 12003-12004.
[25] Wang, T. M.S. Thesis (Chemistry), SUNY at Stony Brook, 2005.
[26] (a) Zhao, X. Q.; Chang, Y. L.; Fowler, F. W.; Lauher, J. W. *J. Am. Chem. Soc.* **1990**, *112*, 6627-6634.; (b) Chang, Y. L.; West, M. A.; Fowler, F. W.; Lauher, J. W. *J. Am. Chem. Soc.* **1993**, *115*, 5991-6000.; (c) Coe, S.; Kane, J.; Nguyen, T.; Toledo, L.; Wininger, E.; Fowler, F. W.; Lauher, J. W. *J. Am. Chem. Soc.* **1997**, *119*, 86-93.
[27] Li, Z. Ph.D. Thesis (Chemistry), SUNY at Stony Brook, 2008.

Chapter 3. Synthesis of Pyridine-Based Diacetylene Macrocycle and Covalent Bonded Tubular Structure (Part I) – Experimental Plan

3.1 Research Goal and Hypothesis

The goal of this project is to construct a covalently bonded tubular structure. Even though tubular structures had been constructed successfully by supramolecular means, as shown in Chapter 1, the synthesis of a tubular structure with covalent bond linkages (beside carbon nanotubes) has not been done. To achieve this goal, we will apply the 1,4-polymerization of diacetylene to connect each macrocycle covalently in solid state. We have also introduced some hydrogen bonding features into our designed macrocycles, such as the pyridine ring in **4** and **4a**, as shown in Figure 3.1. This feature will enable hydrogen bonding to other molecules either inside or outside of the macrocycles. The oxygen from these macrocycles may also contribute as hydrogen bond acceptor that can bind molecules inside these macrocycles. The benzoic acid-based macrocycle **4c**, is expected to have a hydrogen bonding network with each macrocycle unit by their carboxyl groups. Based on our design, the diacetylene linkages in the macrocycles are expected to polymerize if the spacing of each macrocycle unit is correct. The introduction of acetylenic 1,4-polymerization aspect into our designed macrocycle may also enable our covalent bonded tubular structure to obtain conductivity and optical properties. The Host-Guest strategy may also be applicable in our macrocycle project. Using an appropriate host molecule, it is possible to lead our macrocycles into the desired spacing distance either from inside (macrocycle **4**) or from outside (macrocycle **4a**) of the macrocycles.

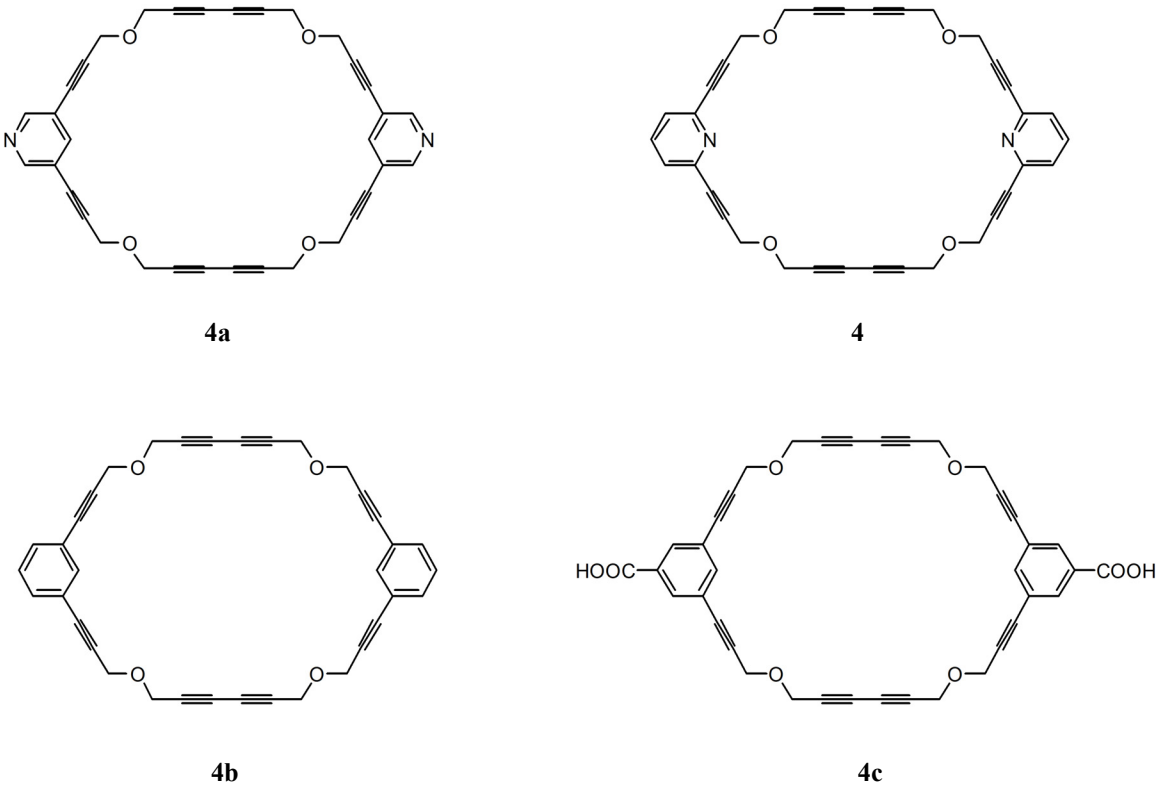

Figure 3.1: The designed macrocycles in this project.

Our designed macrocycle framework is the modified version of macrocycle **4a'**. Macrocycle **4a'** was originally proposed by Curtis. It obtains a better flexibility compare to Tykwinski's macrocycle **3.1** (Figure 3.2).[1,3] The synthetic steps of macrocycle **4a'**, which also proposed by Curtis, is start with Sonogashira coupling of 3,5-dibromopyridine with single TMS-protected 1,4-pentadiyne to give dialkyne **3a'(p)**, then Hay coupling of **3a'(p)** to give macrocycle **4a'** (Scheme 3.1).[3]

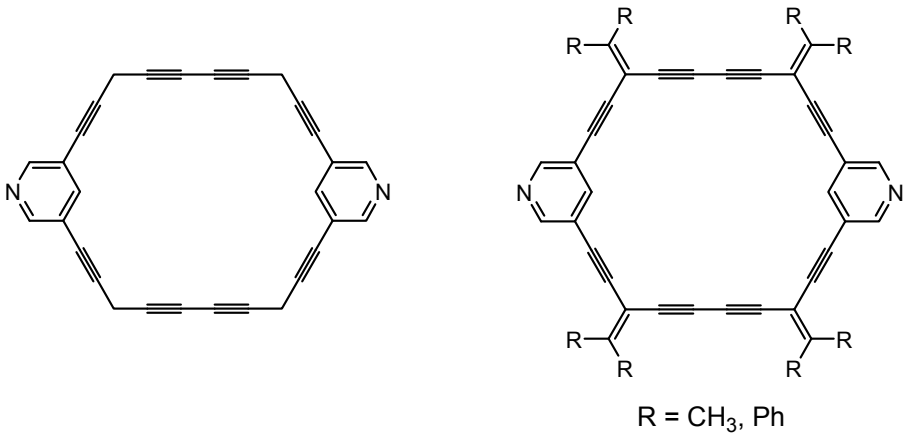

4a' **3.1**

Figure 3.2: Curtis' proposed macrocycle **4a'** in comparison to Tykwinski's macrocycle structure **3.1**.

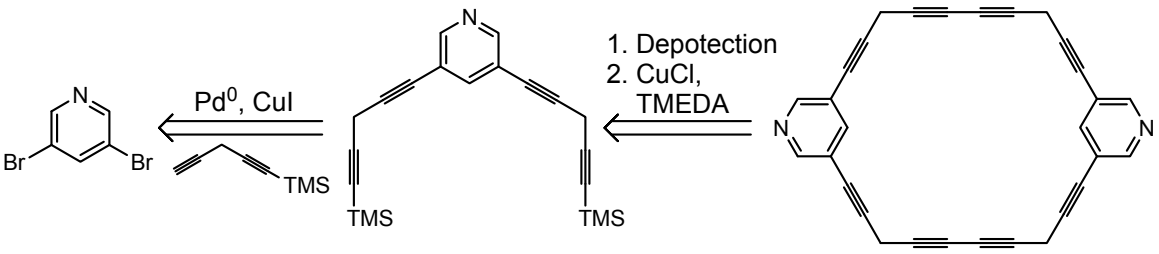

1a **3a'(p)** **4a'**

Scheme 3.1: General scheme for the synthesis of macrocycle **4a'**, proposed by co-worker Sean Curtis.[3]

However, the synthesis of macrocycle **4a'** was difficult. Direct coupling of 3,5-dibromopyridine with single TMS-protected 1,4-pentadiyne under Sonogashira coupling condition was not successful. Curtis hypothesized that an undesired cyclization by-product from single TMS-protected 1,4-pentadiyne was formed during the reaction, which based on a literature that reported a similar observation.[2,3] Further modification of synthetic route to dialkyne **3a'(p)** was also not helpful on synthesizing macrocycle **4a'**. Alkylation of **1a(t)** with TMS-protected propargyl bromide for dialkyne **3a'(p)** was not

successful (Scheme 3.2).[3] Being discouraged by the synthetic attempt for synthesizing macrocycle **4a'**, Curtis later on modified the structure of macrocycle **4a'** to macrocycle **4a**, and proposed the synthetic route for macrocycle **4a**, which we will also apply in this project (Scheme 3.4).[3]

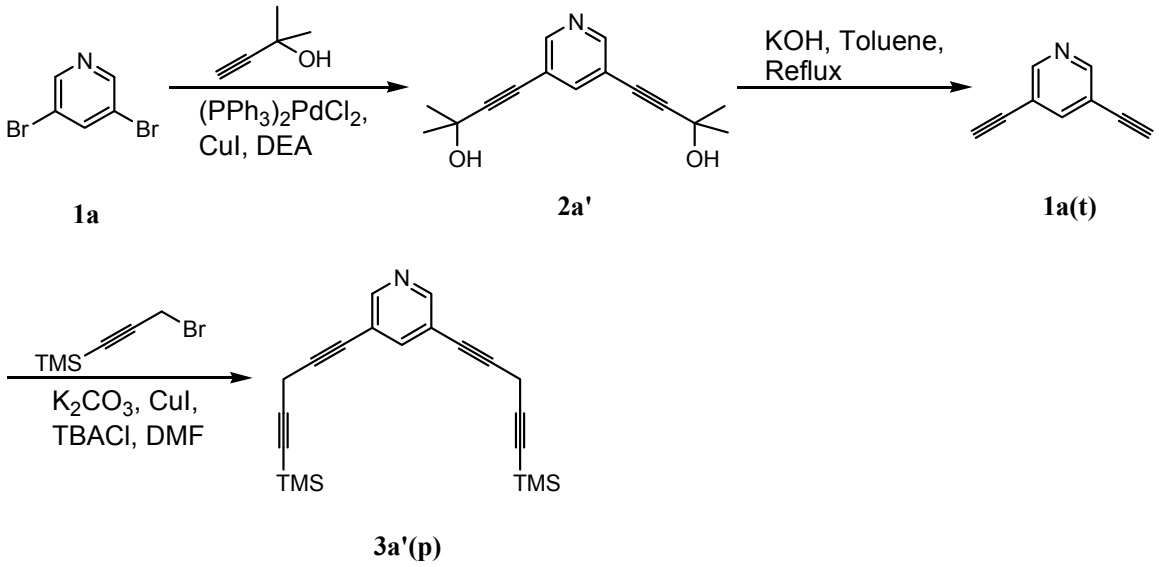

Scheme 3.2: Modified steps for the synthesis of **3a'(p)**. Synthesis was carried on by co-worker Sean Curtis.[3]

Macrocycle **4a** was successfully synthesized by Curtis, and later on repeated by Wang.[3,4] The crystal structure of macrocycle **4a** has also been confirmed by X-ray crystallography.[3,4] Based on the X-ray crystallographic analysis, both Curtis and Wang concluded that the spacing distance of each macrocycle **4a** was only 4.134 Å and the contact distance was 4.293 Å, which was not favorable for the 1,4-polymerization by itself (Figure 3.3).[3,4] An attempt to apply the host-guest strategy for correcting the spacing distance is still in trail and error process, which Wang had reported an unsuccessful attempt to form a co-crystal of macrocycle **4a** with an appropriate host.[4] In

Scheme 3.1, the hypothesis of the formation of co-crystal system with an appropriate host (oxalamide for example) and our designed macrocycle (macrocycle **4a** for example) is shown. It is hypothesized that the proposed co-crystal system may "correct" the spacing of macrocycle **4a** and may lead to a potential 1,4-polymerization (Scheme 3.3). Color change of the co-crystal system is also expected because of a distinctive color obtained by polydiacetylene.[5]

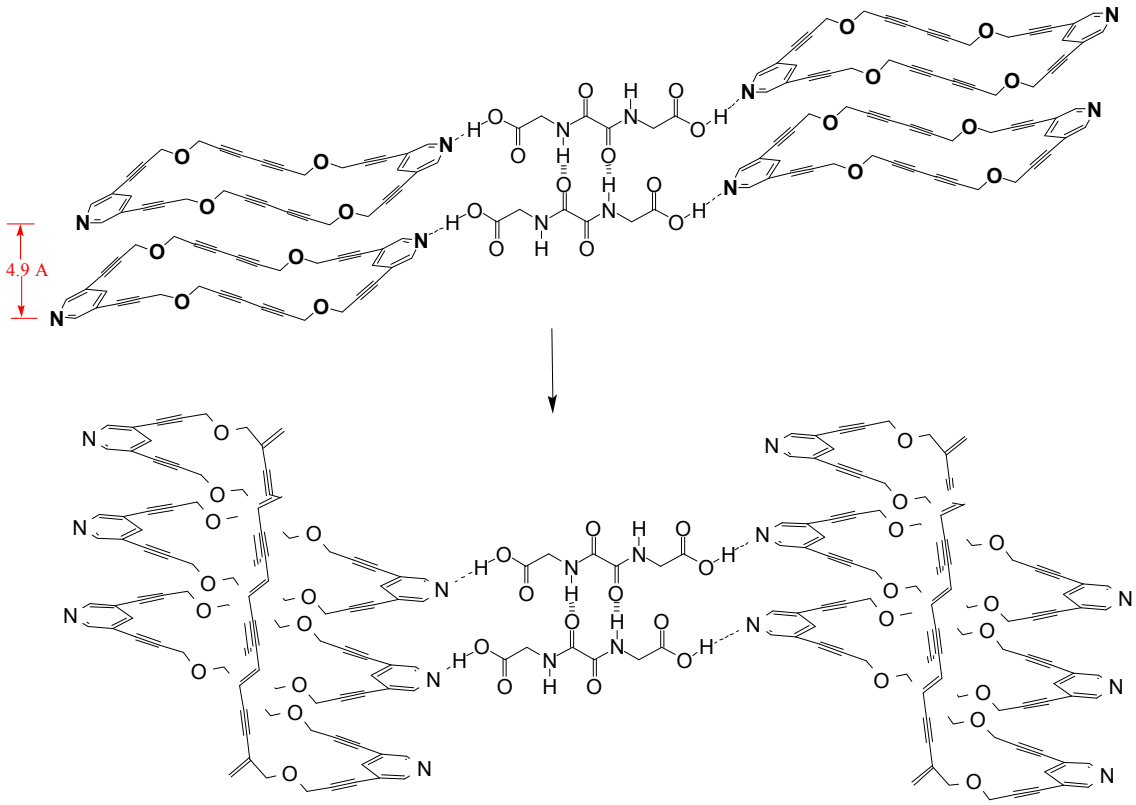

Scheme 3.3: The expected 1,4-polymerization of diacetylene macrocycle **4a** under co-crystal with oxalamide of glycine.

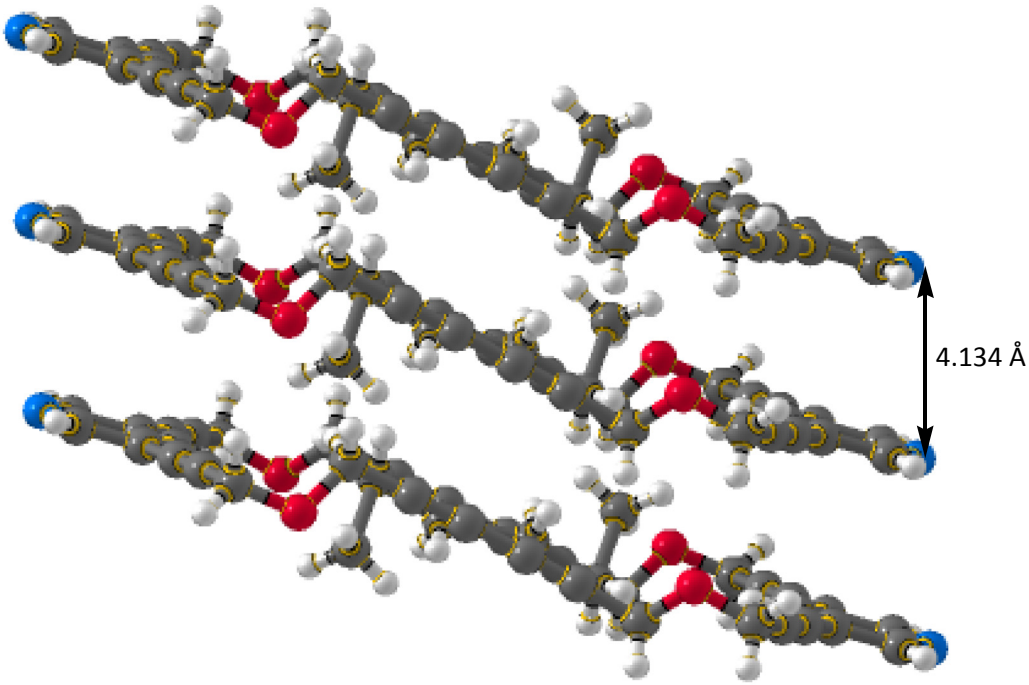

Figure 3.3: The single crystal structure of macrocycle **4a** (with hexane trapped inside the macrocycle), which the spacing distance of each macrocycle unit is only 4.13 Å.

3.2 The Planned Synthetic Route to Pyridine-Based Diacetylene Macrocycles

The general scheme for the synthesis of our pyridine-based diacetylene macrocycles **4**, **4a**, and **4b** are shown in Scheme 3.4.

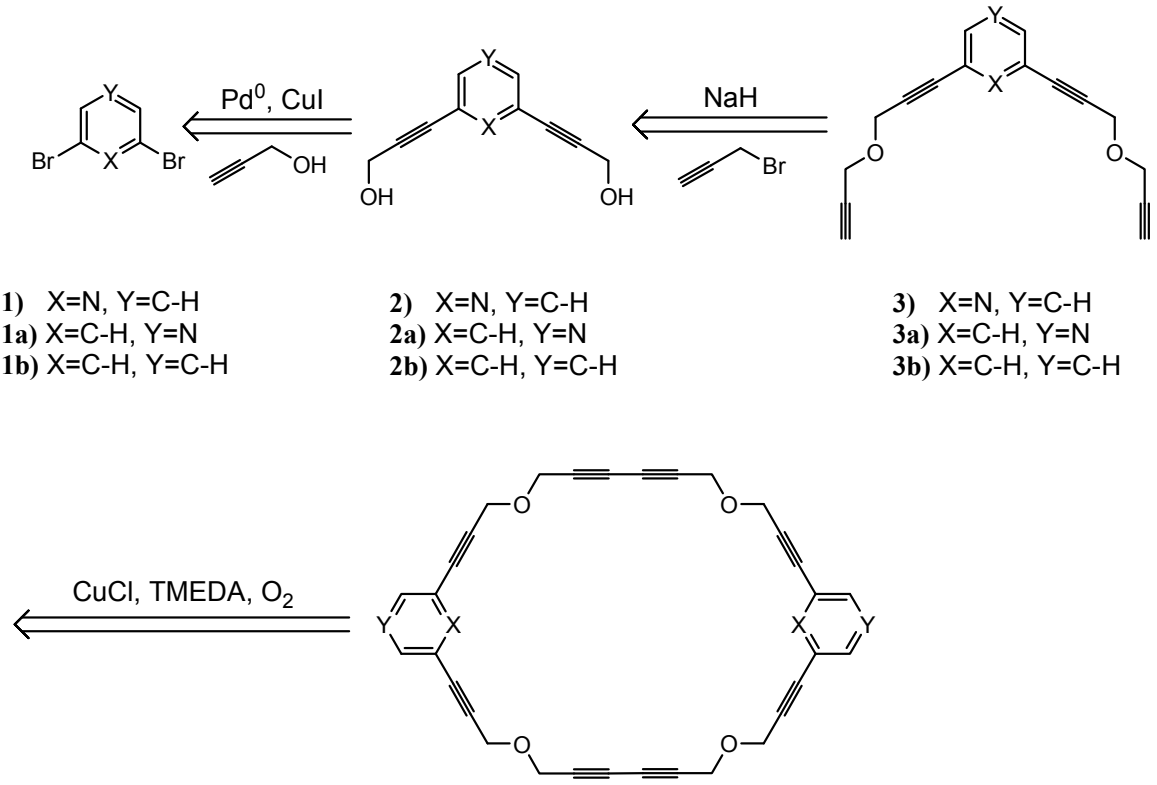

1) X=N, Y=C-H
1a) X=C-H, Y=N
1b) X=C-H, Y=C-H

2) X=N, Y=C-H
2a) X=C-H, Y=N
2b) X=C-H, Y=C-H

3) X=N, Y=C-H
3a) X=C-H, Y=N
3b) X=C-H, Y=C-H

4) X=N, Y=C-H
4a) X=C-H, Y=N
4b) X=C-H, Y=C-H

Scheme 3.4: General scheme for the synthesis of pyridine based diacetylene macrocycle **4**, **4a**, and **4b**.

In general, 2,6-dibromopyridine **1** will couple with propargyl alcohol under the Sonogashira coupling condition to afford pyridyl diol **2**. Then, **2** react with propargyl bromide to yield to pyridyl diether **3**. Diether **3** then undergoes dimerization under Hay coupling condition in high dilution to yield to the desired pyridine-based diacetylene macrocycle **4**.

For the synthesis of macrocycle **4c**, on the other hand, cannot directly follow the general scheme shown in Scheme 3.2 in order to prevent addition of propargyl bromide

into the carboxyl group in 3,5-bis-(3-hydroxy-1-propynyl) benzoic acid, the carboxylic acid form of **2c(p)**. Therefore, a specific synthetic route for macrocycle **4c** is proposed (Scheme 3.5). The preparation of diol **2c(p)** and the ester cleavage from macrocycle **4c(p)** to macrocycle **4c** will follow the procedure accomplished by Blencowe et. al.[6]

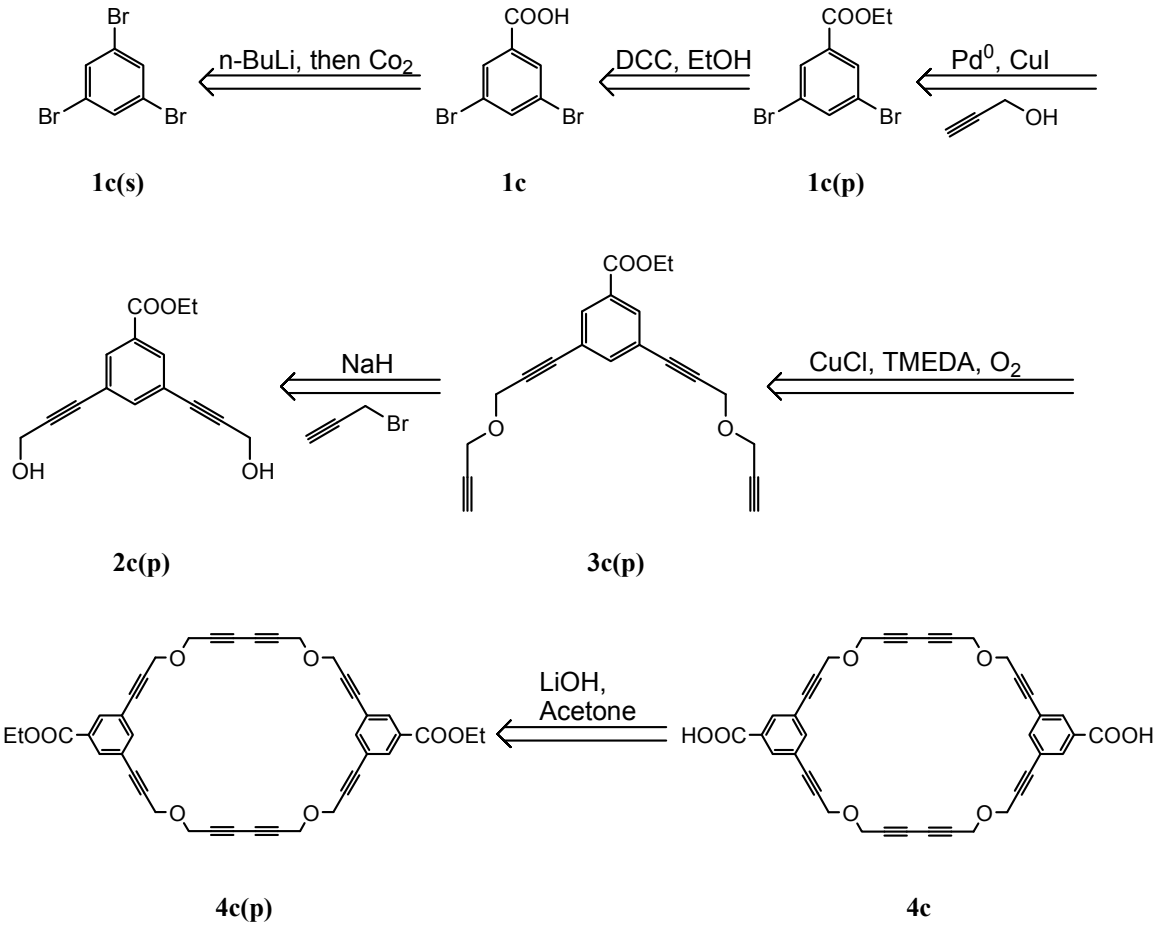

Scheme 3.5: General scheme for the synthesis of macrocycle **4c**.

Macrocycle **4b** and **4c** are still under development by co-workers Guevara, and Burrows and Choi, respectively.[7,8] Guevara had successfully synthesized macrocycle **4b** as a crude product while a defined ^{1}H-NMR spectrum for **4b** has yet to be done.[7] On the other hand, the synthesis of macrocycle **4c** is still underway.[8]

Therefore, this thesis report will mainly focus on the synthesis of macrocycle **4**. This macrocycle is expected to be much more hydrophobic then macrocycle **4a** based on the nitrogen position in the pyridine in the macrocycle. Even though changes were made during the actual synthesis, the synthetic route of macrocycle **4** is identical to **4a**. Despite the success of the synthesis of macrocycle **4a** using the synthetic route shown in Scheme 3.4, the actual synthesis of macrocycle **4** is proven to be difficult. Therefore an alternative route has been proposed and implemented. The actual synthesis of macrocycle **4** and its alternate route will be further discussed in the next chapter.

Endnotes:

[1] (a) Campell, K.; McDonald, R.; Branda, N. R.; Tykwinski, R. R. *Org. Lett.* **2001**, *3*, 1045-1048.; (b) Campell, K.; McDonald, R.; Tykwinski, R. R. *J. Org. Chem.* **2002**, *67*, 1133-1140.
[2] Tan, D. S.; Foley, M. A.; Stockwell, B. R.; Shair, M. D.; Schreiber, S. L. *J. Am. Chem. Soc.* **1999**, *121*, 9073-9087.
[3] Curtis, S. M. Ph.D. Thesis (Chemistry), SUNY at Stony Brook, 2003.
[4] Wang, T. M.S. Thesis (Chemistry), SUNY at Stony Brook, 2005.
[5] (a) Enkelmann, V. Advances in Polymer Science 63 – Polydiacetylenes, Springer-Verlag, Berlin, 1984, pp91-136.; (b) Enkelmann, V. *Chem. Mater.* **1994**, *6*, 1337-1340.
[6] Blencowe, A.; Davidson, L.; Hayes, W. *Eur. Polym. J.* **2003**, *39*, 1955-1963.
[7] Guevara, R. REU Research Report (Chemistry), SUNY at Stony Brook, 2007.
[8] Burrows, N. REU Research Report (Chemistry), SUNY at Stony Brook, 2006.

Chapter 4. Synthesis of Pyridine-Based Diacetylene Macrocycle and Covalent Bonded Tubular Structure (Part II) – Result and Discussion

4.1 Molecular Synthesis

Curtis and Wang have synthesized the 3,5-pyridine based macrocycle **4a** by first, Sonogashira coupling reaction with 3,5-dibromopyridine and propargyl alcohol, then, a propargyl group addition, and finally, the Hay coupling reaction for dimerization (Scheme 4.1).[1,2] In the first attempt for the synthesis of 2,6-pyridine-based macrocycle **4**, same synthetic route was applied (Scheme 4.2).

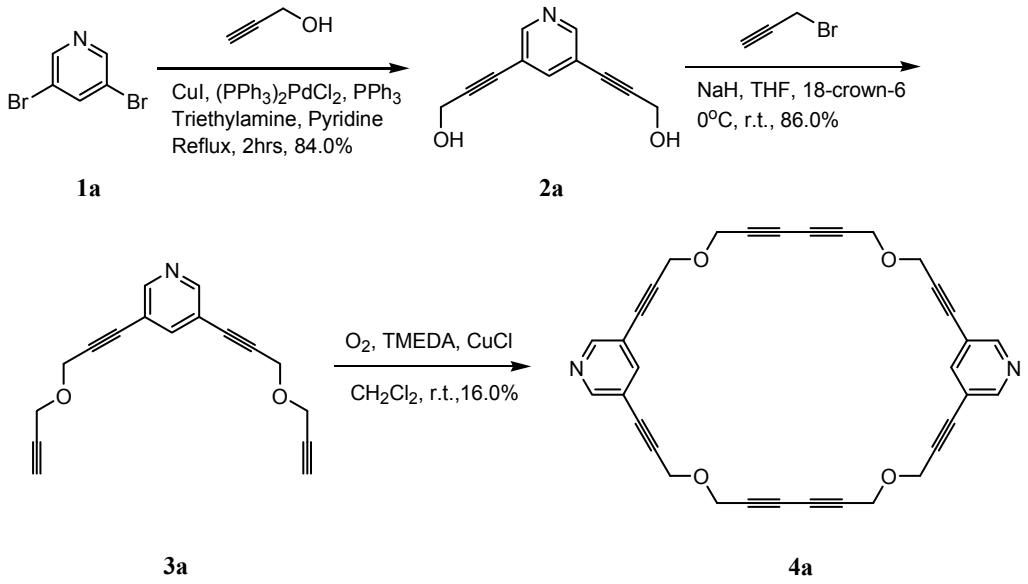

Scheme 4.1: The synthesis steps of 3,5-pyridine-based macrocycle **4a**. The synthesis was carried out by co-worker Curtis and Wang.[1,2]

In the synthesis steps of 3,5-pyridine-based macrocycle **4a**, based on the earlier results obtained from Curtis and Wang, the most difficult step is the dimerization from diether **3a** to macrocycle **4a**. Diether **3a** underwent cyclization with itself and formed a [1 + 1]

product (the monomer). It also formed a trimer or a tetramer.[1,2] Even so, the desired product **4a** was the major product despite of such complication. The yield of macrocycle **4a**, however, was unsatisfactory.

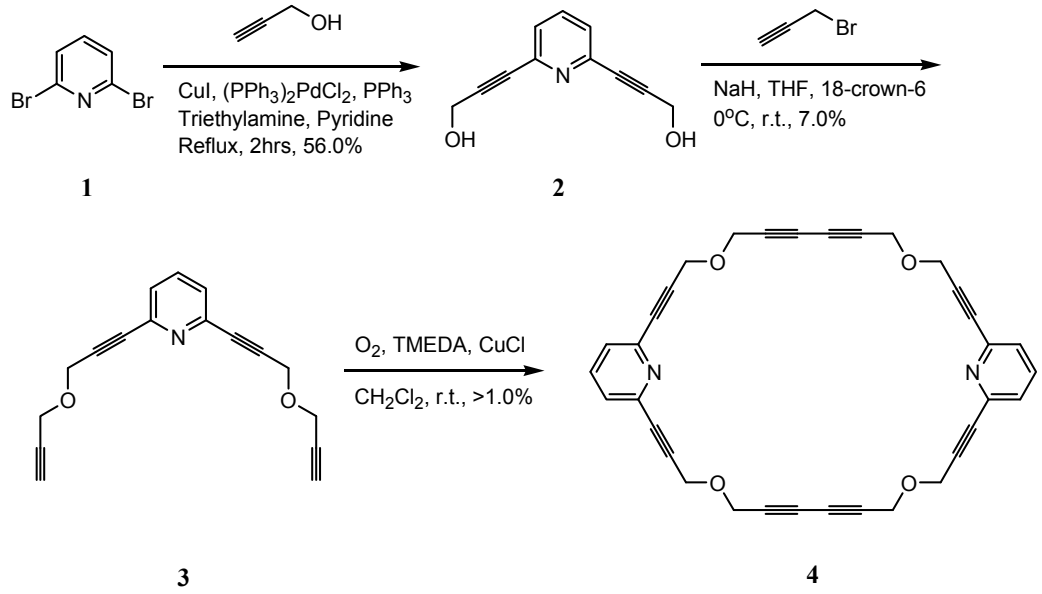

Scheme 4.2: The first synthetic steps of 2,6-pyridine-based macrocycle **4**.

In the case on the synthesis of 2,6-pyridine-based macrocycle **4**, the yield for the formation of diol **2** via the coupling of propargyl alcohol with 2,6-dibromopyridine **1** was moderate, but still acceptable. The purification process had become one of the major difficulties for this reaction because the formation of by-products are very likely under the Sonogashira coupling condition, and it was very likely to yield undesired homo-coupled by-products.[3] In attempt to solve this problem, a modified coupling system introduced by Liang et. al.[4] was applied in this case (Scheme 4.3). Even though the purification problem had been solved, the yield of this reaction was about the same as the pervious reaction system.

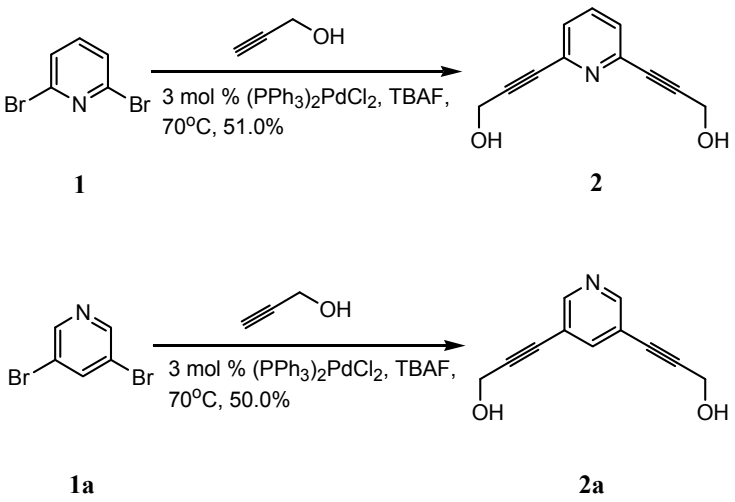

Scheme 4.3: The copper-free Sonogashira coupling reaction system applies in the coupling of 2,6-dibromopyridine **1** and 3,5-dibromopyridine **1a** with propargyl alcohol.[4]

The propargyl group addition that forms **3** also gave an unsatisfactory result. The total yield for this reaction was lower then 20%. Even though 18-crown-6 was used in order to trap the sodium cation and increase the nucleophilicity of dialkoxide form of **2**,[1,2] the reaction still was not as efficient as the conversion from **2a** to **3a**. Therefore, a direct Sonogashira coupling of 2,6-dibromoryridine with propargyl ether was attempted. Even though undesired side products were unpreventable, **2** were produced efficiently with a moderate yield (Scheme 4.4). The reaction time was also shortened, only requires approximately 45 minutes to 1 hour to complete the reaction. The purification of crude product **2** via column chromatography was much better then the purification of crude product **1**. An attempt to optimize the yield for this reaction by replacing the co-solvent pyridine with THF enhanced the yield by 10%.

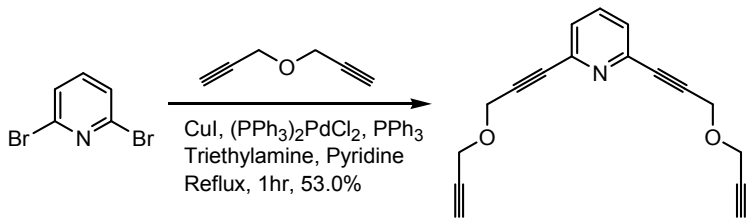

1 **3**

Scheme 4.4: Sonogashira coupling of 2,6-dibromopyridine with propargyl ether using standard reaction system.

The crude product obtained from the dimerization of **3** via the Hay Coupling condition is insoluble in common solvents. The only isolatable product, however, is an intermolecular cyclization product **4(m)** (Scheme 4.5). The yield of this macrocyclic monomer, however, was roughly 10%. The structure of **4(m)** was later confirmed by X-ray crystallographic analysis (See Section 4.3). The desired 2,6-diacetylene-based macrocycle **4**, on the other hand, was obtained in only a trace amount and was insufficient to obtain a meaningful ^{1}H-NMR spectrum. Direct recrystallization using hexane/ethyl acetate mixture from crude product after the removal of solvent was also unsuccessful. The insoluble residue, is hypothesized to be the oligomers.

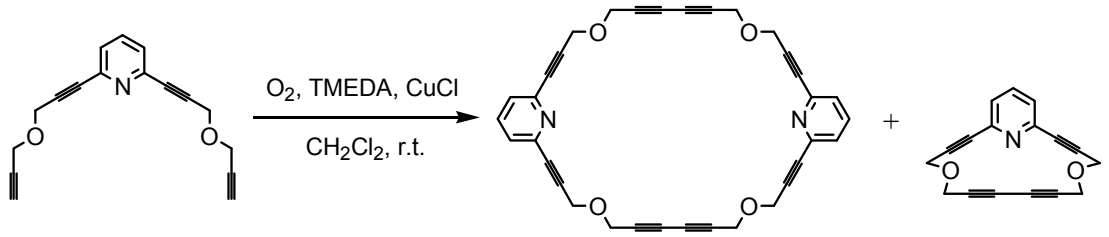

3 **4** >1.0% **4(m)** 4.4%

Scheme 4.5: Homocoupling of **3** via Hay coupling condition. The major product in this reaction was **4(m)**.

Compare to the dimerization of **3a** using the same condition, the formation of macrocycle **4a** was more favorable then macrocycle **4**. The inner nitrogen in the pyridine ring may be the reason that affects the reaction mechanism during the Hay coupling reaction. It is hypothesized that the coordination of cooper metal with pyridine nitrogen in **3** favored intramolecular cyclization and formed the [1 + 1] product **4(m)**. An attempt to increase the dimerization probability by using $1/10^{th}$ of the original amount (25ml) was also not successful, which most of **3** polymerized and neither the presence of **4(m)** or **4** were detected after the reaction.

4.2 Alternate Synthetic Steps

Since the direct coupling of **3** was facing complications, an alternate route that leads to the desired 2,6-pyridine-based macrocycle **4** was developed in attempt to avoid such difficulties (Scheme 4.6).

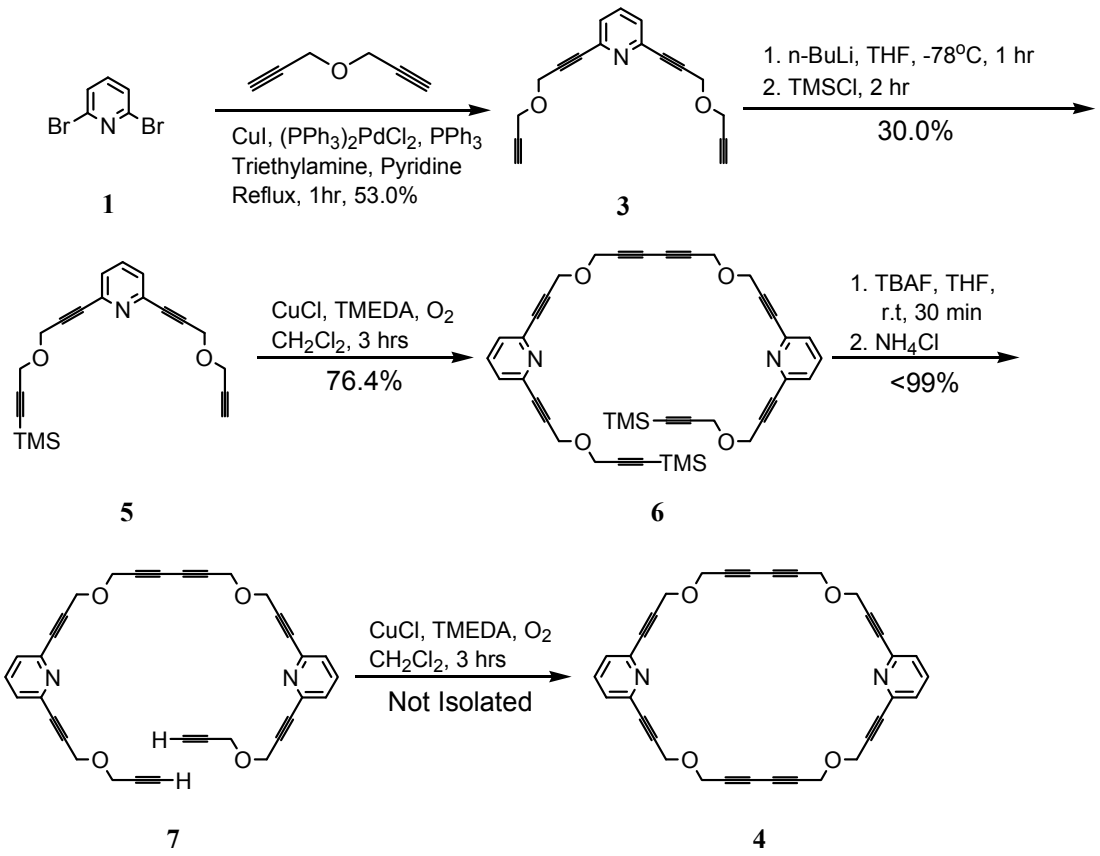

Scheme 4.6: The alternative synthetic route for the synthesis of 2,6-pyridine-based macrocycle **4**.

The advantage of this new synthetic route is that it can prevent the mono-cyclization by protecting one side of the terminal alkyne. The dimerization of the single protected diether **3** (compound **5**) via Hay coupling can be proceeded without any undesired side products. Even though high dilution will still be needed for the second homo coupling of **7** into **4**, this mono-cyclization should be more favorable while probability of polymerization can be reduced by excess solvent.

The regio-control of single protection of **3** was difficult and the yield of **5** was statistical. Even though the percent yield of **5(d)** was more then the percent yield of **5**

despite of the amount equivalence of base added for the reaction, the percent yield of **5** was moderate but it was still sufficient to go on for the next reaction (Scheme 4.7).

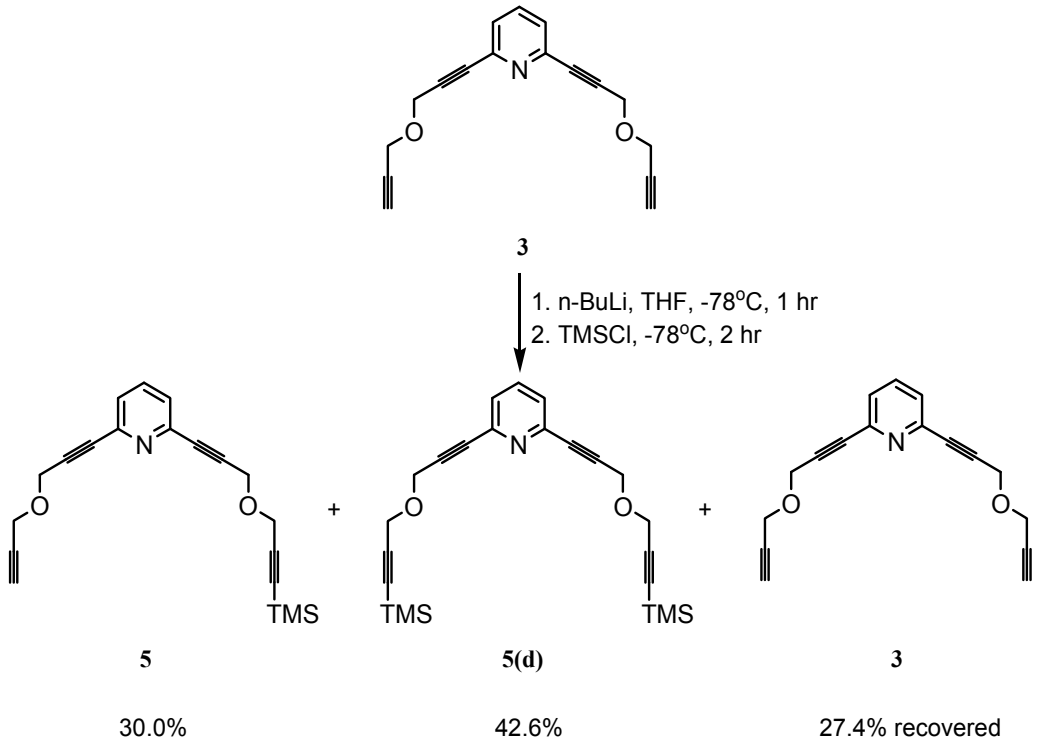

Scheme 4.7: Reaction scheme for the terminal alkyne protection. The reaction is not yet optimized.

The first homo-coupling from **5** to **6** via the Hay coupling condition was very successful. Using 10 mol. equivalent of CuCl as the catalyst, the reaction proceeded very smoothly and 76% yield was obtained. After the first homo coupling, deprotection of TMS group using TBAF was carried out in quantitative yield. The deprotected diether dimer **7** was expected to be less stable then protected dimer **6**; however, its ^{1}H-NMR spectrum had showed that no significant changes of peaks after dimer **7** had stored in the vial in room temperature for a period of time. Deprotected diether dimer **7** can be purified by recrystallization with methanol. Even though the purified **7** exists as a white solid,

crystal analysis of **7** has not yet been obtained because the quality of the solid product was not suitable for X-ray crystallographic analysis. Therefore, compound **7** was characterized by only ^{1}H-NMR and ^{13}C-NMR.

The second homo coupling reaction was not as smooth as expected. The crude product of this coupling reaction is insoluble in common solvents. Therefore, it is extremely difficult to obtain a well-defined ^{1}H-NMR spectrum. Based on the current observations, it is unfortunately still not clear if the second Hay coupling reaction is either a success or a failure.

In an attempt to dissolve the insoluble residue in the crude product, acetic acid and trifluoroacetic acid were used as solvent. The reason for using these acids as solvent is to use the hydrogen bonding inside the macrocycle in order to enhance the solubility. This attempt was also unsuccessful while the insoluble residue remains and was not soluble in either acetic acid or trifluoroacetic acid.

4.3 Crystal Structure Analysis and Comparison

Even though a pure sample of macrocycle **4** has yet to be obtained for its single crystal structure by X-ray crystal analysis, the [1 + 1] side product **4(m)** had been analyzed via-X-ray crystallography. The **4(m)** crystal was obtained by recrystallization with hexane and ethyl acetate. The crystal is needle-like and colorless. After X-ray crystallographic analysis, the analyzed structure had shown that the single crystal structure of [1 + 1] side product **4(m)** has a C_2/c space group. The single crystal structure of **4(m)** is shown in Figure 4.1a. For comparison, the crystal structure of previously made 3,5-pyridine-based [1 + 1] side product **4a(m)**, is also shown in Figure 4.1b.[2] To compare

their space group and their unit cells' dimension, unit cell parameters of these macrocycles are shown in Table 4.1.

Cyclic Monomer	*a* (Å)	*b* (Å)	*c* (Å)	*α*	*β*	*γ*	Space Group	Cross Section (Å^2)
4(m)	15.5098	10.0215	8.8020	90.00	102.14	90.00	C2/c	8.859 × 3.702
4a(m)	4.1345	28.0533	11.6880	90.00	90.12	90.00	$P2_1/c$	9.034 × 2.763

Table 4.1: Unit cell parameters for [1 + 1] side products **4(m)** and **4a(m)**. The cross section of macrocycle **4(m)** is measured from nitrogen to the middle acetylenic carbon; The cross section of macrocycle **4a(m)** is measured from the inner hydrogen to the middle acetylenic carbon.

Based on this comparison, the cross section area of **4(m)** is larger then **4a(m)**. Even so, no solvent molecules were trapped inside the macrocycle in either case, as shown in both Figure 4.1a and Figure 4.1b.

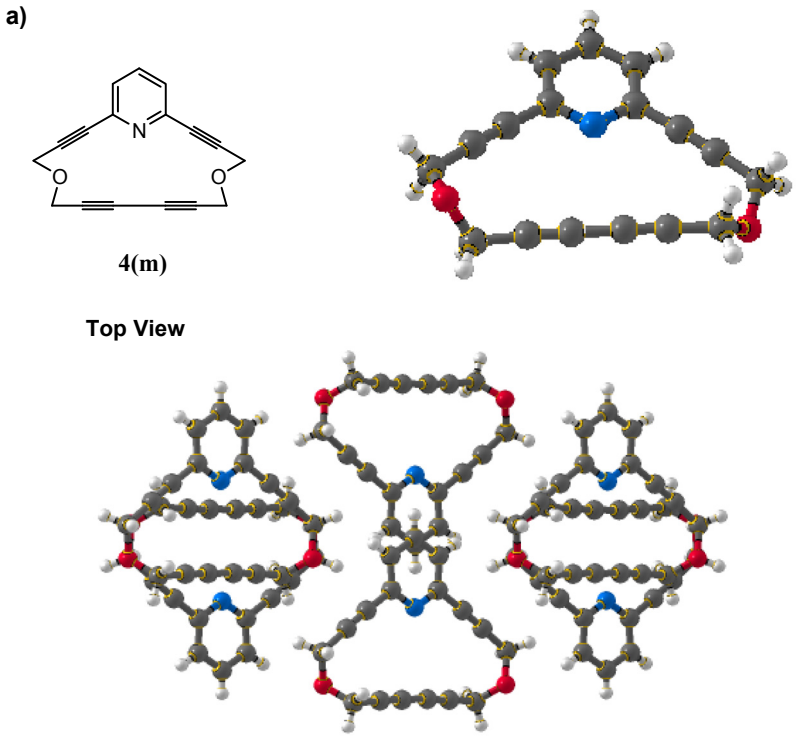

Side View:

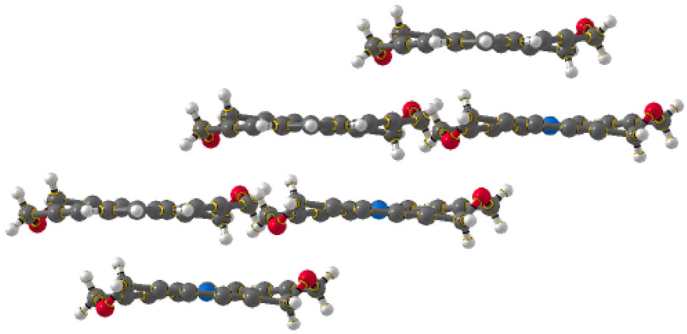

Figure 4.1a: Crystal structure of 2,6-pyridine-based macrocycle monomer **4(m)**.

b)

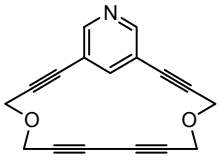

4a(m)

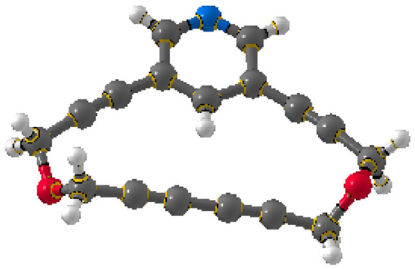

Top View:

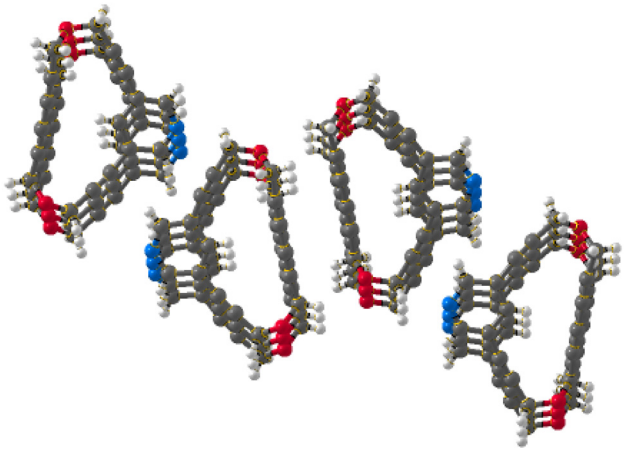

Side View:

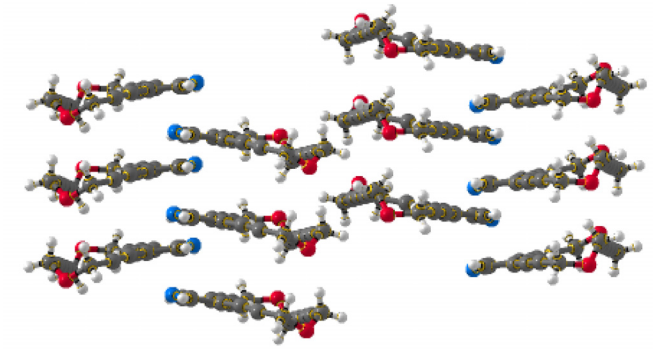

Figure 4.1b: Crystal structure of 3,5-pyridine-based macrocycle monomer **4a(m)**.[2]

The organization patterns of these macrocyclic side products are also interesting. By switching the position of the nitrogen atom in the pyridine ring, their organization pattern has been significantly changed. The intermolecular interaction that organizes these macrocycle is mainly by π-π stacking interaction. In the case of **4(m)**, as shown in Figure 4.2a, each macrocycle building block stacks in an alternating pattern. Therefore, no tubular structure is observed in this case. Because they do not stack on top of each other, there is no proper diacetylene line-up. The spacing distance between each macrocycle building block is approximately 3.666 Å (Figure 4.2). On the other hand, previously synthesized **4a(m)**, also shown in Figure 4.2, obtains a proper diacetylene line-up while these macrocycle building blocks stacks on top of each other. However, the spacing distance is too short (4.134 Å) and the C1-C4 distance is too long (4.172 Å). Therefore, a single crystal of **4a(m)** cannot be able to perform the 1,4-polymerization by itself.

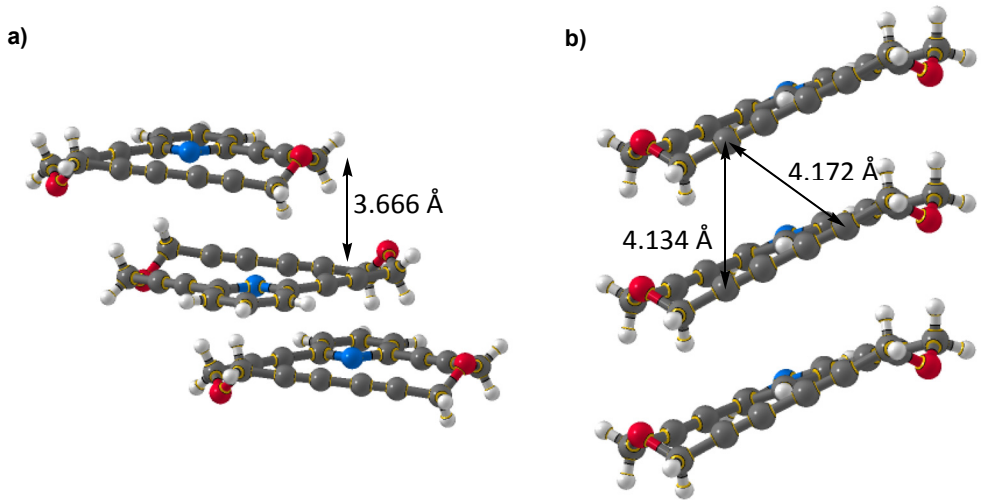

Figure 4.2: The side view of (a) the 2,6-pyridine-based macrocycle monomer **4(m)**, and (b) the 3,5-pyridine-based macrocycle monomer **4a(m)**.[2]

4.4 Future Plan

Even though the results obtained from this research project are both encouraging and disappointing, there are still different modifications that are worthwhile to attempt. First, further optimization of the alternate synthetic route can be done in order to maximize the synthetic steps' performance for attaining a better yield of macrocycle **4**. It is also worthwhile to try crystallizing macrocycle **4** right from the crude product without remove all the solvent from the crude product solution. This attempt was done by Tykwinski et. al. while they reported the similar difficulty in their macrocycle synthesis when they attempted to redissolve their crude product. They isolated their 2,6-pyridine-based pyridinophane and obtained 62% yield using such isolation technique.[5] While Tykwinski et. al. added acetone into their crude product solution and obtained their purified product via precipitation, we may also apply such technique in attempt to isolate the desired macrocycle **4**.

There are also studies that show the electronic property of aromatic rings in a macrocycle may affect its stacking feature, and its formation. Macrocycles that have electron withdrawing groups are seems to be more favorable on crystal formation and macrocyclic formation then those with electron donating groups.[6] Therefore, it may be reasonable to introduce an electron withdrawing group to 2,6-pyridine-based macrocycle **4** (Figure 4.3a). It will also be interesting if the macrocyclic formation for macrocycle **4** can be altered by introducing an electron withdrawing group into diol **2**. We can also introduce a new macrocycle structure that formed by homocoupling of diether **3** and **3a** (Figure 4.3b), in order to observe how the electronic property of our designed macrocycles affects the reactivity during macrocyclic formation, and their stacking behavior.

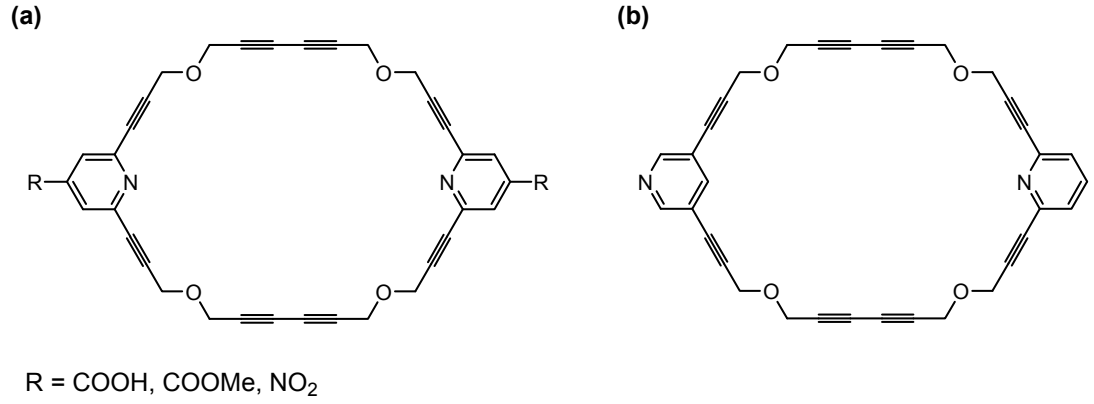

Figure 4.3: (a) The proposed refinement of macrocycle **4** by introducing electron withdrawing group. (b) The proposed new macrocycle structure form by homocoupling of **3** and **3a**. This structure is expected to obtain an unique electronic property in its framework.

Another mechanism problem that is worthwhile to solve is the dimerization under the Hay coupling condition in the original synthetic route. As mentioned before, it is hypothesized that copper metal may coordinated with the pyridine position of diether **3**

and favored the formation of macrocycle monomer **4(m)**. Therefore, it is worthwhile to try to obtain the structure of the coordination complex of copper metal and diether **3**. The hypothesized complex structure is shown in Figure 4.4.

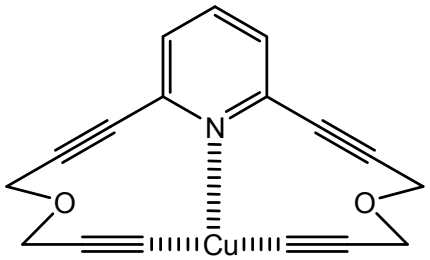

Figure 4.4: A plausible copper-diether **3** coordination complex that may alter the favorability during the Hay coupling condition on the original synthetic route.

If we can confirm the existence of this coordination complex, it can be very helpful for the synthetic route modification in order to enhance the product yield for the desired macrocycle **4** or its derivatives.

4.5 Conclusion

Even though a pure sample of 2,6-pyridine-based macrocycle **4** is still needed to be obtained for characterization and crystal analysis, a pure sample of a by-product **4(m)** is obtained and is subjected to X-ray diffraction for its crystal structure analysis. The intermolecular spacing of **4(m)**, however, is not a match for the proper diacetylene line-up. Thus the 1,4-polymerization of **4(m)** in its single crystal state is not possible. The alternative synthetic route toward macrocycle **4**, even though it eliminates the complications on the purification of crude product and on the undesirable formation of the mono-cyclization product, the similar solubility problem of its crude product for further purification remains. The introduction of an electron withdrawing group may be

able to alter the macrocyclic formation step for our desired macrocycle, and the macrocycle's stacking features. New macrocycle derivatives that have a different electronic properties then macrocycle **4** are proposed in order to study how electronic property of our designed macrocycles affects their stacking features and their macrocyclic formation. Mechanistic studies on the Hay coupling of diether **3** are also suggested, which may be helpful to resolve the synthetic complications during the oxidative homocoupling reactions in the final step of both the original and the new alternate route for our desired macrocycle **4**.

Endnotes:

[1] Curtis, S. M. Ph.D. Thesis (Chemistry), SUNY at Stony Brook, 2003.
[2] Wang, T. M.S. Thesis (Chemistry), SUNY at Stony Brook, 2005.
[3] Siemsen, P.; Livingston, R. C.; Diederich, F. *Angew. Chem. Int. Ed.* **2000**, *39*, 2632-2657.
[4] Liang, Y.; Xie, Y.-X.; Li, J.-H. *J. Org. Chem.* **2006**, *71*, 379-381.
[5] Campbell, K.; Tiemstra, N. M.; Prepas-Strobeck, N. S.; McDonald, R.; Ferguson, M. J.; Tykwinski, R. R. *Synlett.* **2004**, *1*, 182-186
[6] (a) Zhao, D.; Moore, J. S. *Chem. Commun.* **2003**, 807-818.; (b) Lahiri, S.; Thompson, J. L.; Moore, J. S. *J. Am. Chem. Soc.* **2000**, *112*, 11315-11319.; (c) Brunsveld, L.; Folmer, B. J. B.; Meijer, E. W.; Sijbesma, R. P. *Chem. Rev.* **2001**, *101*, 4071-4097.; (d) Tobe, Y.; Utsumi, N.; Kawabata, K.; Nagano, A.; Adachi, K.; Araki, S.; Sonoda, M.; Hirose, K.; Naemura, K. J. Am. Chem. Soc. 2002, 124, 5350-5364.

Chapter 5. Experimental Section

- ^{1}H-NMR spectra were recorded and obtained on a Varian Gemini 300MHz or 400MHz instrument. ^{13}C-NMR spectra, on the other hand, were recorded and obtained on a Varian Gemini 400MHz instrument. Both ^{1}H-NMR and ^{13}C-NMR experiments were using the solvent as an internal standard. All chemical shifts are recorded in parts per million (ppm). Coupling constants are reported in hertz (Hz). Peaks and their coupling patterns are described as singlet (s), doublet (d), triplet (t), quartet (q), quintet (qt), multiplet (m), doublet of doublets (dd), and doublet of triplets (dt).

- Melting points were recorded on a Fisher-Johns melting point apparatus and are uncorrected.

- Column chromatography was performed using Sorbent Technologies silica gel 60, 230-400 mesh.

- Chemicals were purchased from Fisher Scientific Company or Aldrich Chemical Company.

- All reactions are not yet optimized and will undergo optimizations in the near future.

- Beside 3,5-bis-(3-prop-2-ynyloxy-prop-1-ynyl) pyridine (Compound **3a**), the synthesis of **3,5-**bis-(3-prop-2-ynyloxy-prop-1-ynyl) pyridine (Compound **3a**), macrocycle **4a**, and macrocycle **4a(m)** was carried out by co-worker Ti Wang.[1]

5.1 Synthesis of Macrocycle 4 and 4(m)

2,6-bis-(3-hydroxy-1-propynyl) pyridine (2):

Method A: 3.00 g (12.6 mmol) of 2,6-dibromopyridine, 0.36 g (1.40 mol) of Ph_3P, and purified 0.096 g (0.5 mmol) of CuI were mixed with 60 mL of triethylamine, and 24 mL of dry pyridine under N_2. 0.27 g (0.38 mmol) of $(PPh_3)_2PdCl_2$ was then added into the reaction mixture under N_2. After the catalyst was dissolved into the reaction mixture, 6.0 mL (107 mmol) of propargyl alcohol was added dropwise into the reaction system. The reaction mixture was brought to reflux and TLC was used to monitor the reaction. After approximately 3 hours, the insoluble solid was filtered and was washed with ether. The filtered mixture was contracted and was purified with column chromatography (Hex: EtOAc 1:2) and afforded 1.32 g (56.0% yield) of white solid.

Method B: 3.00 g (12.6 mmol) of 2,6-dibromopyridine and 0.27 g (0.38 mmol) of $(PPh_3)_2PdCl_2$ were dissolved in 55.0 mL solution of tetrabutylammonium fluoride in THF under N_2, after all solids were dissolved in solution, 6.00 mL (107 mmol) of propargyl alcohol was added dropwise in room temperature under N_2. The reaction mixture was then heated to 70˚C and the reaction was monitored by TLC. After approximately 4 hours, the reaction mixture was quenched with water and filtered with celite. The filtered mixture was extracted with ether, dried with $MgSO_4$, and concentrated to afford oil with brownish color. The brown oil was purified via column chromatography (Hex: EtOAc 1:2) and afforded 1.20 g (50.9% yield) of white solid.

Melting point: 107-109˚C. ^{1}H-NMR (300MHz, d_6-DMSO): δ4.37 (d, 4H, J = 6 Hz), 5.50 (t, 2H, J = 6 Hz), 7.51 (d, 2H, J = 7.8 Hz), 7.85 (t, 1H, J = 7.8 Hz). ^{13}C-NMR (400MHz, d_6-DMSO): δ49.2, 82.8, 89.7, 126.1, 137.4, 142.4.

2,6-bis-(3-prop-2-ynyloxy-prop-1-ynyl) pyridine (3):

Method A: Inside a 250 mL round bottom flask, 2,6-dibromopyridine (2.37 g, 10.0 mmol), Ph_3P (0.43 g, 1.65 mmol), and CuI (0.08 g, 0.40 mmol) were mixed with 100 mL triethylamine and 50 mL THF under N_2. In a separate 25 mL round bottom flask, propargyl ether (5.60 mL, 55.0 mmol) and $(PPh_3)_2PdCl_2$ (0.21 g, 0.30 mmol) were mixed under N_2. This mixture was then added dropwise into the reaction mixture in 15 minutes, and then heated to 80˚C for 1 hour. After the reaction mixture was cooled down to room temperature, the insoluble triethylamine salt was removed. Ethyl acetate was used to wash the solid until the ethyl acetate washings were clear. The combined filtrate was concentrated and then purified by column chromatography (Hex: EtOAc 3:1) and 1.66 g (63.1% yield) of brown oil was obtained as the product.

Method B: 0.25 g (1.34 mmol) of diol **2** was dissolved in 5.0 mL of dry THF in a round bottom flask under N_2. The solution was then transferred into a 7.5 mL of dry THF with 0.58 g (24.2 mmol) of sodium hydride via syringe or cannula under 0˚C and N_2. The reaction mixture was stirred for approximately 20 minutes, then 0.72 g (2.73 mmol) 18-crown-6 was added into the reaction mixture. After an extra 20 minutes stirring, 0.36 mL (4.03 mmol) propargyl bromide was added dropwise via syringe. After the addition, the reaction mixture was stirred overnight at room temperature. After approximately 15 hrs,

cold water was used to quench the reaction. The reaction mixture was extracted with ether, dried with $MgSO_4$, and concentrated. A brown oil was observed. After column chromatography (Hex: EtOAc 2:1), the product was a brownish oil with 0.028 g (7.90% yield).

^{1}H-NMR (300MHz, $CDCl_3$): δ2.47 (t, 2H, *J* = 2.4 Hz), 4.31 (d, 4H, *J* = 2.4 Hz), 4.49 (s, 4H), 7.37 (d, 2H, *J* = 8.1 Hz), 7.62 (t, 1H, *J* = 7.5 Hz). ^{13}C-NMR (400MHz, $CDCl_3$): δ56.6, 56.8, 75.3, 78.7, 84.7, 85.3, 126.5, 136.5, 142.7.

2-(3-Prop-2-ynyloxy-prop-1-ynyl)-6-[3-(3-trimethylsilanyl-prop-2-ynyloxy)-prop-1-ynyl] pyridine (5):

A solution of diether **3** (0.33 g, 1.25 mmol) in 10.0 mL dry THF was cooled down to -78˚C under N_2. 0.9 M solution of Lithium bis(trimethylsilyl) amide in methylcyclohexane (1.50 mL, 1.38 mmol) was added dropwise over 30 minutes. The reaction mixture was stirred for 2 hours and trimethylsilyl chloride (0.17 mL, 1.38 mmol) was added dropwise. The reaction mixture was then stirred for another 1 hour and the reaction was quenched by a saturated solution of NH_4Cl. The mixture was then extracted with ether and the combined organic layer was dried with $MgSO_4$. The organic layer was then concentrated and the product was purified by column chromatography (Hex: EtOAc 5:1). The purified product was a yellowish oil and weighted 0.123 g (30.0% yield).

^{1}H-NMR (400MHz, $CDCl_3$): δ0.18 (s, 9H), 2.47 (t, 1H, *J* = 2.4 Hz), 4.31 (s, 2H), 4.32 (d, 2H, *J* = 2.4 Hz), 4.48 (s, 2H), 4.50 (s, 2H), 7.37 (d, 2H, *J* = 8 Hz), 7.62 (t, 1H, *J* = 7.6 Hz).

^{13}C-NMR (400MHz, $CDCl_3$): δ-0.01, 57.0, 57.1, 57.2, 57.8, 75.4, 78.9, 85.0, 85.3, 85.5, 85.7, 92.6, 100.6, 126.7, 126.8, 136.7, 143.1, 143.2.

2,6-bis-[3-(3-trimethylsilanyl-prop-2-ynyloxy)-prop-1-ynyl]-pyridine [5(d)]:

This compound was the undesired by-product of the pervious reaction. After column chromatography (Hex: EtOAc 10:1), this purified compound was a white crystal and weighted 0.217 g (42.6% yield).

Melting Point: 89-90˚C. ^{1}H-NMR (400MHz, $CDCl_3$): δ0.18 (s, 18H), 4.31 (s, 4H), 4.48 (s, 4H), 7.38 (d, 2H, J = 7.6 Hz), 7.63 (t, 1H, J = 8 Hz). ^{13}C-NMR (400MHz, $CDCl_3$): δ-0.02, 57.2, 57.8, 85.3, 85.5, 92.5, 100.6, 126.8, 136.8, 143.2.

Dimer of 2-(3-Prop-2-ynyloxy-prop-1-ynyl)-6-[3-(3-trimethylsilanyl-prop-2-ynyloxy)-prop-1-ynyl] pyridine (6):

In 50.0 mL solution of **5** (0.20g, 0.60 mmol) in dry CH_2Cl_2, a solution of CuCl (0.59 g, 6.0 mmol) and TMEDA (3.20 mL, 21.0 mmol) in 10.0 mL dry CH_2Cl_2 was added dropwise. The reaction mixture was then stirred for 3 hours in room temperature with oxygen gas bubbling into it. The reaction mixture was then quenched with saturated NH_4Cl solution and was extracted with CH_2Cl_2. The combined organic layer was then further washed with saturated NH_4Cl solution and was dried with $MgSO_4$. The organic layer was then concentrated, a yellowish oil was obtained as the product (0.15 g, 76.4% yield). The product proceeded to next step without purification.

^{1}H-NMR (400MHz, $CDCl_3$): δ0.17 (s, 18H), 4.30 (s, 4H), 4.40 (s, 4H), 4.47 (s, 4H), 4.48 (s, 4H), 7.40 (dd, 4H, *J* = 1.2 Hz, 7.6 Hz), 7.62 (t, 2H, *J* = 7.8 Hz). ^{13}C-NMR (400MHz, $CDCl_3$): δ-0.05, 57.1, 57.4, 57.8, 71.2, 74.9, 84.7, 85.3, 85.5, 85.9, 92.6, 100.6, 126.75, 126.78, 136.7, 143.0, 143.2.

Dimer of 2,6-bis-(3-prop-2-ynyloxy-prop-1-ynyl) pyridine (7):

Tetrabutylammonium fluoride trihydrate (0.14 g, 0.44 mmol) was added into a solution of **6** (0.15 g, 0.20 mmol) in 20.0 mL THF. The reaction mixture was stirred in room temperature in 1 hour. The reaction mixture was quenched and washed with NH_4 brine. The organic layer was then dried with $MgSO_4$ and concentrated. A white solid (0.10 g, >99% yield) was obtained. The solid was purified via recrystallization by methanol.

Melting Point: 93-94˚C. ^{1}H-NMR (300MHz, $CDCl_3$): δ2.47 (t, 2H, *J* = 2.4 Hz), 4.32 (d, 4H, *J* = 2.4 Hz), 4.41 (s, 4H), 4.50 (s, 4H), 4.51 (s, 4H), 7.38 (dd, 4H, *J* = 1.5 Hz, 7.8 Hz), 7.64 (t, 2H, *J* = 8.1 Hz). ^{13}C-NMR (400MHz, $CDCl_3$): 56.9, 57.0, 57.4, 75.4, 78.8, 84.9, 85.0, 85.5, 85.7, 126.69, 126.74, 136.7, 142.9.

5,12,24,31-tetraoxa-39,40-diaza-tricyclo[33.3.1.1^{16,20}]tetraconta-1(39),16,18,20(40),35,37-hexaene-2,7,9,14,21,26,28,33-octayne (Macrocycle 4):

Method A: A solution of CuCl (0.05 g, 0.52 mmol) and TMEDA (0.3 mL, 1.75 mmol) in 2.00 mL dry CH_2Cl_2 was added into a solution of **7** (0.0027 g, 0.005 mmol) in 5.00 mL dry CH_2Cl_2 dropwise. The reaction mixture was then stirred with bubbling O_2 in room

temperature for 3 hours. The reaction mixture was quenched with saturated NH_4Cl solution and was extracted with CH_2Cl_2. The combined organic layer was further washed with NH_4Cl brine, dried with $MgSO_4$, and concentrated under reduced pressure. The crude product obtained was a white solid (0.002 g). Because the crude product is insoluble in common organic solvents (such as hexane, acetone, ethyl acetate, chloroform, methanol, ethanol, water, even the original solvent that was used in the reaction: methylene chloride), the desired product (Macrocycle **4**) had not been isolated.

Method B: Diether **3** (0.028 g, 0.10 mmol) was dissolved in 250 mL of dry CH_2Cl_2. CuCl (0.073g, 0.70 mmol) and TMEDA (0.16 mL, 1.80 mmol) were added into the solution. O_2 was bubbled in the solution for approximately 2 hours. The reaction mixture was quenched with saturated NH_4Cl solution, extracted with CH_2Cl_2, washed with more NH_4Cl solution, dried with $MgSO_4$, and concentrated to afford a green oil with a white solid. The oil was purified with column chromatography for by-product **4(m)**, and the remaining white solid was insoluble in common organic solvents. Therefore the desired product was not isolated.

5,12-Dioxa-20-aza-bicyclo[14.3.1]icosa-1(19),16(20),17-triene-2,7,9,14-tetrayne [Macrocycle 4(m)]:

Same procedure as the 2,6-macrocycle (as shown in Method B) and this compound was a side product of this reaction. The green oil from the crude product was purified with column chromatography (Hex: EtOAc 2:1), the purified compound was a white crystal and weighted 0.0012 g (4.4% yield).

Melting Point: 148-150˚C (Decompose). ^{1}H-NMR (400MHz, $CDCl_3$): δ4.41 (s, 8H), 7.23 (d, 2H, *J* = 7.5 Hz), 7.58 (t, 1H, *J* = 7.8 Hz). ^{13}C-NMR (400MHz, $CDCl_3$): 56.6, 56.8, 75.3, 78.7, 84.7, 85.3, 126.5, 136.5, 142.7.

5.2 Synthesis of Macrocycle 4a and 4a(m)

3,5-bis-(3-hydroxy-1-propynyl) pyridine (2a):

Same procedure as 2,6-bis-(3-hydroxy-1-propynyl) pyridine **2**. The product was a white solid with 1.99 g (84.0% yield) using method A and 0.10 g (54.5% yield) using method B.

Melting Point: 126-128˚C. ^{1}H-NMR (300MHz, d_6-DMSO): δ4.32 (d, 4H, *J* = 6 Hz), 5.44 (t, 2H, *J* = 6 Hz), 7.87 (t, 1H, *J* = 2.1 Hz), 8.58 (d, 2H, *J* = 2.1 Hz). ^{13}C-NMR (400 MHz, d_6-DMSO): δ50.2, 80.3, 94.7, 120.0, 140.8, 151.3.

3,5-bis-(3-prop-2-ynyloxy-prop-1-ynyl) pyridine (3a):

Same procedure as 2,6-bis-(3-prop-2-ynyloxy-prop-1-ynyl) pyridine **3** (see Method B). The product was a brown oil with 0.64 g (86.0% yield).

^{1}H-NMR (400MHz, $CDCl_3$): δ2.49 (t, 2H, *J* = 2.1 Hz), 4.32 (d, 4H, *J* = 2.1 Hz), 4.50 (s, 4H), 7.77 (t, 1H, *J* = 1.8 Hz), 8.59 (d, 2H, *J* = 1.8 Hz). ^{13}C-NMR (400 MHz, $CDCl_3$): δ56.8, 57.1, 75.3, 78.6, 82.5, 88.4, 119.1, 140.1, 151.2.

5,12,24,31-tetraoxa-18,37-diaza-tricyclo[33.3.1.1^{16,20}]tetraconta-1(39),16,18,20(40),35,37-hexaene-2,7,9,14,21,26,28,33-octayne (Macrocycle 4a):

Same procedure as the macrocycle **4** and **4(m)** (using method B). The compound was a white crystal and weighted 0.042 g (16.0% yield).

^{1}H-NMR (400MHz, $CDCl_3$): δ4.41 (s, 8H), 4.50 (s, 8H), 7.84 (t, 2H, *J* = 1.8 Hz), 8.60 (d, 4H, *J* = 1.8 Hz). ^{13}C-NMR (300 MHz, $CDCl_3$): δ57.4, 57.6, 71.4, 75.0, 83.3, 88.4, 141.8, 151.6.

5,12-Dioxa-18-aza-bicyclo[14.3.1]icosa-1(19),16(20),17-triene-2,7,9,14-tetrayne [Macrocycle 4a(m)]:

Same procedure as the macrocycle **4** and **4(m)** (as shown in Method B) and this compound was a side product of this reaction. The compound was a white crystal and weighted 0.016g (6.0% yield).

Melting Point: 150˚C (Decompose). ^{1}H-NMR (400MHz, $CDCl_3$): δ4.42 (s, 8H), 8.43 (s, 1H), 8.50 (s, 2H). ^{13}C-NMR (300 MHz, $CDCl_3$): δ59.8, 61.0, 70.6, 77.3, 84.4, 90.5, 119.7, 141.4, 148.1.

Endnotes:

[1] Wang, T. M.S. Thesis (Chemistry), SUNY at Stony Brook, 2005.

Bibliography

Basak, A., S. S. Bag, P. A. Majumder, A. K. Das, and V. Bertolasi. 2004. Effect of Remote Trigonal Carbons on the Kinetics of Bergman Cyclization: Synthesis and Chemical Reactivity of Pyridazinedione-Based Enediynes. Journal of Organic Chemistry 69:6927-6930.

Blencowe, A., L. Davidson, and W. Hayes. 2003. Synthesis and characterization of hyperbranched polyesters incorporating the AB_2 monomer 3,5-bis(3-hydroxylprop-1-ynyl)benzoic acid. European Polymer Journal 39:1955-1963.

Bong, D. T., T. D. Clark, J. R. Granja, and M. R. Ghadiri. 2001. Self-assembling organic nanotubes. Angewandte Chemie, International Edition 40:988-1011.

Bradley, K., J.-C. P. Gabriel, and G. Grünert. 2003. Flexible nanotube transistors. Nano Letters 3:1353-1355.

Burnsveld, L., B. J. B. Folmer, E. W. Meijer, and R. P. Sijbesma. 2001. Supramolecular Polymers. Chemical Reviews 101:4071-4097.

Bunz, U. H. F. 1997. A soft spot for alkynes. Synlett. 1117-1127.
---. 1996. Synthesis of novel liquid crystalline organometallic polymers. Pure and Applied Chemistry 68:309-312.

Busch, D. H., and N. A. Stephenson. 1990. Molecular Organization, Portal to Supramolecular Chemistry. Coordination Chemistry Reviews 110:119-154.

Campell, K., R. McDonald, and R. R. Tykwinski. 2002. Functionalized Macrocyclic Ligands for Use in Supramolecular Chemistry. Journal of Organic Chemistry 67:1133-1140.

Campell, K., R. McDonald, N. R. Branda, and R. R. Tykwinski. 2001. Rigid, Cross-Conjugated Macrocycles: A Cyclic Alternative to 4,4'-Bipyridines in Supramolecular Chemistry. Organic Letters 3:1045-1048.

Campbell, K., N. M. Tiemstra, N. S. Prepas-Strobeck, R. McDonald, M. J. Ferguson, and R. R. Tykwinski. 2004. Synthesis of a Pyridinophane with endo-Annular Donor Sites. Synlett 1:182-186

Chang, Y. L., M. A. West, F. W. Fowler, J. W. Lauher. 1993. An approach to the design of molecular solids. Strategies for controlling the assembly of molecules into two-dimensional layered structures. Journal of the American Chemical Society 115:5991-6000.

Chiang, C. K., M. A.; Druy, S. C. Gau, A. J. Heeger, E. J. Louis, A. G. MacDiarmid, Y. W. Park, and H. Shirakawa. 1978. Synthesis of highly conducting films of derivatives of polyacetylene, $(CH)_x$. Journal of the American Chemical Society 100:1013-1015.

Chodkiewicz, W. 1957. Synthesis of acetylenic compounds. Ann. Chim. (Paris) [13] 2:819-869.

Chodkiewicz, W., and P. Cadiot. 1955. New synthesis of symmetrical and asymmetrical conjugated polyacetylene. Compt. Rend. 241:1055-1057.

Chodkiewicz, W., J. S. Alhuwalia, P. Cadiot, and A. Willemart. 1957. Preparation of aliphatic bifunctional compounds. Compt. Rend. 245:322-324.

Coe, S., J. Kane, T. Nguyen, L. Toledo, E. Wininger, F. W. Fowler, and J. W. Lauher. 1997. Molecular Symmetry and the Design of Molecular Solids: The Oxalamide Functionality as a Persistent Hydrogen Bonding Unit. Journal of the American Chemical Society 119:86-93.

Collins, P. G., M. S. Arnold, and P. Avouris. 2001. Engineering Carbon Nanotubes and Nanotube Circuits Using Electrical Breakdown. Science 292:706-709.

Cram, D. J., N. L.; Allinger, and H. Steinberg. 1954. Macro Rings. VII. The Spectral Consequences of Bringing Two Benzene Rings Face to Face. Journal of the American Chemical Society 76:6132-6141.

Curtis, S. M. Designed Supramolecular Systems for the Polymerization of Diacetylenes. Ph.D. Dissertation (Chemistry). Stony Brook University, 2003.

Dai, W., J. L. Petersen, and K. K. Wang. 2005. Synthesis of Indeno-Fused Derivatives of Quinolizinium Salts, Imidazo[1,2-*a*]pyridine, Pyrido[1,2-*a*]indole, and 4*H*-Quinolizin-4-one via Benzannulated Enyne-Allenes. Journal of Organic Chemistry 70:6647-6652.

Dalton, A. B., S. Collins, E. Muñoz, J. M. Razal, V. E. Ebron, J. P. Ferraris, J. N. Coleman, B. G. Kim, and R. H. Baughman. 2003. Super-tough carbon-nanotube fibers. Nature 423.6941:703.

DeSantis, P., S. Morosetti, and R. Rizzo. 1974. Conformational Analysis of Regular Enantiomeric Sequences. Macromolecules 7:52-58.

Desiraju, G. R. Crystal Engineering: The Design of Organic Solids. Amsterdam: Elsevier, 1989.

---. 1995. Supramolecular Synthons in Crystal Engineering - A New Organic Synthesis. Angewandte Chemie, International Edition in English 34:2311-2327.

Eastmond, R., and D. R. M. Walton. 1972. Silylation as a protective method in Cadiot-Chodkiewicz couplings Synthesis of aryl-butadiynes and –hexatriynes. Tetrahedron 28:4591-4599.

Eastmond, R., T. R. Johnson, and D. R. M. Walton 1972. Silylation as a protective method for terminal alkynes in oxidative couplings. A general synthesis of the parent polyynes $H(C{=}C)_nH$ (n = 4–10, 12). Tetrahedron 28:4601-4616.

Eisenberg, B. 1998. Ionic Channels in Biological Membranes: Natural Nanotubes. Accounts of Chemical Research 31:117-123.

Enkelmann, V. Advances in Polymer Science 63 – Polydiacetylenes. Berlin: Springer-Verlag, 1984. 91-136.
---. 1994. Solid-State Reactivity of Triacetylenes. Chemistry of Materials 6:1337-1340.

Etter, M. C. 1990. Encoding and decoding hydrogen-bond patterns of organic compounds. Accounts of Chemical Research 23:120-126.

Fowler, F. W., and J. W. Lauher. 2000. A rational design of molecular materials. Journal of Physical Organic Chemistry 13:850-857.

Gabriel, J. C.-P. 2003. Large Scale Production of Carbon Nanotube Transistors: A Generic Platforms for Chemical Sensors. Material Research Society Symposium Proceedings 776:271-277.

Gannon, C. J., P. Cherukuri, B. I. Yakobson, L. Cognet, J. S. Kanzius, C. Kittrell, R. B. Weisman, M. Pasquali, H. K. Schmidt, R. E. Smalley, and S. A. Curley. 2007. Carbon nanotube-enhanced thermal destruction of cancer cells in a noninvasive radiofrequency field. Cancer 110:2654-2665.

Ghadiri, M. R., J. R. Granja, R. A. Milligan, D. E. McRee, and N. Khazanovich. 1993. Self-assembling organic nanotubes based on a cyclic peptide architecture. Nature 366:324-327.

Hartgerink, J. D., J. R. Granja, R. A. Milligan, and M. R. Ghadiri. 1996. Self-Assembling Peptide Nanotubes. Journal of the American Chemical Society 118:43-50.
Hay, A. S. 1960. Communications- Oxidative Coupling of Acetylenes. Journal of Organic Chemistry 25:1275-1276.
---. 1962. Oxidative Coupling of Acetylenes. II. Journal of Organic Chemistry 27:3320-3321.

Hide, F., M. A. Diaz-Garcia, B. J. Schwartz, M. R. Andersson, Q. Pei, and A. J. Heegar. 1996. Semiconducting Polymers: A New Class of Solid-State Laser Materials. Science 273:1833-1836.

Höger, S. J. 1999. Highly efficient methods for the preparation of shape-persistent macrocyclics. Polymer Science Part A: Polymer Chemistry 37:2685-2698.

Höger, S., A.-D. Meckenstock, and H. Pellen. 1997. High-Yield Macrocyclization via Glaser Coupling of Temporary Covalent Templated Bisacetylenes. Journal of Organic Chemistry 62:4556-4557.

Höger, S., K. Bonrad, A. Mourran, U. Beginn, and M. Möller. 2001. Synthesis, Aggregation, and Adsorption Phenomena of Shape-Persistent Macrocycles with Extraannular Polyalkyl Substituents. Journal of the American Chemical Society 123:5651-5659.

Horwich, A. L., E. U. Weber-Ben, and D. Finley. Chaperone Rings in Protein Folding and Degradation. 1999. Proceedings of the National Academy of Sciences of the United States of America 96:11033-11040.

Hunter, C. A., and J. K. M. Sanders. 1990. The nature of .pi.-.pi. interactions. Journal of the American Chemical Society 112:5525-5534.

Illuminati, G. and L. Mandolini. 1981. Ring Closure Reactions of Bifunctional Chain Molecules. Accounts of Chemical Research 14:95-102.

Itoh, T., H. Shirakawa, and S. J. Ikeda. 1974. Simultaneous polymerization and formation of polyacetylene film on the surface of concentrated soluble Ziegler-type catalyst solution. Journal of Polymer Science: Polymer Chemistry Edition 12:11-20.

Jeffrey, G. A. An Introduction to Hydrogen Bonding. Oxford: Oxford University Press, 1997.

Jozefiak, T. H., E. J. Ginsburg, C. B. Gorman, R. H. Grubbs, N. S. Lewis. 1993. Voltammetric characterization of soluble polyacetylene derivatives obtained from the ring-opening metathesis polymerization (ROMP) of substituted cyclooctatetraenes. Journal of the American Chemical Society 115:4705-4713.

Kakamura, K., M. Okubo, and M. Yamaguchi. 2001. Synthesis and Self-aggregation of Cyclic Alkynes Containing Helicene. Organic Letters 3:1097-1099.

Kane, J. J., R.-F. Liao, J. W. Lauher, and F. W. Fowler. 1995. Preparation of layered diacetylenes as a demonstration of strategies for supramolecular synthesis. Journal of the American Chemical Society 117:12003-12004.

Kane, J. J., T.; Nguyen, J. Xiao, F. W. Fowler, and J. W. Lauher. 2001. The Host Guest Co-Crystal Approach to Supramolecular Structure. Molecular Crystals and Liquid Crystals 356:449-458.

Katayev, E. A., J. L. Sessler, V. N. Khrustalev, and Y. A. Ustynyuk. 2007. Synthetic Model of the Phosphate Binding Protein: Solid-State Structure and Solution-Phase Anion Binding Properties of a Large Oligopyrrolic Macrocycle. Journal of Organic Chemistry 72:7244-7252.

Koopal, C. G. J., M. C. Feiters, R. J. M. Nolte, and R. B. M. de Ruiter. 1992. Polypyrrole microtubules and their use in the construction of a third generation biosensor. Synthetic Metals 51:397-405.

Liang, Y., Y.-X. Xie, and J.-H. Li. 2006. Modified Palladium-Catalyzed Sonogashira Cross-Coupling Reactions under Copper-, Amine-, and Solvent-Free Conditions. Journal of Organic Chemistry 71:379-381.

Martin, R. B. 1996. Comparisons of Indefinite Self-Association Models. Chemical Reviews 96:3043-3064.

Martin, R. E., T.; Mäder, and F. Diederich. 1999. Monodisperse Poly(triacetylene) Rods: Synthesis of a 11.9 nm Long Molecular Wire and Direct Determination of the Effective Conjugation Length by UV/Vis and Raman Spectroscopies. Angewandte Chemie, International Edition. 38:817-821.

Martin, R. E., U. Gubler, C. Boudon, V. Gramlich, C. Bosshard, J.-P. Gisselbrecht, P. Günter, M. Gross, and F. Diederich. 1997. Poly(triacetylene) oligomers: synthesis, characterization, and estimation of the effective conjugation length by electrochemical, UV/Vis, and nonlinear optical methods. Chemistry : A European Journal 3:1505-1512.

McQuade, D. T., A. E. Pullen, and T. M. Swager. 2000. Conjugated Polymer-Based Chemical Sensors. Chemical Reviews 100:2537-2574.

Moore, J. S. 1997. Shape-Persistent Molecular Architectures of Nanoscale Dimension. Accounts of Chemical Research 30:402-413.

Moroni, M., J. Le Moigne, and S. Luzzati. 1994. Rigid rod conjugated polymers for nonlinear optics: 1. Characterization and linear optical properties of poly(aryleneethynylene) derivatives. Macromolecules 27:562-571.

Novak, P., K. Muller, K. S. V. Santhanam, and O. Haas. 1997. Electrochemically Active Polymers for Rechargeable Batteries. Chemical Reviews 97:207-281.

Nugent, W. A., D. L. Thorn, and R. L. Harlow. 1987. Cyclization of diacetylenes to E,E exocyclic dienes. Complementary procedures based on titanium and zirconium reagents. Journal of the American Chemical Society 109:2788-2796.

Pattil, A. O., A. J. Heegar, and F. Wudl. 1998. Optical properties of conducting polymers. Chemical Reviews 88:183-200.

Pedersen, C. J. 1967. Cyclic polyethers and their complexes with metal salts. Journal of the American Chemical Society 89:7017-7036.

Pimental, G. C., and A. L. McClellan. The Hydrogen Bond. San Francisco: Freeman, 1960.

Postma, H. W. C., T. Teepen, Z. Yao, M. Grifoni, and C. Dekker. 2001. Carbon Nanotube Single-Electron Transistors at Room Temperature. Science 293:76-79.

Sailor, M. J., F. L.; Klavetter, R. H. Grubbs, and N. S. Lewis. 1990. Electronic properties of junctions between silicon and organic conducting polymers. Nature 346:155-157.

Sailor, M. J., E. J. Ginsburg, C. B. Gorman, A. Kumar, R. H. Grubbs, and N. S. Lewis. 1990. Thin Films of Conducting Polymers: An n-Si/Poly-$(CH_3)_3$Si-cyclooctatetraene Solar Cell and Layered Polymeric Structures. Science 249:1146-1149.

Sakwattanasinitt, M., D.-C. Lee, M. Kim. X. Wang, L. Li, J. Kumar, S. K. Tripathy, and D. J. Sandman. 1999. New Processable, Functionalizable Polydiacetylenes. Macromolecules 32:7361-7369.

Sarkar, A., S. Okada, H, Nakanishi, and H. Matsuda. 1998. Polydiacetylenes from Asymmetrically Substituted Diacetylenes Containing Heteroaryl Side Groups for Third-Order Nonlinear Optical Properties. Macromolecules 31:9174-9180.

Sarkar, A., S. Okada, H. Matsuzawa, H. Matsuda, and H. Nakanishi. 2000. Novel polydiacetylenes for optical materials: beyond the conventional polydiacetylenes. Journal of Materials Chemistry 10:819-828.

Shimizu, L. S., A. D. Hughes, M. D. Smith, M. J. Davis, B. P. Zhang, H.-C. Loye, and K. D. Shimizu. 2003. Self-Assembled Nanotubes that Reversibly Bind Acetic Acid Guests. Journal of the American Chemical Society 125:14972-14973.

Shirakawa, H., E. J. Louis, A. G. MacDiarmid, C. K. Chiang, and A. J. Heeger. 1977. Synthesis of electrically conducting organic polymers: halogen derivatives of polyacetylene, $(CH)_x$. Journal of the Chemical Society, Chemical Communications. 578-580.

Siemsen, P., R. C. Livingston, and F. Diederich. 2000. Acetylenic Coupling: A Powerful Tool in Molecular Construction. Angewandte Chemie, International Edition 39:2632-2657.

Siemsen, P., U. Gubler, C. Bosshard, P. Günter, and F. Diederich. 2001. Pt-Tetraethynylethene Molecular Scaffolding: Synthesis and Characterization of a Novel Class of Organometallic Molecular Rods. Chemistry : A European Journal 7:1333-1341.

Sigler, P. B., Z. Xu, H. S. Rye, S. G. Burston, W. A. Fenton, and A. L. Horwich. 1998. Structure and function in GroEL-mediated protein folding. Annual Review of Biochemistry 67:581-608.

Simmons, T. J., D. Hashim, R. Vajtai, and P. M. Ajayan. 2007. Large Area-Aligned Arrays from Direct Deposition of Single-Wall Carbon Nanotube Inks. Journal of the American Chemical Society 129:10088-10089.

Singh, R., D. Pantarotto, D. McCarthy, O. Chaloin, J. Hoebeke, C. D. Partidos, J.-P. Briand, M. Prato, A. Bianco, and K. Kostarelos. 2005. Binding and Condensation of Plasmid DNA onto Functionalized Carbon Nanotubes: Toward the Construction of Nanotube-Based Gene Delivery Vectors. Journal of the American Chemical Society 127:4388-4396.

Son, S. U., Y. A. Yoon, D. S. Choi, J. K. Park, B. M. Kim, and Y. K. Chung. 2001. Dicobalt Octacarbonyl Catalyzed Carbonylated Cycloaddition of Triynes to Functionalized Tetracycles. Organic Letters 3:1065-1067.

Sondheimer, F., Y. Amiel, and R. Wolovsky. 1957. Unsaturated Macrocyclic Compounds. IV. The Oxidation of Terminal Diacetylenes to Macrocyclic Tetraacetylenes. Journal of the American Chemical Society 79:6263-6257.

Sonogashira, K., Y. Tohda, and N. Hagihara. 1975. Convenient synthesis of acetylenes. Catalytic substitutions of acetylenic hydrogen with bromo alkenes, iodo arenes, and bromoptridines. Tetrahedron Letters. 4467-4470.

Srinivasan, M., S. Sankararaman, H. Hopf, I. Dix, and P. G. Jones. 2001. Syntheses and Structures of Isomeric [6.6]- and [8.8]Cyclophanes with 1,4-Dioxabut-2-yne and 1,6-Dioxahexa-2,4-diyne Bridges. Journal of Organic Chemistry 66:4299-4303.

Steed, J. W., and J. L. Atwood. Supramolecular Chemistry. Chichester: John Wiley & Sons, 2000.

Takahashi, S., Y. Koroyama, K. Sonogashira, and N. Hagihara. 1980. Synthesis 12:627-631.

Tan, D. S., M. A. Foley, B. R. Stockwell, M. D. Shair, and S. L. Schreiber. 1999. Synthesis and Preliminary Evaluation of a Library of Polycyclic Small Molecules for Use in Chemical Genetic Assays. Journal of the American Chemical Society 121:9073-9087.

Tobe, Y., N. Utsumi, K. Kawabata, A. Nagano, K. Adachi, S. Araki, M. Sonoda, K. Hirose, and K. Naemura. 2002. *m*-Diethynylbenzene Macrocycles: Syntheses and Self-Association Behavior in Solution. Journal of the American Chemical Society 124:5350-5364.

Trost, B. M., and M. T. Rudd. 2005. Ruthenium-Catalyzed Cycloisomerizations of Diynols. Journal of the American Chemical Society 127:4763-4776.

Tseng, Y.-C., P., Xuan, A. Javey, R. Malloy, Q. Wang, J. Bokor, and H. Dai. 2004. Monolithic Integration of Carbon Nanotube Devices with Silicon MOS Technology. Nano Letters 4:123-127.

Viehe, H. G. Chemistry of Acetylene. New York: Marcel Dekker, 1969.

Voges, D., P. Zwickl, and W. Baumeister. 1999. The 26S Proteasome: A Molecular Machine Designed for Controlled Proteolysis. Annual Review of Biochemistry 68:1015-1068.

Wang, T. The Topochemical Polymerization of Diacetylenes using Supramolecular Host-Guest Chemistry. M.S. Thesis (Chemistry). Stony Brook University, 2005.

Wegner, G. Z. 1969. Naturforsch. (b) 24:824.

Werz, D. B., R. Gleiter, and F. Rominger. 2004. Cyclic Tetra- and Hexaynes Containing 1,4-Donor-Substituted Butadiyne Units: Synthesis and Supramolecular Organization. Journal of Organic Chemistry 69:2945-2952.

Wilson, G. S., and H. L. Anderson. 1999. A conjugated triple strand porphyrin array. Chemical Communications. 1539-1540.

Zhang, M., S. Fang, A. A. Zakhidou, S. B. Lee, A. E. Aliev, C. D. Williams, K. R. Atkinson, and R. H. Baughman. 2005. Strong, Transparent, Multifunctional, Carbon Nanotube Sheets. Science 309:1215-1219.

Zhang, W., and J. S. Moore. 2006. Shape-Persistent Macrocycles: Structures and Synthetic Approaches from Arylene and Ethynylene Building Blocks. Angewandte Chemie, International Edition 45:4416-4439.

Zhao, D., and J. S. Moore. 2003. Shape-persistent arylene ethynylene macrocycles: syntheses and supramolecular chemistry. Chemical Communications. 807-818.

Zhao, X. Q., Y. L. Chang, F. W. Fowler, and J. W. Lauher. 1990. An approach to the design of molecular solids. The ureylene dicarboxylic acids. Journal of the American Chemical Society 112:6627-6634.

Zhou, Q., P. J. Carroll, and T. M. Swager. 1994. Synthesis of Diacetylene Macrocycles Derived from 1,2-Diethynyl Benzene Derivatives: Structure and Reactivity of the Strained Cyclic Dimer. Journal of Organic Chemistry 59:1294-1301.

Zuercher, W. J., M. Scholl, and R. H. Grubbs. 1998. Ruthenium-Catalyzed Polycyclization Reactions. Journal of Organic Chemistry 63:4291-4298.

Zumdahl, S. S. Chemistry-4th Edition. Boston: Houghton Mifflin, 1997.

Appendix

Crystallographic Data for Compound 2

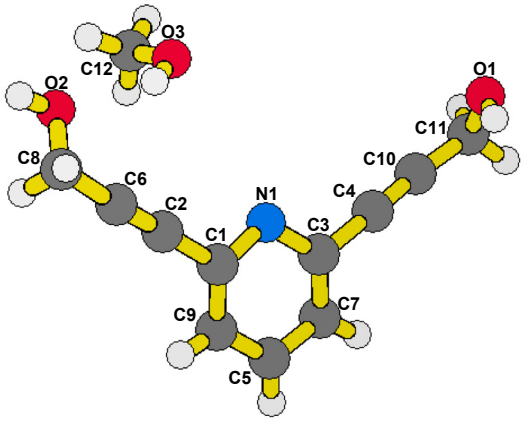

Table 1. Crystal data and structure refinement for Compound **2**.

Identification code	Compound **2** (Note: Obtain methanol)	
Empirical formula	C12 H11 N O3	
Formula weight	217.22	
Temperature	273(2) K	
Wavelength	0.71073 Å	
Crystal system	Triclinic	
Space group	P-1	
Unit cell dimensions	a = 4.2383(18) Å	□α = 105.351(8)°
	b = 9.724(4) Å	□β = 96.702(9)°
	c = 13.226(6) Å	□γ = 90.351(9)°
Volume	521.7(4) $Å^3$	
Z	2	
Density (calculated)	1.383 Mg/m^3	
Absorption coefficient	0.100 mm^{-1}	
F(000)	228	
Theta range for data collection	1.61 to 28.75°	
Index ranges	-5<=h<=5, -8<=k<=12, -17<=l<=16	
Reflections collected	3359	
Independent reflections	2333 [R(int) = 0.0518]	
Completeness to theta = 28.75°	85.7 %	
Absorption correction	None	
Refinement method	Full-matrix least-squares on F^2	
Data / restraints / parameters	2333 / 0 / 149	
Goodness-of-fit on F^2	3.193	
Final R indices [I>2sigma(I)]	R1 = 0.3883, wR2 = 0.6434	
R indices (all data)	R1 = 18.1136, wR2 = 0.7750	
Largest diff. peak and hole	549.053 and -556.748 $e.Å^{-3}$	

Table 2. Atomic coordinates ($\times 10^4$) and equivalent isotropic displacement parameters ($Å^2 \times 10^3$) for Compound **2**. U(eq) is defined as one third of the trace of the orthogonalized U^{ij} tensor.

	x	y	z	U(eq)
O(1)	8930(70)	-4220(30)	1390(20)	66(8)
N(1)	5890(60)	1180(30)	2750(20)	39(7)
O(2)	3090(70)	3180(30)	6608(18)	59(8)
C(1)	4350(90)	2450(30)	2920(20)	39(8)
C(2)	3300(90)	2890(30)	3960(30)	44(9)
C(3)	6830(80)	750(30)	1760(30)	39(9)
C(4)	8310(90)	-650(40)	1540(30)	54(11)
C(5)	5000(80)	2840(30)	1250(30)	49(10)
O(3)	2780(80)	300(30)	5690(30)	83(10)
C(6)	2370(90)	3250(40)	4820(30)	48(9)
C(7)	6490(100)	1530(40)	1050(30)	54(11)
C(8)	1240(110)	3650(50)	5880(30)	62(12)
C(9)	3910(90)	3310(40)	2230(30)	56(11)
C(10)	9530(90)	-1810(40)	1400(20)	43(9)
C(11)	10780(100)	-3170(40)	1160(30)	63(12)
C(12)	5178(15)	1278(10)	6310(5)	1134(14)

Table 3. Bond lengths [Å] and angles [°] for Compound **2**.

O(1)-C(11)	1.40(5)
N(1)-C(1)	1.37(4)
N(1)-C(3)	1.38(4)
O(2)-C(8)	1.34(5)
C(1)-C(9)	1.39(5)
C(1)-C(2)	1.46(5)
C(2)-C(6)	1.21(5)
C(3)-C(7)	1.35(5)
C(3)-C(4)	1.47(5)
C(4)-C(10)	1.22(5)
C(5)-C(7)	1.40(5)
C(5)-C(9)	1.40(5)
O(3)-C(12)	1.41(3)
C(6)-C(8)	1.49(5)
C(10)-C(11)	1.40(5)
C(1)-N(1)-C(3)	113(3)
N(1)-C(1)-C(9)	127(3)
N(1)-C(1)-C(2)	112(3)
C(9)-C(1)-C(2)	120(3)
C(6)-C(2)-C(1)	179(4)
N(1)-C(3)-C(7)	124(3)
N(1)-C(3)-C(4)	114(3)
C(7)-C(3)-C(4)	123(3)
C(10)-C(4)-C(3)	177(4)
C(7)-C(5)-C(9)	116(3)
C(2)-C(6)-C(8)	179(4)
C(5)-C(7)-C(3)	123(3)
O(2)-C(8)-C(6)	113(3)
C(1)-C(9)-C(5)	118(3)
C(4)-C(10)-C(11)	175(4)
O(1)-C(11)-C(10)	114(3)

Table 4. Anisotropic displacement parameters ($Å^2 \times 10^3$) for Compound **2**. The anisotropic displacement factor exponent takes the form: $-2\pi^2[h^2 a^{*2}U^{11} + ... + 2 h k a^* b^* U^{12}]$

	U^{11}	U^{22}	U^{33}	U^{23}	U^{13}	U^{12}
O(1)	80(20)	43(15)	70(19)	9(14)	23(16)	4(15)
N(1)	47(18)	32(15)	36(16)	5(13)	1(13)	0(13)
O(2)	90(20)	53(16)	30(14)	7(12)	14(14)	8(14)
C(1)	60(20)	33(18)	29(18)	8(15)	4(17)	-4(17)
C(2)	70(30)	34(18)	30(18)	21(15)	-16(18)	0(17)
C(3)	50(20)	23(18)	40(20)	5(15)	3(18)	-7(16)
C(4)	60(30)	60(30)	40(20)	-2(18)	21(19)	-30(20)
C(5)	70(30)	40(20)	40(20)	16(17)	-6(19)	4(18)
O(3)	110(20)	55(17)	80(20)	0(16)	31(19)	10(16)
C(6)	60(30)	40(20)	40(20)	12(17)	0(19)	0(17)
C(7)	80(30)	40(20)	40(20)	1(17)	30(20)	-20(20)
C(8)	70(30)	60(30)	60(30)	10(20)	30(20)	10(20)
C(9)	70(30)	25(19)	70(30)	4(18)	30(20)	-6(18)
C(10)	70(30)	40(20)	21(17)	20(16)	5(17)	5(19)
C(11)	60(30)	50(30)	70(30)	0(20)	30(20)	10(20)
C(12)	1282(18)	2000(30)	784(12)	1447(18)	257(10)	952(17)

Table 5. Hydrogen coordinates ($\times 10^4$) and isotropic displacement parameters ($Å^2 \times 10^3$) for Compound **2**.

	x	y	z	U(eq)
H(1)	7179	-4302	1032	98
H(2)	2640	3576	7199	88
H(5)	4747	3365	752	58
H(3)	1085	703	5674	125
H(7)	7282	1188	406	65
H(8A)	1165	4681	6124	74
H(8B)	-910	3259	5823	74
H(9)	2923	4180	2425	67
H(11A)	11032	-3456	416	76
H(11B)	12878	-3123	1555	76
H(12A)	4452	1769	6966	1701
H(12B)	5667	1958	5935	1701
H(12C)	7050	774	6447	1701

Crystallographic Data for Compound 5(d)

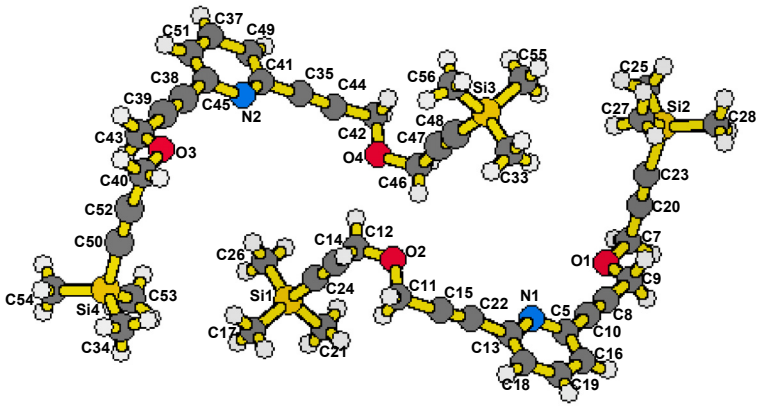

Table 1. Crystal data and structure refinement for Compound **5(d)**.

Identification code	Compound **5(d)**	
Empirical formula	C23 H29 N O2 Si2	
Formula weight	407.65	
Temperature	273(2) K	
Wavelength	0.71073 Å	
Crystal system	Triclinic	
Space group	P1	
Unit cell dimensions	a = 6.113(2) Å	□α = 99.098(8)°
	b = 10.970(4) Å	□β = 99.125(7)°
	c = 19.261(6) Å	□γ = 106.196(8)°
Volume	1196.4(7) $Å^3$	
Z	2	
Density (calculated)	1.132 Mg/m^3	
Absorption coefficient	0.165 mm^{-1}	
F(000)	436	
Theta range for data collection	1.10 to 28.95°	
Index ranges	-8<=h<=7, -14<=k<=12, -25<=l<=25	
Reflections collected	7921	
Independent reflections	6482 [R(int) = 0.1042]	
Completeness to theta = 28.95°	86.1%	
Absorption correction	None	
Refinement method	Full-matrix least-squares on F^2	
Data / restraints / parameters	6482 / 3 / 505	
Goodness-of-fit on F^2	0.625	
Final R indices [I>2sigma(I)]	R1 = 0.0900, wR2 = 0.2225	
R indices (all data)	R1 = 0.3605, wR2 = 0.3613	
Absolute structure parameter	-0.2(8)	
Largest diff. peak and hole	0.376 and -0.303 $e.Å^{-3}$	

Table 2. Atomic coordinates ($\times 10^4$) and equivalent isotropic displacement parameters ($Å^2 \times 10^3$) for Compound **5(d)**. U(eq) is defined as one third of the trace of the orthogonalized U^{ij} tensor.

	x	y	z	U(eq)
Si(1)	8960(16)	7937(8)	1689(5)	77(3)
Si(2)	865(16)	-6020(8)	-641(5)	74(3)
O(2)	3600(40)	4064(15)	2500(9)	66(6)
O(1)	-1560(40)	-2130(18)	-1448(9)	80(7)
C(5)	-5240(50)	130(20)	41(12)	51(7)
N(1)	-3470(40)	910(20)	520(12)	58(6)
C(7)	-1050(50)	-3130(20)	-1877(15)	60(8)
C(8)	-4170(40)	-1540(30)	-876(15)	63(8)
C(9)	-3790(60)	-2540(30)	-1377(17)	76(9)
C(10)	-4730(50)	-810(30)	-494(16)	73(9)
C(11)	1600(40)	4500(20)	2384(16)	57(8)
C(12)	5780(50)	4930(30)	2939(16)	109(12)
C(13)	-4050(50)	1790(30)	1001(15)	61(8)
C(14)	6690(60)	5860(30)	2488(19)	104(12)
C(15)	-480(60)	3480(30)	1889(17)	82(10)
C(16)	-7640(50)	40(30)	-22(15)	73(10)
C(17)	8650(70)	9500(30)	2084(17)	117(14)
C(18)	-6220(50)	1800(30)	1006(13)	61(8)
C(19)	-7940(40)	970(30)	537(15)	58(7)
C(20)	-250(50)	-4070(20)	-1447(14)	69(8)
C(21)	7280(70)	7340(40)	696(15)	130(16)
C(22)	-1950(50)	2690(30)	1515(13)	54(8)
C(23)	70(50)	-4840(30)	-1162(16)	81(9)
C(28)	-1480(50)	-7680(30)	-1032(19)	95(12)
C(24)	7630(60)	6750(30)	2175(19)	94(11)
C(25)	3830(50)	-6070(30)	-719(17)	81(11)
C(26)	12210(60)	8040(30)	1830(20)	109(15)
C(27)	480(70)	-5520(30)	304(15)	110(12)
Si(3)	-7630(15)	-1006(8)	4364(5)	78(3)
Si(4)	552(16)	12934(9)	6685(5)	82(3)
O(4)	-2120(30)	2843(18)	3551(10)	78(6)
O(3)	2880(30)	9068(15)	7497(9)	63(6)
C(33)	-10590(50)	-1070(30)	4295(15)	86(9)
C(34)	-2340(50)	13030(30)	6798(18)	87(11)
C(35)	3470(50)	4210(30)	4531(18)	83(9)
N(2)	4930(50)	5930(30)	5541(15)	72(7)
C(37)	9580(50)	5970(30)	5554(18)	91(9)
C(38)	6170(50)	7680(30)	6498(15)	54(8)
C(39)	5760(50)	8530(30)	6926(15)	77(9)
C(40)	1860(60)	9900(30)	7918(15)	105(12)

Table 2. (Continued)

	x	y	z	U(eq)
C(41)	5270(50)	5130(30)	5058(13)	57(7)
C(42)	-350(50)	2240(30)	3647(17)	99(11)
C(43)	5210(40)	9640(30)	7364(15)	80(9)
C(44)	1680(50)	3430(30)	4111(14)	64(8)
C(45)	6740(60)	6800(30)	6016(14)	72(10)
C(46)	-4200(50)	1810(20)	3109(15)	62(9)
C(47)	-5260(40)	880(30)	3572(15)	53(7)
C(48)	-6110(50)	190(30)	3866(14)	71(9)
C(49)	7500(50)	5040(30)	4968(17)	98(11)
C(50)	1150(50)	11760(30)	7167(15)	76(8)
C(51)	8900(50)	6800(30)	6042(16)	80(9)
C(52)	1790(50)	10910(30)	7525(18)	99(12)
C(53)	260(60)	12360(30)	5693(15)	97(10)
C(54)	2780(60)	14530(30)	7088(19)	106(12)
C(55)	-7360(50)	-2650(30)	3962(18)	87(11)
C(56)	-6160(60)	-500(30)	5314(16)	94(10)

Table 3. Bond lengths [Å] and angles [°] for Compound **5(d)**.

Si(1)-C(24)	1.81(4)
Si(1)-C(17)	1.83(3)
Si(1)-C(21)	1.94(3)
Si(1)-C(26)	1.93(3)
Si(2)-C(25)	1.86(3)
Si(2)-C(23)	1.88(3)
Si(2)-C(27)	1.89(3)
Si(2)-C(28)	1.92(3)
O(2)-C(12)	1.44(3)
O(2)-C(11)	1.43(3)
O(1)-C(9)	1.35(3)
O(1)-C(7)	1.40(3)
C(5)-N(1)	1.29(3)
C(5)-C(16)	1.43(4)
C(5)-C(10)	1.47(4)
N(1)-C(13)	1.39(4)
C(7)-C(20)	1.56(3)
C(8)-C(10)	1.16(3)
C(8)-C(9)	1.44(4)
C(11)-C(15)	1.50(4)
C(12)-C(14)	1.49(5)
C(13)-C(18)	1.33(4)
C(13)-C(22)	1.48(4)
C(14)-C(24)	1.27(5)
C(15)-C(22)	1.11(4)
C(16)-C(19)	1.43(4)
C(18)-C(19)	1.29(3)
C(20)-C(23)	1.12(3)
Si(3)-C(33)	1.78(3)
Si(3)-C(56)	1.83(3)
Si(3)-C(48)	1.87(3)
Si(3)-C(55)	1.91(3)
Si(4)-C(50)	1.79(3)
Si(4)-C(54)	1.85(3)
Si(4)-C(53)	1.88(3)
Si(4)-C(34)	1.84(3)
O(4)-C(42)	1.41(3)
O(4)-C(46)	1.48(3)
O(3)-C(40)	1.46(3)
O(3)-C(43)	1.47(3)
C(35)-C(44)	1.25(4)
C(35)-C(41)	1.40(4)
N(2)-C(41)	1.25(4)
N(2)-C(45)	1.34(4)

Table 3. (Continued)

C(37)-C(51)	1.40(4)
C(37)-C(49)	1.54(4)
C(38)-C(39)	1.25(4)
C(38)-C(45)	1.39(4)
C(39)-C(43)	1.52(4)
C(40)-C(52)	1.45(4)
C(41)-C(49)	1.43(4)
C(42)-C(44)	1.55(4)
C(45)-C(51)	1.31(4)
C(46)-C(47)	1.53(4)
C(47)-C(48)	1.09(3)
C(50)-C(52)	1.34(4)
C(24)-Si(1)-C(17)	107.9(16)
C(24)-Si(1)-C(21)	106.8(17)
C(17)-Si(1)-C(21)	110.8(16)
C(24)-Si(1)-C(26)	106.4(16)
C(17)-Si(1)-C(26)	110.5(17)
C(21)-Si(1)-C(26)	114(2)
C(25)-Si(2)-C(23)	109.5(15)
C(25)-Si(2)-C(27)	115.5(16)
C(23)-Si(2)-C(27)	106.9(14)
C(25)-Si(2)-C(28)	112.4(15)
C(23)-Si(2)-C(28)	106.9(15)
C(27)-Si(2)-C(28)	105.2(16)
C(12)-O(2)-C(11)	120(2)
C(9)-O(1)-C(7)	110(2)
N(1)-C(5)-C(16)	128(2)
N(1)-C(5)-C(10)	116(3)
C(16)-C(5)-C(10)	116(3)
C(5)-N(1)-C(13)	113(2)
O(1)-C(7)-C(20)	114(2)
C(10)-C(8)-C(9)	172(3)
O(1)-C(9)-C(8)	108(2)
C(8)-C(10)-C(5)	175(3)
O(2)-C(11)-C(15)	113(2)
O(2)-C(12)-C(14)	105(2)
C(18)-C(13)-N(1)	124(3)
C(18)-C(13)-C(22)	125(3)
N(1)-C(13)-C(22)	111(2)
C(24)-C(14)-C(12)	173(3)
C(22)-C(15)-C(11)	177(3)
C(5)-C(16)-C(19)	111(3)
C(13)-C(18)-C(19)	120(2)

Table 3. (Continued)

C(18)-C(19)-C(16)	123(2)
C(23)-C(20)-C(7)	172(3)
C(15)-C(22)-C(13)	171(3)
C(20)-C(23)-Si(2)	175(3)
C(14)-C(24)-Si(1)	177(3)
C(33)-Si(3)-C(56)	108.7(15)
C(33)-Si(3)-C(48)	111.2(15)
C(56)-Si(3)-C(48)	108.7(14)
C(33)-Si(3)-C(55)	111.6(14)
C(56)-Si(3)-C(55)	109.8(14)
C(48)-Si(3)-C(55)	106.8(14)
C(50)-Si(4)-C(54)	108.9(16)
C(50)-Si(4)-C(53)	110.7(15)
C(54)-Si(4)-C(53)	114.8(17)
C(50)-Si(4)-C(34)	106.8(15)
C(54)-Si(4)-C(34)	109.3(15)
C(53)-Si(4)-C(34)	106.0(16)
C(42)-O(4)-C(46)	106(2)
C(40)-O(3)-C(43)	119(2)
C(44)-C(35)-C(41)	172(3)
C(41)-N(2)-C(45)	120(3)
C(51)-C(37)-C(49)	112(3)
C(39)-C(38)-C(45)	176(3)
C(38)-C(39)-C(43)	172(3)
O(3)-C(40)-C(52)	104(2)
N(2)-C(41)-C(35)	124(3)
N(2)-C(41)-C(49)	125(3)
C(35)-C(41)-C(49)	111(3)
O(4)-C(42)-C(44)	99(2)
C(39)-C(43)-O(3)	105(2)
C(35)-C(44)-C(42)	168(3)
N(2)-C(45)-C(51)	122(3)
N(2)-C(45)-C(38)	115(3)
C(51)-C(45)-C(38)	122(3)
C(47)-C(46)-O(4)	110(2)
C(48)-C(47)-C(46)	176(3)
C(47)-C(48)-Si(3)	179(3)
C(41)-C(49)-C(37)	115(3)
C(52)-C(50)-Si(4)	175(3)
C(45)-C(51)-C(37)	124(3)
C(50)-C(52)-C(40)	165(3)

Table 4. Anisotropic displacement parameters ($Å^2 \times 10^3$) for Compound **5(d)**. The anisotropic displacement factor exponent takes the form: $-2\pi^2[h^2 a^{*2}U^{11} + ... + 2 h k a^* b^* U^{12}]$

	U^{11}	U^{22}	U^{33}	U^{23}	U^{13}	U^{12}
Si(1)	88(7)	71(6)	66(6)	11(5)	11(6)	20(5)
Si(2)	87(7)	65(6)	78(6)	17(5)	27(5)	31(5)
O(2)	107(16)	38(10)	62(12)	16(9)	26(11)	29(11)
O(1)	77(15)	79(15)	77(13)	-22(11)	17(11)	34(13)
C(5)	64(18)	63(17)	40(13)	13(13)	33(13)	30(15)
N(1)	51(12)	56(14)	49(13)	-19(11)	1(11)	11(11)
C(7)	76(16)	33(14)	90(20)	37(14)	60(14)	17(11)
C(8)	43(14)	70(20)	80(20)	3(17)	12(14)	42(15)
C(9)	100(20)	34(15)	100(20)	3(14)	53(19)	29(16)
C(10)	70(19)	90(20)	80(20)	31(18)	25(17)	49(18)
C(11)	40(13)	35(13)	80(20)	-1(13)	-1(13)	8(11)
C(12)	110(20)	70(20)	90(20)	-3(17)	25(18)	-47(16)
C(13)	70(20)	54(19)	45(19)	7(15)	-1(17)	13(17)
C(14)	90(20)	80(20)	110(20)	-48(18)	-63(19)	49(19)
C(15)	100(30)	70(20)	90(20)	3(18)	70(20)	29(19)
C(16)	80(20)	100(30)	80(20)	47(19)	68(17)	60(20)
C(17)	190(40)	46(17)	100(30)	9(17)	0(20)	30(20)
C(18)	48(15)	76(19)	60(16)	-14(14)	8(13)	39(15)
C(19)	14(12)	110(20)	57(16)	2(15)	-2(12)	36(14)
C(20)	100(20)	28(13)	74(16)	26(12)	4(15)	19(13)
C(21)	150(30)	160(30)	47(17)	26(18)	-30(20)	20(30)
C(22)	53(19)	50(16)	44(15)	-24(12)	5(14)	16(15)
C(23)	100(20)	100(20)	90(20)	48(18)	38(19)	63(19)
C(28)	65(18)	60(20)	120(30)	0(20)	-11(19)	-18(16)
C(24)	90(20)	58(17)	130(30)	19(18)	0(20)	34(17)
C(25)	63(17)	110(30)	90(20)	20(20)	24(17)	50(20)
C(26)	60(20)	100(30)	190(40)	60(30)	40(20)	35(19)
C(27)	190(30)	51(19)	72(17)	4(14)	24(18)	23(18)
Si(3)	73(6)	66(6)	87(7)	23(5)	4(6)	15(5)
Si(4)	91(7)	76(7)	79(7)	21(5)	20(6)	25(6)
O(4)	40(11)	77(14)	87(14)	-2(12)	-21(10)	1(10)
O(3)	79(14)	49(11)	72(14)	36(10)	24(11)	23(10)
C(33)	72(19)	120(20)	81(19)	30(17)	36(15)	37(18)
C(34)	70(20)	70(20)	120(30)	30(20)	40(20)	26(17)
C(35)	80(19)	100(20)	90(20)	60(20)	19(18)	41(19)
N(2)	90(19)	80(18)	54(16)	28(14)	25(15)	28(15)
C(37)	130(20)	44(14)	60(18)	-7(13)	-18(16)	-8(14)
C(38)	68(18)	39(17)	43(17)	0(14)	-1(14)	6(14)
C(39)	52(16)	90(20)	56(18)	32(15)	-16(14)	-23(15)
C(40)	180(30)	90(20)	58(17)	1(15)	-19(17)	100(20)

Table 4. (Continued)

	U^{11}	U^{22}	U^{33}	U^{23}	U^{13}	U^{12}
C(41)	64(18)	69(19)	36(15)	6(13)	-8(13)	28(15)
C(42)	52(15)	110(20)	110(20)	-42(17)	-31(15)	50(15)
C(43)	20(13)	140(30)	64(18)	-21(17)	8(12)	18(14)
C(44)	68(17)	60(20)	70(20)	12(16)	-11(15)	38(16)
C(45)	100(20)	48(18)	37(17)	-18(15)	-44(16)	15(17)
C(46)	67(18)	40(15)	67(19)	29(15)	-35(16)	14(14)
C(47)	53(14)	56(16)	59(17)	23(14)	19(13)	23(12)
C(48)	75(18)	68(19)	52(17)	26(15)	-3(15)	-5(15)
C(49)	43(18)	130(30)	120(20)	70(20)	-6(16)	8(18)
C(50)	90(20)	55(17)	80(20)	4(14)	23(16)	23(15)
C(51)	59(17)	80(20)	70(20)	-11(17)	-18(16)	12(16)
C(52)	61(17)	90(20)	110(20)	-64(19)	54(18)	-9(17)
C(53)	120(20)	130(30)	58(18)	14(17)	50(15)	56(19)
C(54)	110(30)	52(17)	150(30)	19(19)	50(20)	3(18)
C(55)	77(17)	60(20)	130(30)	-10(20)	46(18)	30(16)
C(56)	110(20)	79(18)	70(20)	-2(16)	-1(17)	9(16)

Crystallographic Data for Macrocycle 4(m)

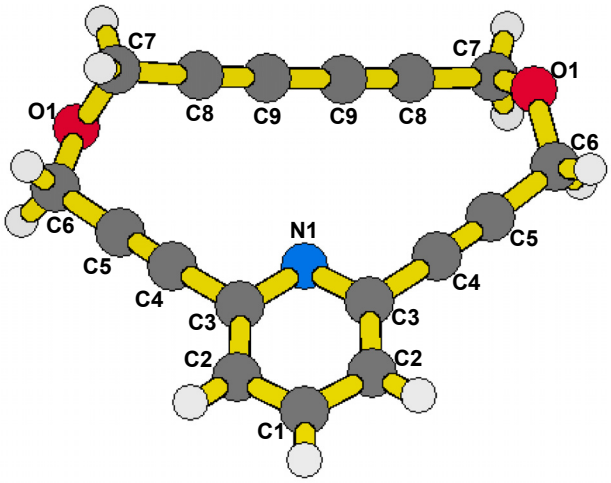

Table 1. Crystal data and structure refinement for Macrocycle **4(m)**.

Identification code	Macrocycle **4(m)**	
Empirical formula	C17 H11 N O2	
Formula weight	261.27	
Temperature	273(2) K	
Wavelength	0.71073 Å	
Crystal system	Monoclinic	
Space group	C2/c	
Unit cell dimensions	a = 15.510(3) Å	□α = 90°
	b = 10.021(2) Å	□β = 102.139(4)°
	c = 8.8020(18) Å	□γ = 90°
Volume	1337.5(5) $Å^3$	
Z	4	
Density (calculated)	1.297 Mg/m^3	
Absorption coefficient	0.086 mm^{-1}	
F(000)	544	
Theta range for data collection	2.44 to 28.70°	
Index ranges	-19<=h<=19, -11<=k<=13, -11<=l<=11	
Reflections collected	4195	
Independent reflections	1560 [R(int) = 0.0535]	
Completeness to theta = 28.70°	89.9 %	
Absorption correction	None	
Refinement method	Full-matrix least-squares on F^2	
Data / restraints / parameters	1560 / 0 / 92	
Goodness-of-fit on F^2	0.732	
Final R indices [I>2sigma(I)]	R1 = 0.0632, wR2 = 0.1874	
R indices (all data)	R1 = 0.1578, wR2 = 0.2726	
Largest diff. peak and hole	0.153 and -0.289 $e.Å^{-3}$	

Table 2. Atomic coordinates ($\times 10^4$) and equivalent isotropic displacement parameters ($Å^2 \times 10^3$) for Macrocycle **4(m)**. U(eq) is defined as one third of the trace of the orthogonalized U^{ij} tensor.

	x	y	z	U(eq)
N(1)	5000	7624(4)	2500	60(1)
O(1)	7356(1)	10676(2)	1035(3)	72(1)
C(1)	5603(2)	6930(3)	1932(4)	59(1)
C(2)	5619(2)	5562(4)	1903(5)	73(1)
C(3)	5898(2)	11285(3)	1369(5)	68(1)
C(4)	5328(2)	11254(3)	2078(4)	66(1)
C(5)	6752(2)	8445(4)	954(4)	68(1)
C(6)	5000	4881(5)	2500	83(2)
C(7)	6241(2)	7730(4)	1367(4)	65(1)
C(8)	7372(2)	9361(4)	442(5)	73(1)
C(9)	6569(2)	11364(4)	428(5)	82(1)

Table 3. Bond lengths [Å] and angles [°] for Macrocycle **4(m)**.

N(1)-C(1)	1.343(3)
N(1)-C(1)#1	1.343(3)
O(1)-C(9)	1.406(4)
O(1)-C(8)	1.419(4)
C(1)-C(2)	1.371(5)
C(1)-C(7)	1.441(4)
C(2)-C(6)	1.369(4)
C(3)-C(4)	1.184(4)
C(3)-C(9)	1.462(5)
C(4)-C(4)#1	1.381(6)
C(5)-C(7)	1.182(4)
C(5)-C(8)	1.467(5)
C(6)-C(2)#1	1.369(4)
C(1)-N(1)-C(1)#1	117.6(4)
C(9)-O(1)-C(8)	113.4(3)
N(1)-C(1)-C(2)	122.8(3)
N(1)-C(1)-C(7)	115.0(3)
C(2)-C(1)-C(7)	122.2(3)
C(1)-C(2)-C(6)	118.3(4)
C(4)-C(3)-C(9)	176.9(4)
C(3)-C(4)-C(4)#1	178.3(3)
C(7)-C(5)-C(8)	178.6(4)
C(2)#1-C(6)-C(2)	120.2(5)
C(5)-C(7)-C(1)	176.2(4)
O(1)-C(8)-C(5)	113.8(3)
O(1)-C(9)-C(3)	115.0(3)

Symmetry transformations used to generate equivalent atoms:
#1 -x+1,y,-z+1/2

Table 4. Anisotropic displacement parameters ($Å^2 \times 10^3$) for Macrocycle **4(m)**. The anisotropic displacement factor exponent takes the form: $-2\pi^2[h^2 a^{*2}U^{11} + ... + 2 h k a^* b^* U^{12}]$

	U^{11}	U^{22}	U^{33}	U^{23}	U^{13}	U^{12}
N(1)	56(2)	59(2)	67(2)	0	20(2)	0
O(1)	59(1)	67(2)	93(2)	-9(1)	25(1)	-1(1)
C(1)	54(2)	55(2)	66(2)	-1(2)	13(2)	1(2)
C(2)	66(2)	59(2)	93(3)	-6(2)	17(2)	4(2)
C(3)	59(2)	65(2)	85(3)	9(2)	25(2)	6(2)
C(4)	56(2)	63(2)	81(3)	3(2)	23(2)	2(2)
C(5)	60(2)	72(2)	77(2)	-7(2)	26(2)	4(2)
C(6)	81(4)	51(3)	122(5)	0	28(3)	0
C(7)	60(2)	65(2)	74(2)	-4(2)	24(2)	7(2)
C(8)	69(2)	74(3)	82(3)	-10(2)	31(2)	-3(2)
C(9)	71(2)	85(3)	100(3)	19(2)	42(2)	13(2)

Table 5. Hydrogen coordinates ($\times 10^4$) and isotropic displacement parameters ($Å^2 \times 10^3$) for Macrocycle **4(m)**.

	x	y	z	U(eq)
H(2)	6039	5109	1487	87
H(6)	5000	3953	2500	100
H(8A)	7964	9006	764	88
H(8B)	7236	9399	-684	88
H(9A)	6321	11012	-598	98
H(9B)	6709	12296	305	98

^{1}H-NMR and ^{13}C-NMR Spectra

^{1}H-NMR and ^{13}C-NMR Spectra of synthesized compounds are presented in the following order:

1. 2,6-bis-(3-hydroxy-1-propynyl) pyridine **(2)**, p.99-100
2. 2,6-bis-(3-prop-2-ynyloxy-prop-1-ynyl) pyridine **(3)**, p.101-102
3. 2-(3-Prop-2-ynyloxy-prop-1-ynyl)-6-[3-(3-trimethylsilanyl-prop-2-ynyloxy)-prop-1-ynyl] pyridine **(5)**, p.103-104
4. 2,6-bis-[3-(3-trimethylsilanyl-prop-2-ynyloxy)-prop-1-ynyl]-pyridine **[5(d)]**, p.105-106
5. Dimer of 2-(3-Prop-2-ynyloxy-prop-1-ynyl)-6-[3-(3-trimethylsilanyl-prop-2-ynyloxy)-prop-1-ynyl] pyridine **(6)**, p.107-108
6. Dimer of 2,6-bis-(3-prop-2-ynyloxy-prop-1-ynyl) pyridine **(7)**, p.109-110
7. 5,12-Dioxa-20-aza-bicyclo[14.3.1]icosa-1(19),16(20),17-triene-2,7,9,14-tetrayne **[4(m)]**, p.111-112
8. 3,5-bis-(3-hydroxy-1-propynyl) pyridine **(2a)**, p.113-114

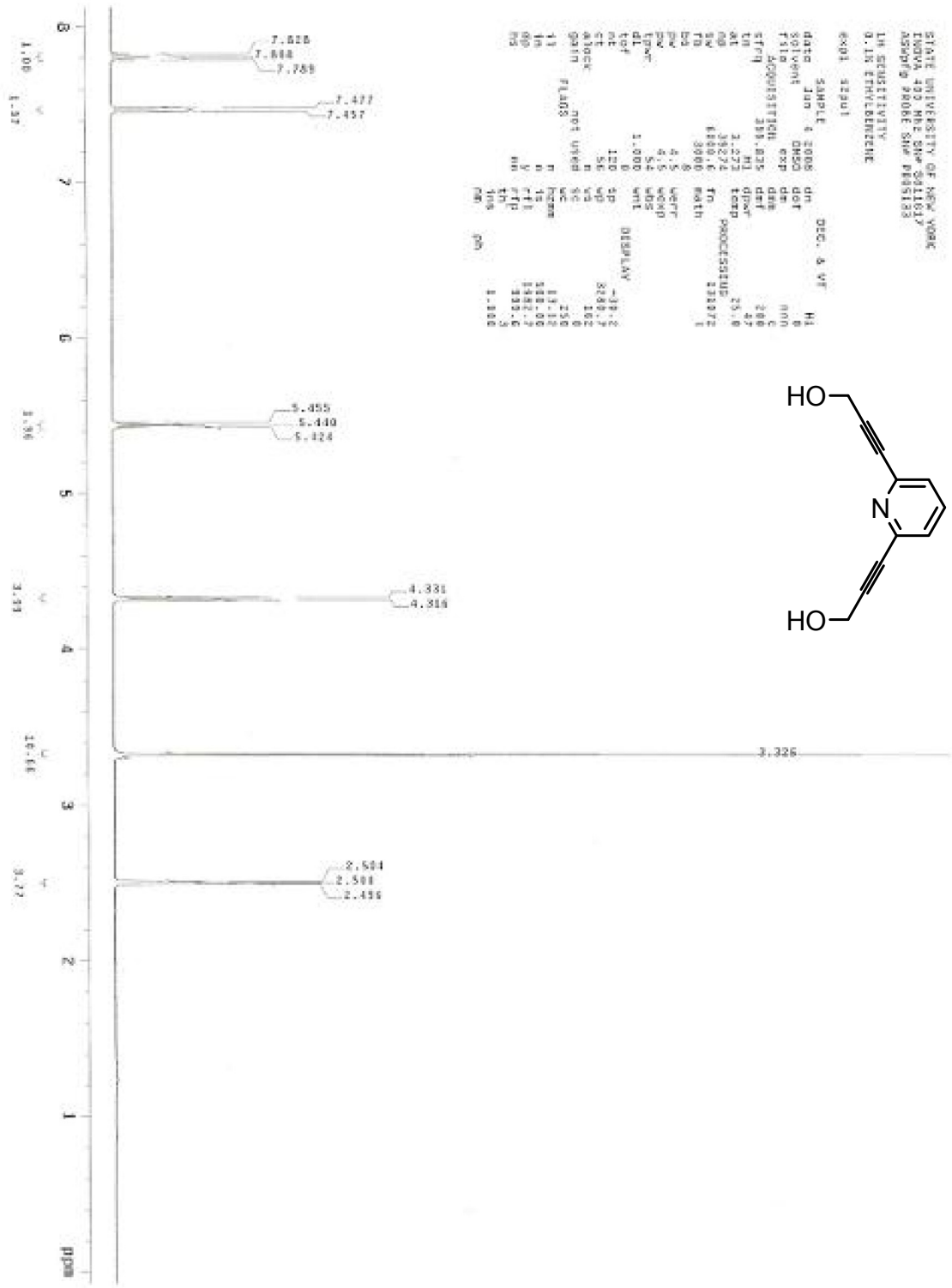
7.828
7.808
7.789
7.477
7.457
5.455
5.440
5.424
4.331
4.316
3.326
2.504
2.488
2.456
HO
N
HO

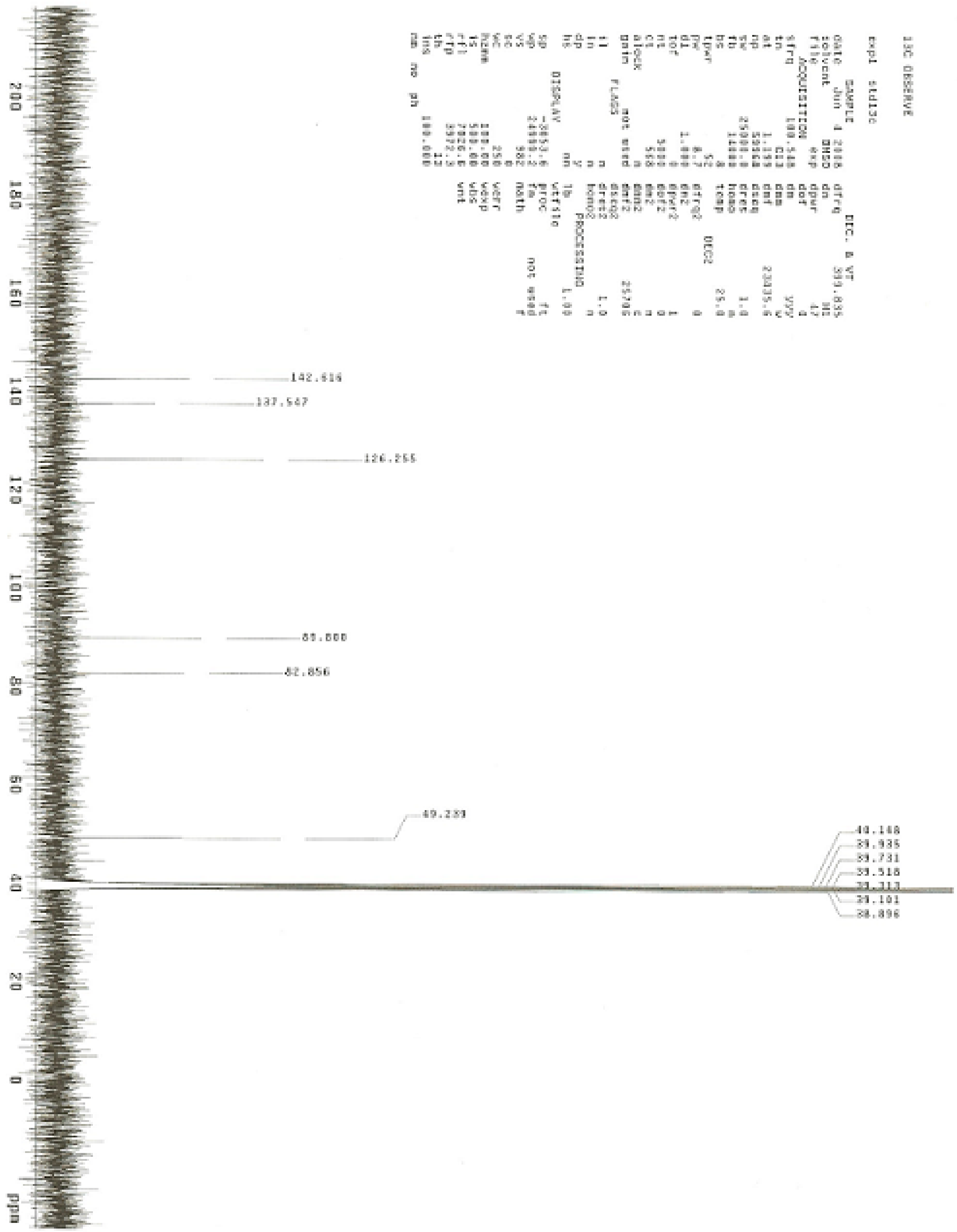

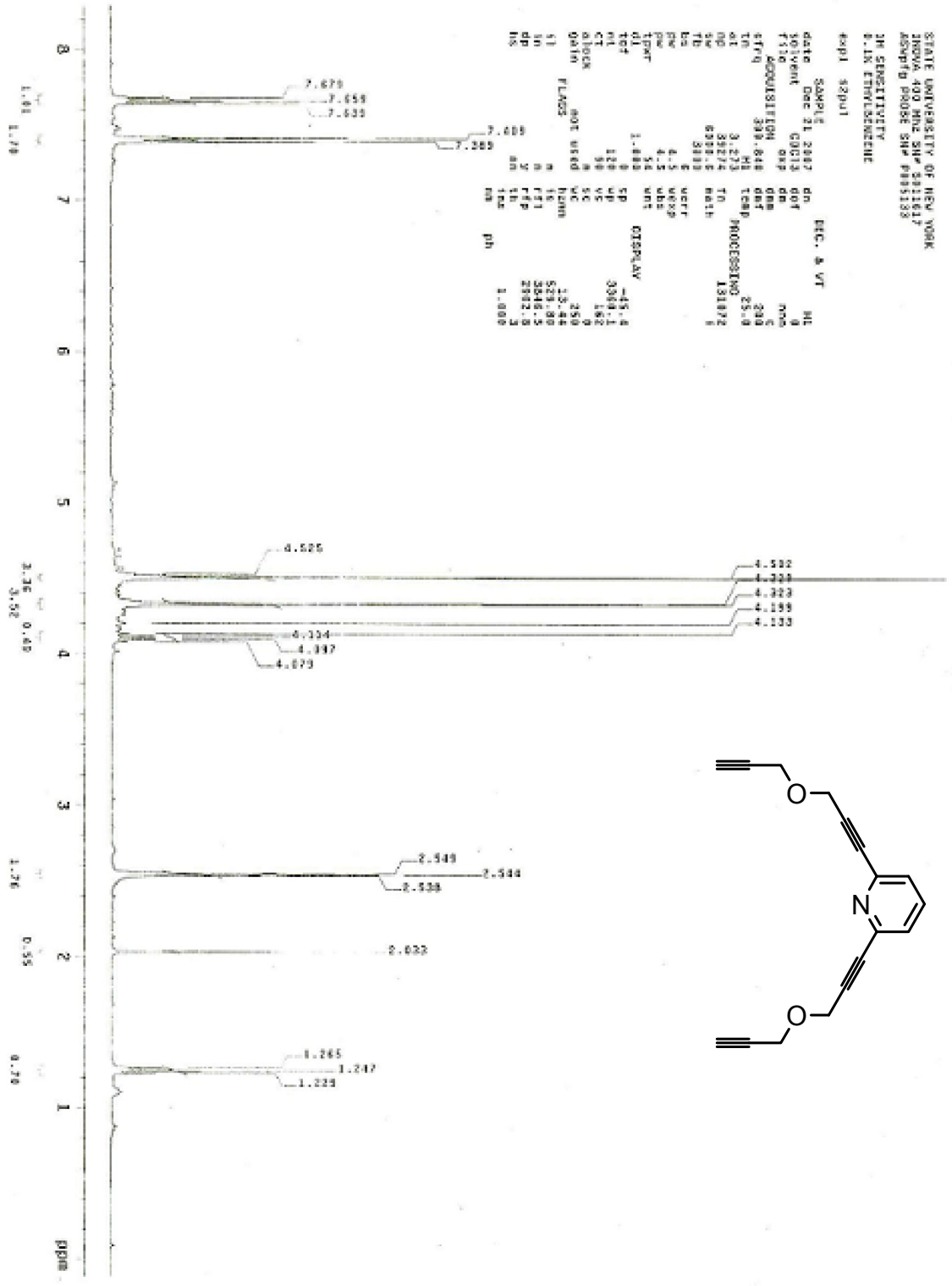
7.679
7.658
7.639
7.405
7.389
4.525
4.502
4.328
4.323
4.199
4.133
4.134
4.097
4.079
2.549
2.544
2.538
2.032
1.265
1.247
1.229
ppm

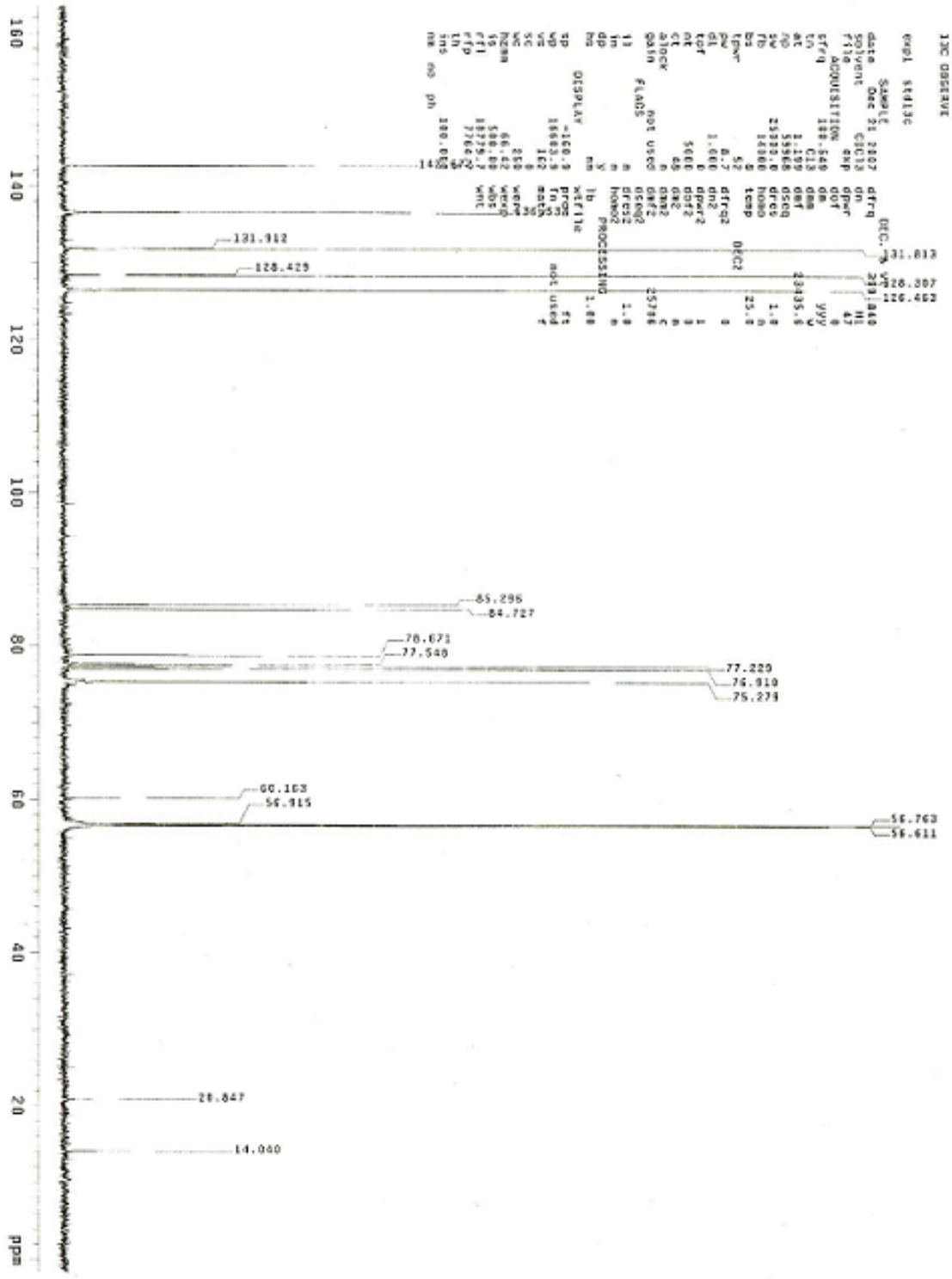
131.813
128.307
126.483
85.298
84.727
78.671
77.548
77.229
76.919
75.278
60.103
56.915
56.763
56.611
28.847
14.040
ppm

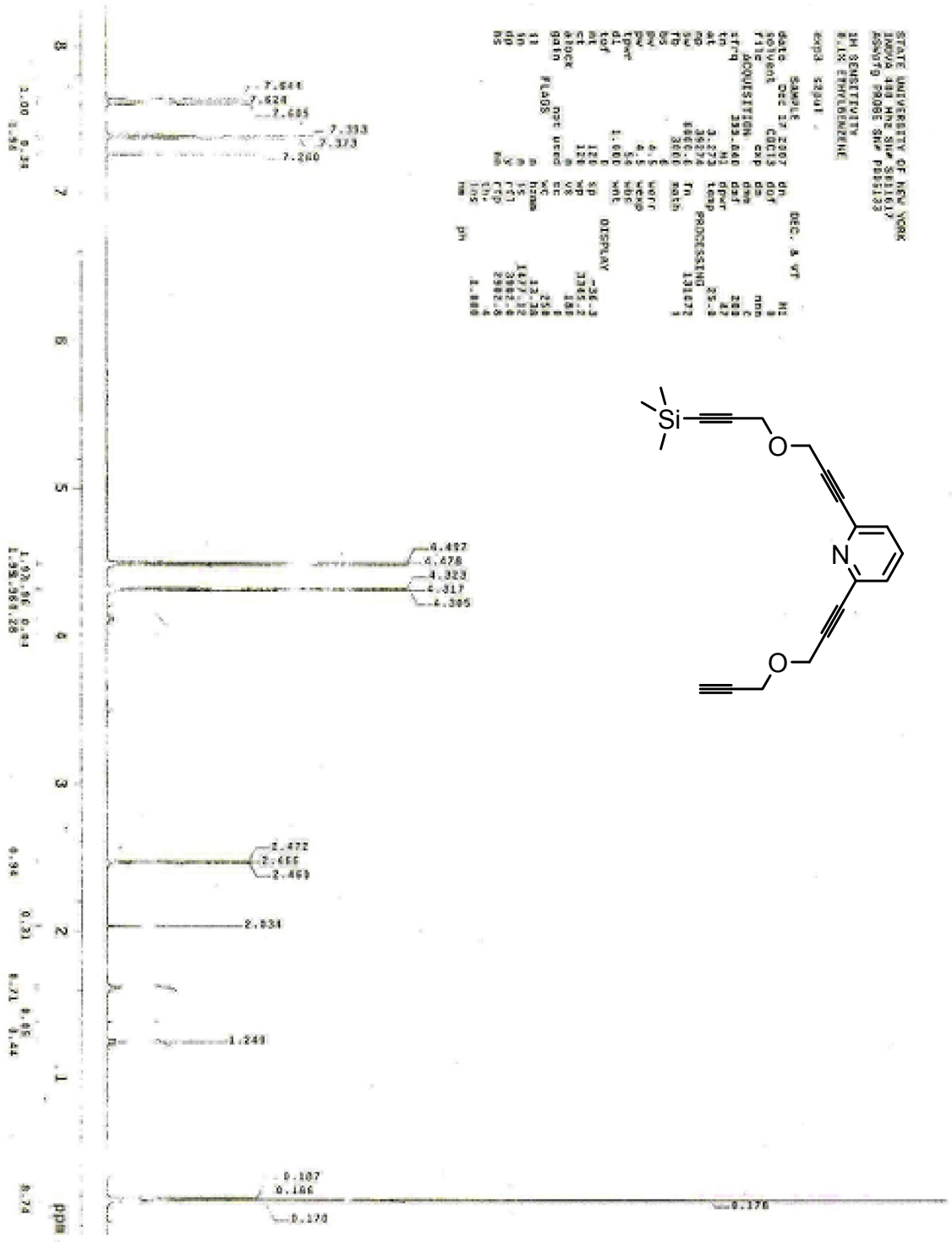
7.644
7.624
7.605
7.333
7.313
7.200
4.407
4.378
4.323
4.317
4.305
2.472
2.455
2.439
2.434
1.249
0.107
0.106
0.170
0.176
Si
O
N
O

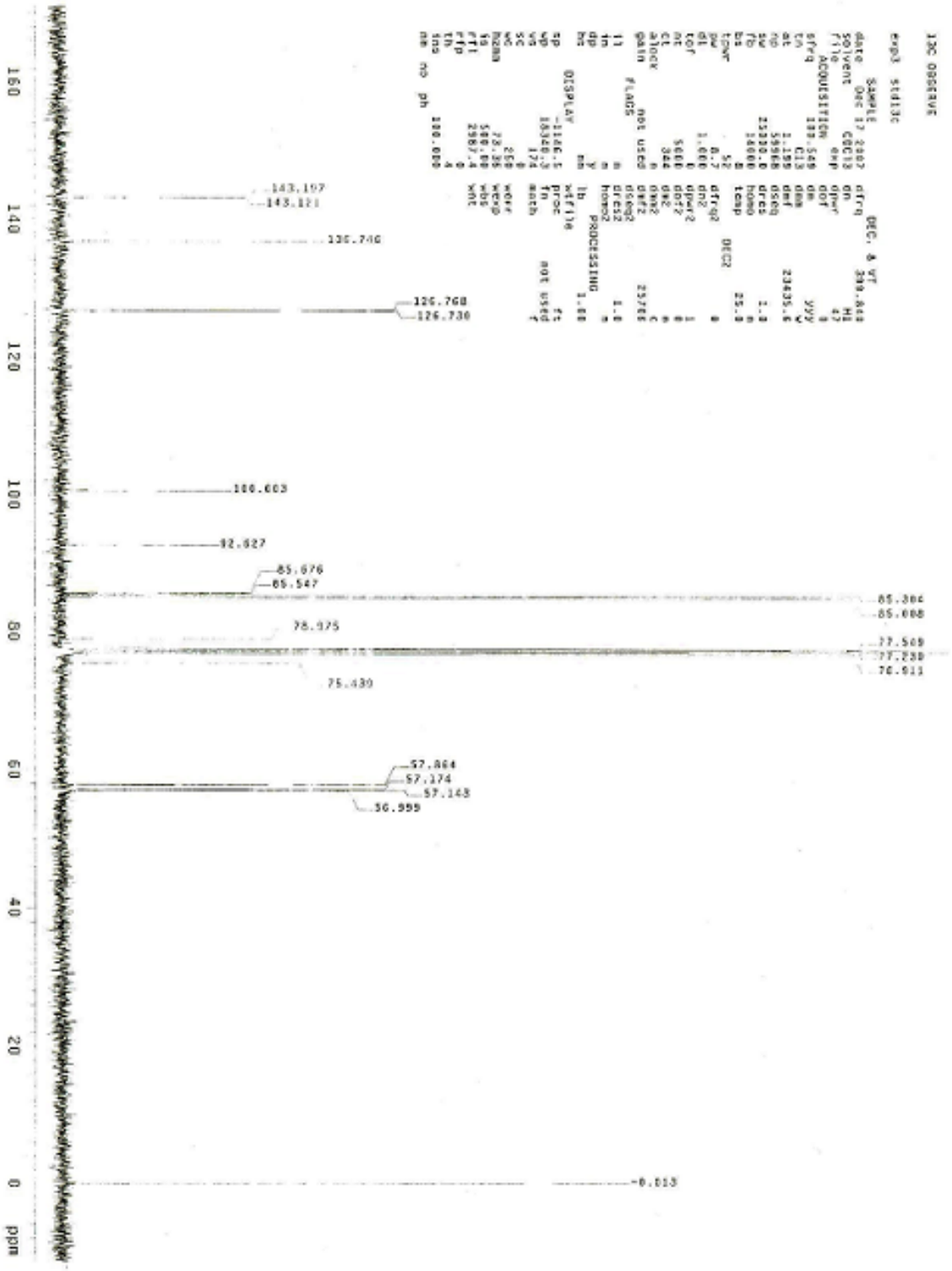
143.197
143.121
130.740
126.768
126.730
100.603
92.627
85.676
85.547
85.384
85.088
78.975
77.569
77.250
76.911
75.430
57.864
57.174
57.143
56.999
-0.013
ppm

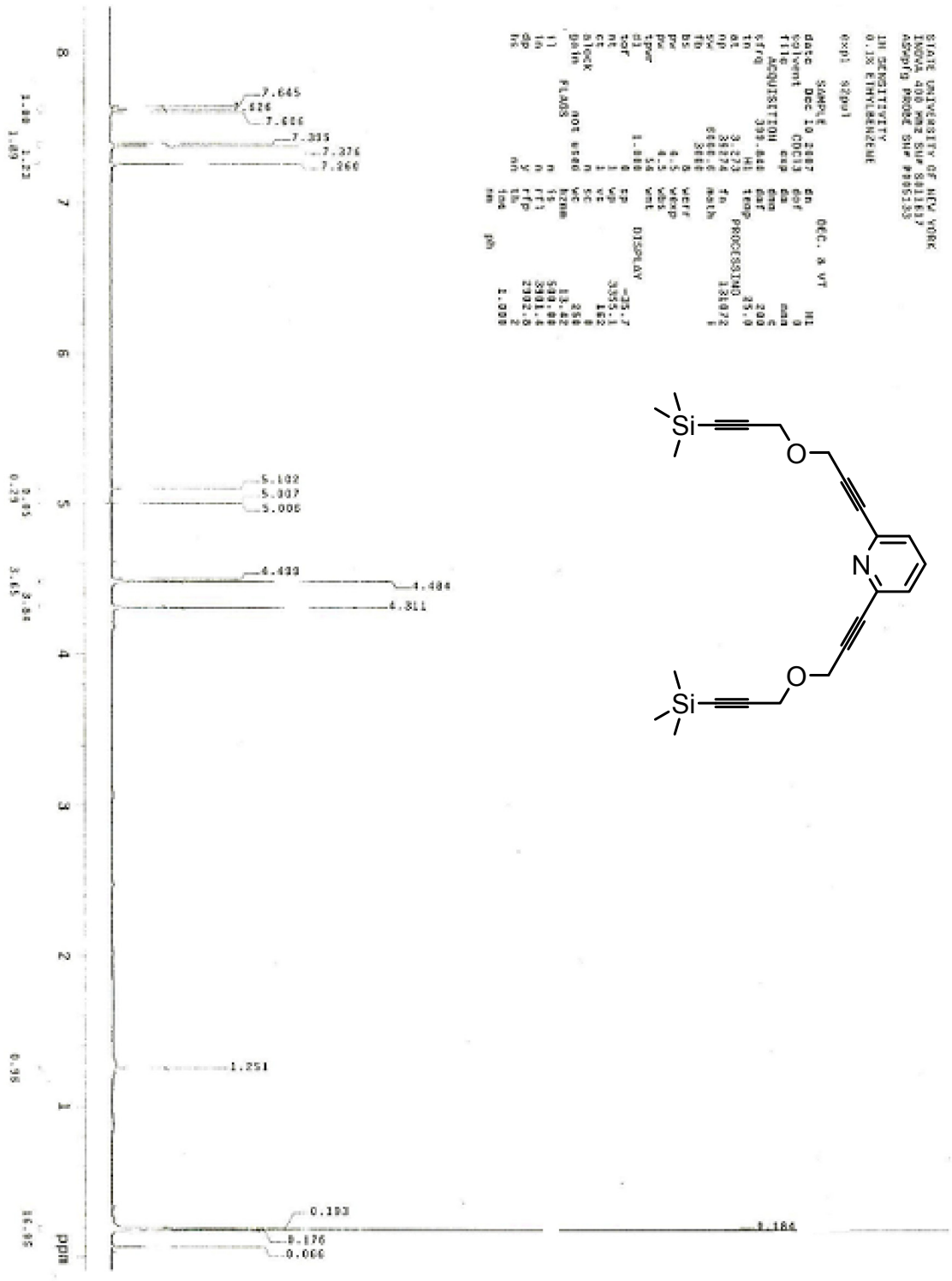
7.645
7.626
7.606
7.385
7.276
7.260
5.102
5.087
5.066
4.488
4.484
4.311
1.251
0.193
0.176
0.066
0.184
Si
O
N
O
Si

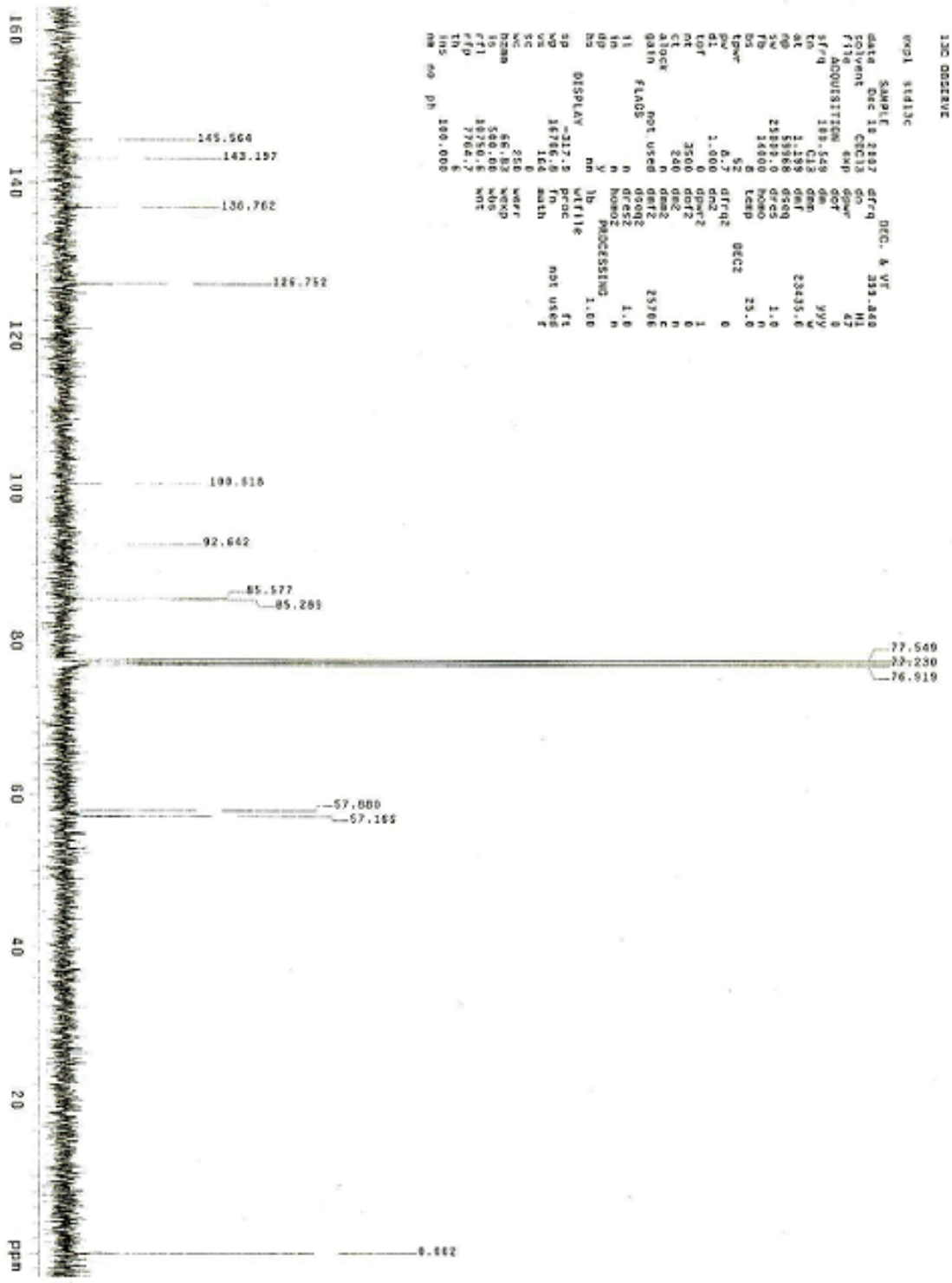
145.564
143.197
136.762
126.752
109.618
92.642
85.577
85.281
77.549
77.230
76.919
57.880
57.165
0.662
ppm

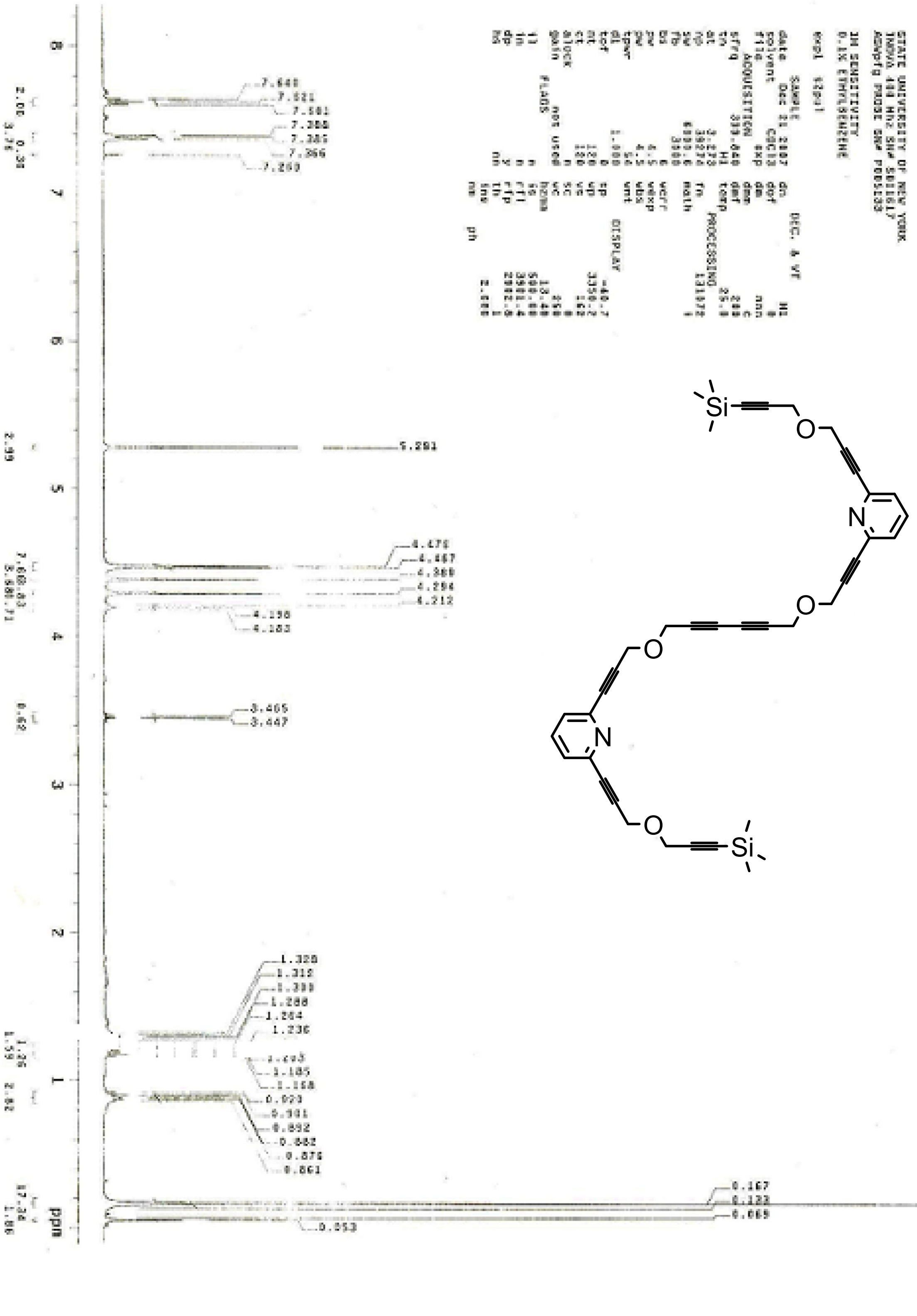

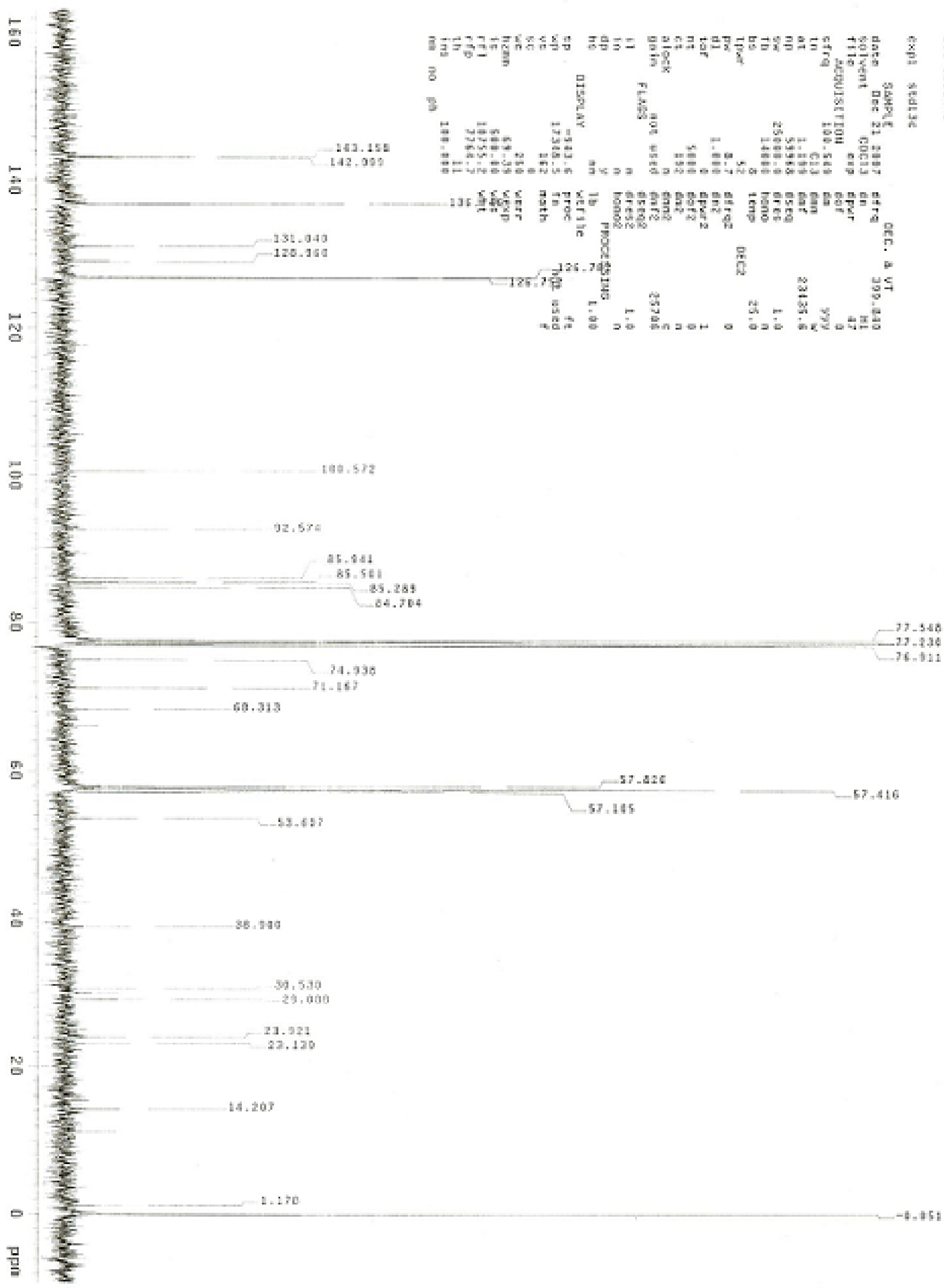

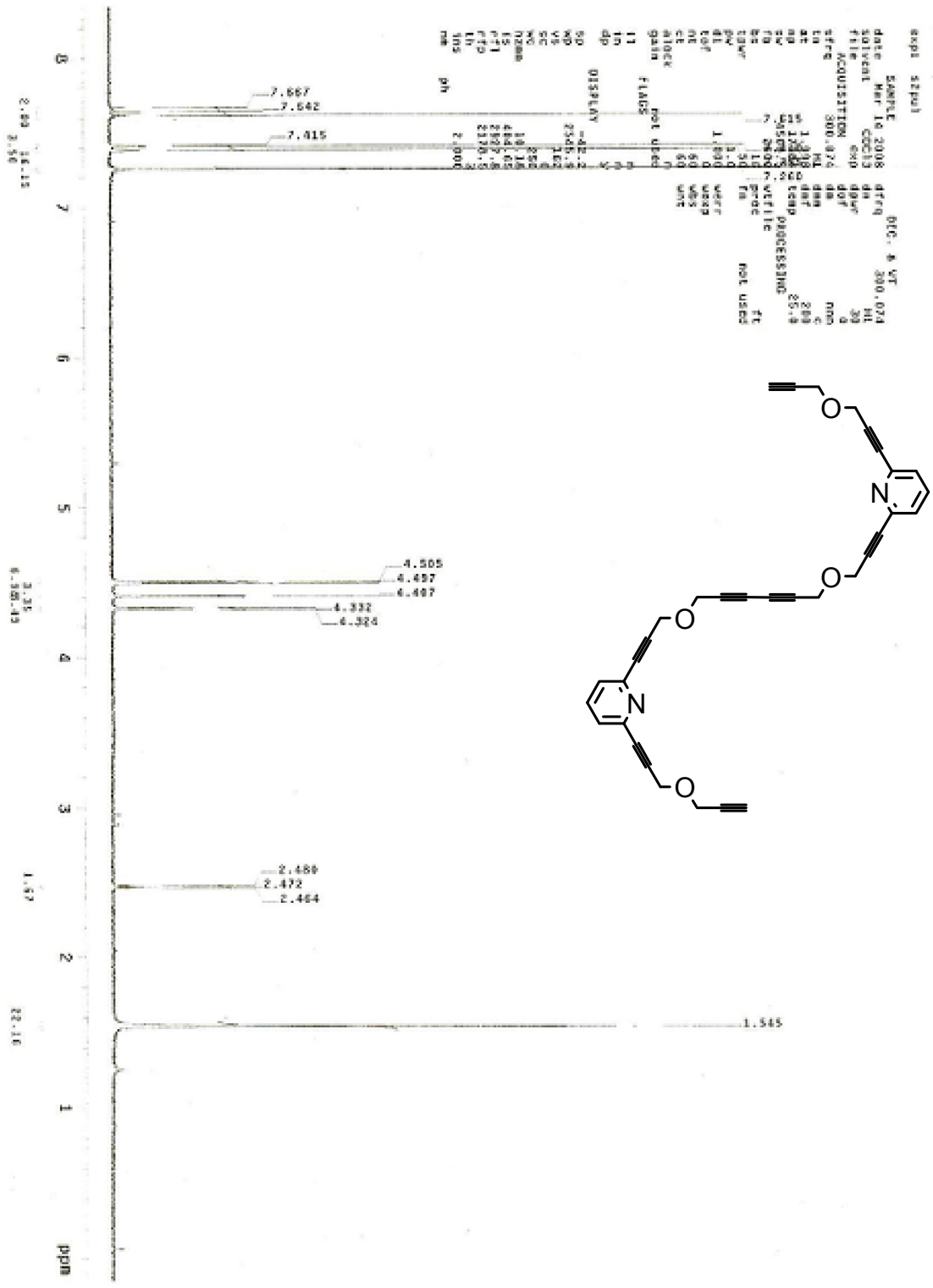
7.667
7.642
7.415
4.505
4.497
4.487
4.332
4.324
2.489
2.472
2.464
1.545
ppm
O
N
O
O
N
O

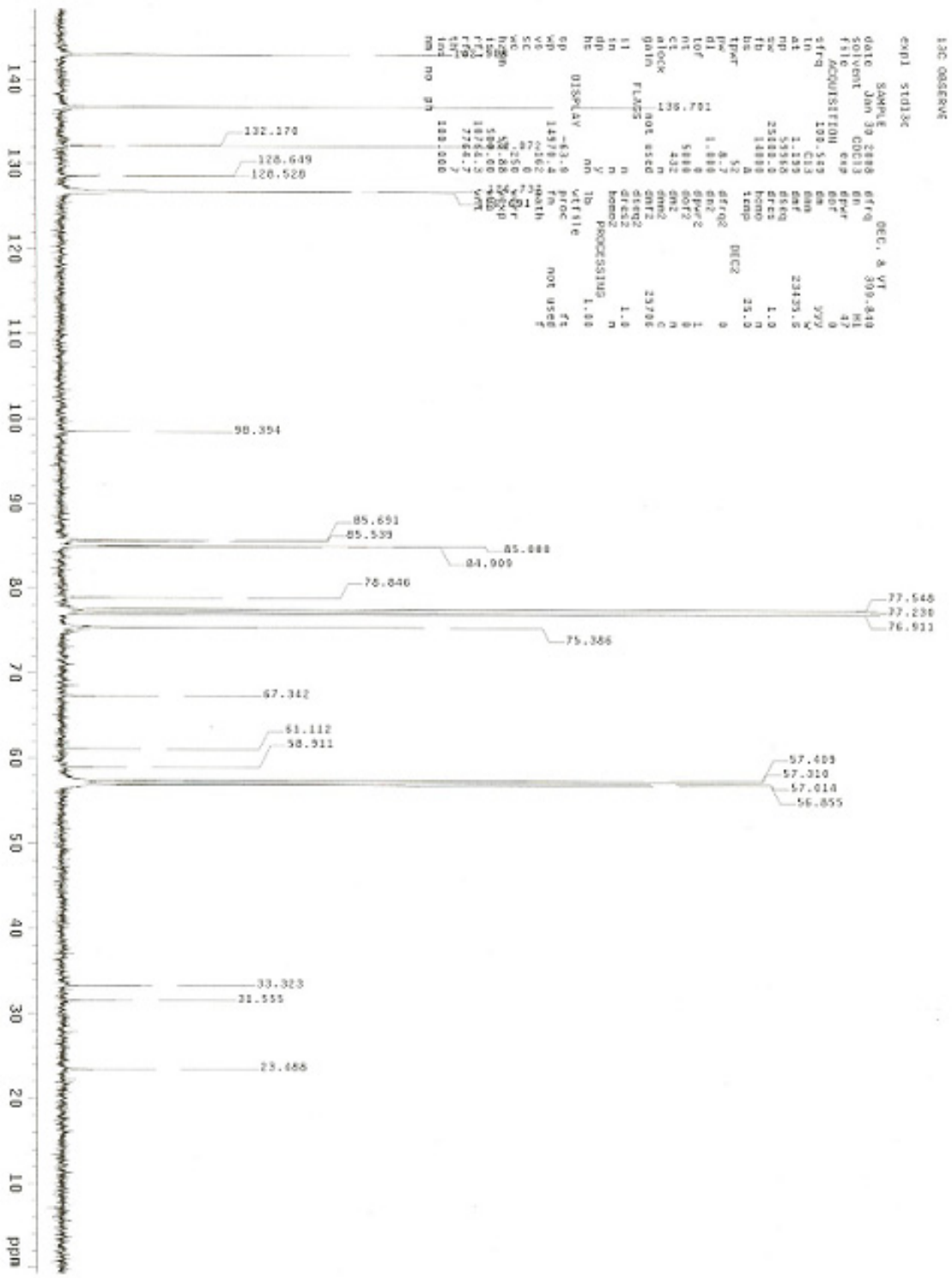
132.170
128.649
128.528
98.354
85.651
85.539
85.088
84.909
78.846
77.548
77.238
76.931
75.386
67.342
61.112
58.911
57.409
57.310
57.014
56.855
33.323
31.555
23.486
ppm

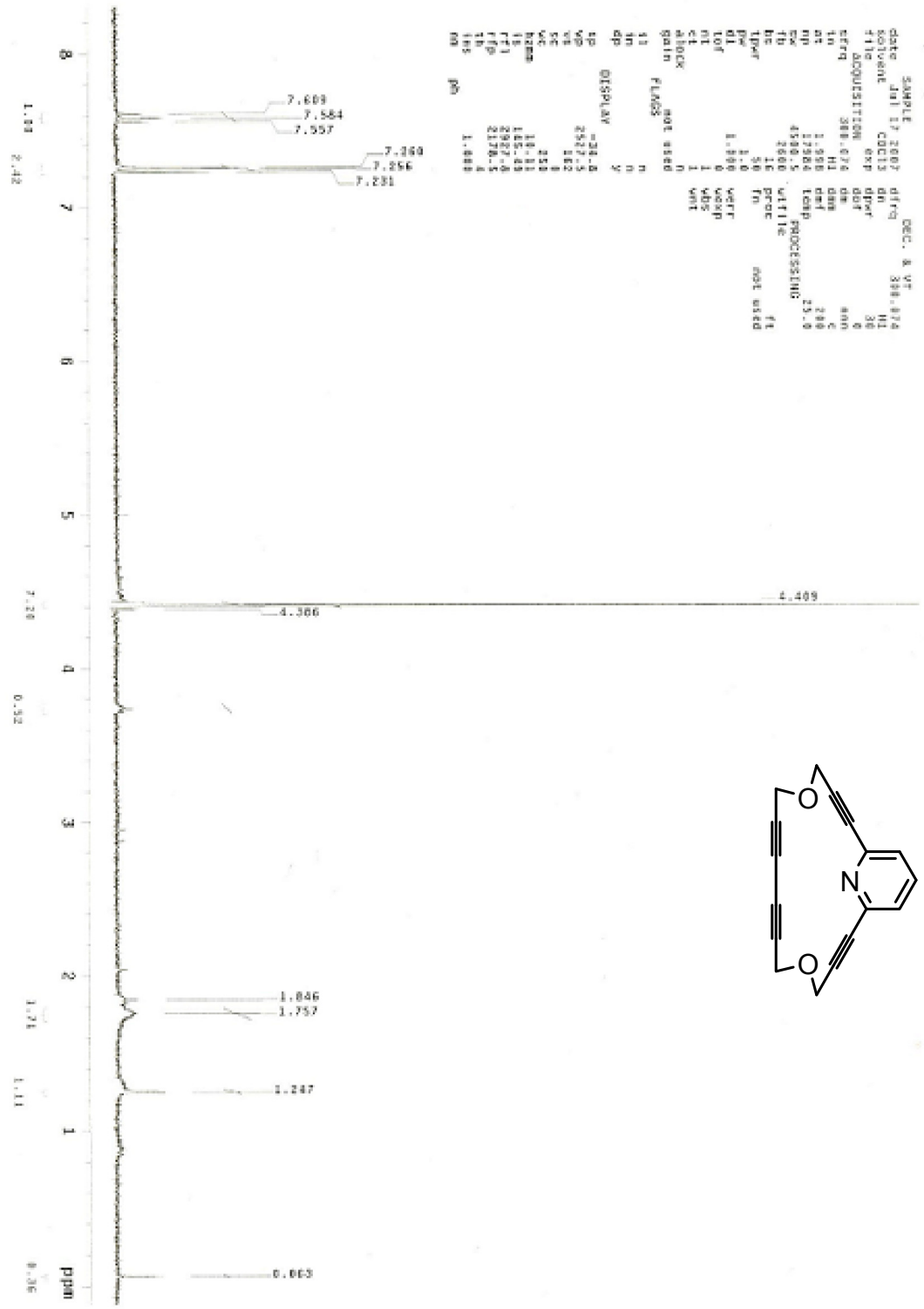
7.609
7.584
7.557
7.369
7.256
7.231
4.386
4.409
1.846
1.757
1.247
0.003
ppm

O
N
O

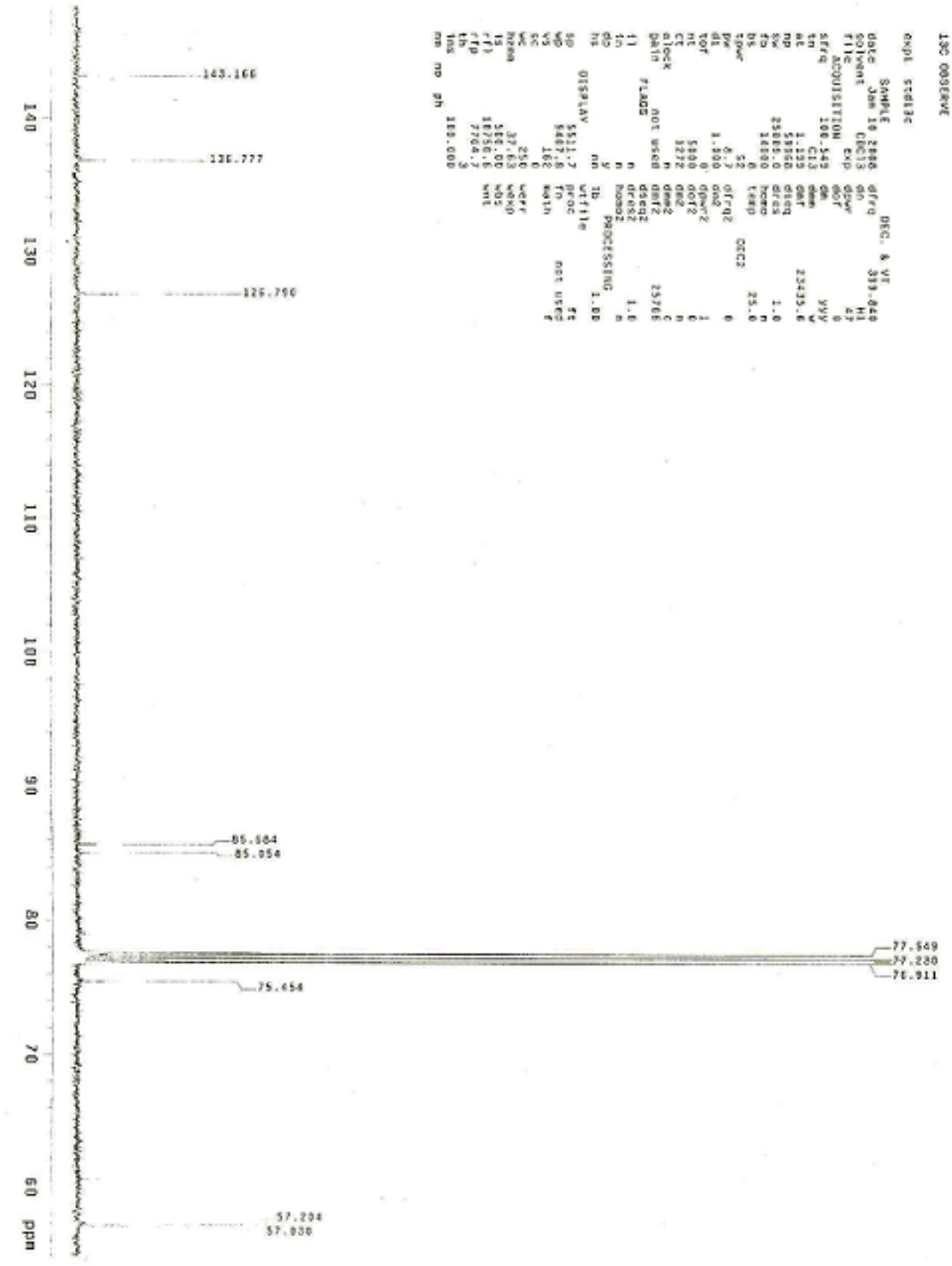
143.169
135.777
125.790
85.684
85.054
77.549
77.230
76.911
75.454
57.204
57.030
ppm

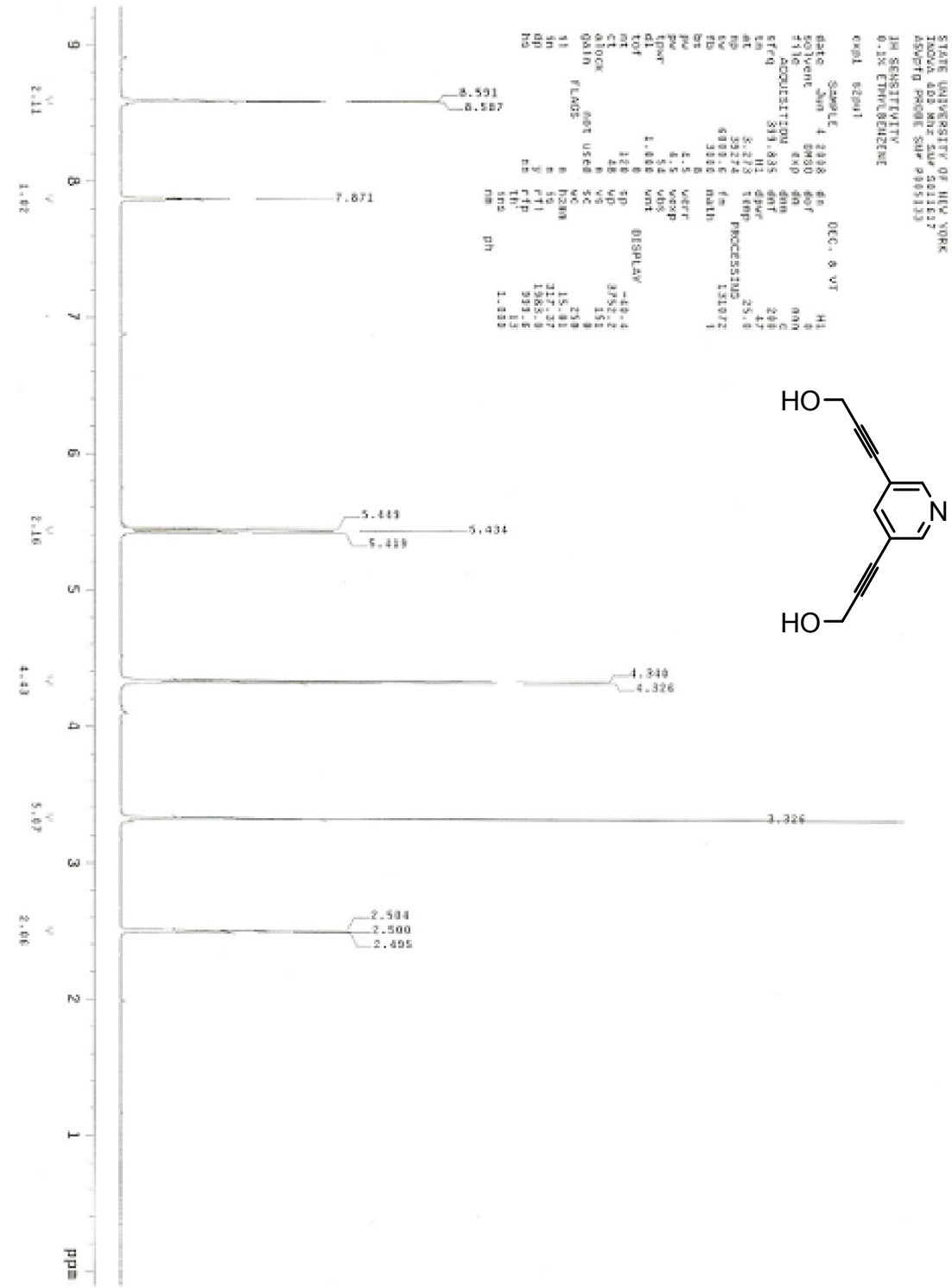
8.591
8.587
7.871
5.449
5.434
5.429
4.349
4.326
3.326
2.504
2.500
2.495
HO
N
HO
ppm

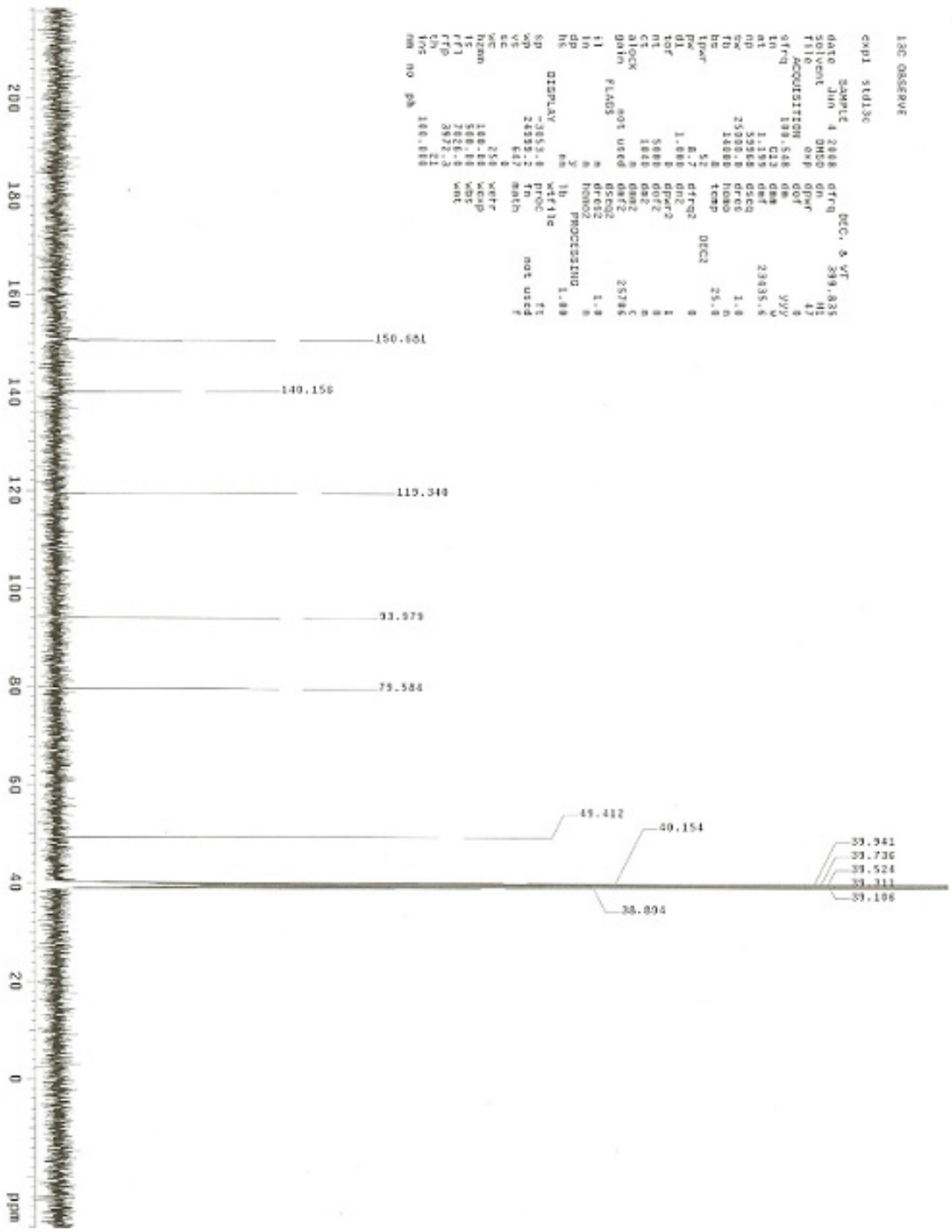
150.681
140.156
119.340
93.979
79.584
49.412
40.154
39.941
39.736
39.524
39.311
39.106
38.894
200
180
160
140
120
100
80
60
40
20
0
ppm